IOP PUBLISHING REPORTS ON PROGRESS IN PHYSICS

Rep. Prog. Phys. **71** (2008) 026001 (43pp) doi:10.1088/0034-4885/71/2/026001

Many-body physics and quantum chaos

Denis Ullmo

Université Paris-Sud, LPTMS, UMR8626, 91405 Orsay Cedex, France
and
CNRS, LPTMS, UMR8626, 91405 Orsay Cedex, France

E-mail: denis.ullmo@u-psud.fr

Received 11 July 2007, in final form 7 November 2007
Published 28 January 2008
Online at stacks.iop.org/RoPP/71/026001

Abstract

Experimental progress in the miniaturization of electronic devices has made routinely available in the laboratory small electronic systems, on the micrometre or sub-micrometre scale, which at low temperature are sufficiently well isolated from their environment to be considered as fully coherent. Some of their most important properties are dominated by the interaction between electrons. Understanding their behaviour therefore requires a description of the interplay between interference effects and interactions.

The goal of this review is to address this relatively broad issue and more specifically to address it from the perspective of the quantum chaos community. I will therefore present some of the concepts developed in the field of quantum chaos which may be applied to the study of many-body effects in mesoscopic and nanoscopic systems. Their implementation is illustrated in a few examples of experimental relevance such as persistent currents, mesoscopic fluctuations of Kondo properties or Coulomb blockade. I will furthermore try to bring out, from the various physical illustrations, some of the specific advantages on more general grounds of the quantum chaos based approach.

(Some figures in this article are in colour only in the electronic version)

This article was invited by Professor S Washburn.

Contents

1. Introduction

The title of this review may seem self-contradictory in two respects. To begin with, it associates chaos, a purely classical notion, with quantum physics. Furthermore it implies that this association, which as we will see refers traditionally to the study of low-dimensional non-interacting quantum systems, will be considered in the context of many-body physics.

The first of these contradictions is however mainly a question of semantics. Indeed, if in an early period of development of the field of quantum chaos, some of the issues addressed had to do with the possible existence of true chaotic dynamics for quantum systems, this was relatively quickly answered, essentially in the negative. Quantum chaos now mainly refers to the study of the consequences, for a quantum system, of the more or less chaotic nature of the dynamics of its classical analogue. It has followed two main avenues. The first one is based on semiclassical techniques—specifically the use of semiclassical Green's functions in the spirit of Gutzwiller's trace formulae (Gutzwiller 1971, 1990, 1991, Balian and Bloch 1972, Berry and Tabor 1977)—which provides a link between a quantum system and its $\hbar \to 0$ limit. The second is associated with the Bohigas Giannoni Schmit conjecture (Bohigas *et al* 1984a, 1984b, Bohigas 1991) or related approaches Peres (1984), which states that the spectral fluctuations of classically chaotic systems can be described using the proper ensembles of random matrices.

Some of the beauty of quantum chaos is that it has developed a set of tools which have found applications in a large variety of different physical contexts, ranging from molecular and atomic physics (Delande and Gay 1986, Wintgen and Friedrich 1986, Wintgen 1987, Delande *et al* 1991) to acoustics (Derode *et al* 1995, Fink 1997, Fink *et al* 2000), nuclear physics (Bohigas and Leboeuf 2002, Olofsson *et al* 2006), cold atoms (Mouchet *et al* 2001, Hensinger *et al* 2001, Steck *et al* 2001, 2002), optical (Nöckel and Stone 1997, Gmachl *et al* 1998) or microwave (Stockmann and Stein 1990, Sridhar 1991, Alt *et al* 1995, Kudrolli *et al* 1995, Pradhan and Sridhar 2000) resonators and of course mesoscopic physics (Richter *et al* 1996b, Richter 2000, Alhassid 2000). With few exceptions (see nevertheless Bohigas and Leboeuf (2002) and Olofsson *et al* (2006)) most of these physical systems share the property of being correctly described by non-interacting, low-dimensional, models.

This is true in spite of the fact that random-matrix ensembles were introduced in the early fifties by Wigner (see the series of papers reprinted in Porter (1965)) to explain the statistics of slow neutron resonances and were therefore applied in the context of strongly interacting systems. In that case however, it was less the notion of chaos than the one of complexity (large number of degrees of freedom, strong and complicated interactions) which was proposed by Wigner to justify this approach.

At any rate, the scope of this review will be concerned with a very different type of interacting system, namely, the Landau–Fermi liquid, for which the system can be explained as a set of quasi-particles interacting weakly through a (renormalized) interaction amenable to perturbative treatment. More specifically, what we have in mind are various realizations of fully coherent, confined electron gasses, with a density high enough that a Landau–Fermi-liquid type description applies. These are typically semiconductor quantum dots or small metallic nano-particles, within which a few tens to a few thousands of electrons interact through a screened Coulomb interaction.

Although this screened interaction between electrons is weak and is therefore well described by a standard perturbative approach (first order perturbation in the simplest cases or eventually with some re-summation of higher-order terms in other situations), some important physical processes are actually largely dominated by them. Moreover, the systems considered are only weakly affected by their environment and can therefore be assumed to be fully coherent. Because of the confinement, translational invariance is then broken, and some new and interesting physics is brought in by the fact that, in the non-interacting limit from which the perturbation scheme is developed, eigenstates are not just plane waves. The mesoscopic fluctuations associated with confinement and interference need to be taken into account for the eigenstates and one-particle energies, either at a statistical level or in a detailed way associated with a given geometry.

Describing these mesoscopic fluctuations and implementing their consequences for many-body effects can be done in a variety of ways. For diffusive systems, techniques based on diagrammatic perturbation expansion in the disorder potential can be used (Altshuler and Aronov 1985, Aleiner *et al* 2002, Akkermans and Montambaux 2007), as well as approaches based on the super-symmetric σ-model (Efetov 1999, Mirlin 2000), which is also appropriate for the description of ballistic chaotic systems (Blanter *et al* 2001a) (see also Andreev *et al* (1996), Leyvraz and Seligman (1997) and Agam *et al* (1997) in this context). In this review, I shall however limit myself to the methods coming from the quantum chaos community. One reason for this limitation of scope is that there are already very good and complete reviews which give an excellent account of the other approaches. Another is that the quantum chaos perspective is in many useful cases more intuitive and somewhat simpler to apply from a technical point of view. As a consequence, this will make it possible to present in an essentially self-contained way the technical tools required to understand a large class of many-body effects relevant for these quantum dots or nano-particles, *as long as they are in the Landau–Fermi-liquid regime*. The goal is that it should be possible to follow almost all of the review with a graduate level in quantum mechanics and, in some cases, basic notions of many-body theory such as can be found in classic textbooks such as Fetter and Walecka (1971). This, I hope, will make it particularly convenient for experimentalists or theoreticians who wish to enter into this field.

Another advantage of the quantum chaos based approach is that it is by nature more flexible and is therefore not limited to chaotic or diffusive dynamics. How much physics is missed by other points of view because of this limitation can be debated, and I will return to this discussion at the end of this review. However, if for metallic nano-particles the choice of a description in terms of a disordered (diffusive) system is

dictated by the actual physics of these materials, it is clear that for semiconductor quantum dots, one reason as to why so much focus has been put on chaotic dynamics is that it is the only description that could be addressed by the more traditional techniques of solid state physics. Having a tool which makes it possible to consider other kinds of dynamics at least gives the possibility of asking the question of whether anything new, or interesting, can be found in these other regimes.

The structure of this review is therefore the following. The first section is devoted to the description of the basic tools necessary to study the physical problems we want to consider. As we want to address different energy scales, or from an experimental point of view different temperature ranges, it will be necessary to introduce a few complementary point of views. Semiclassical techniques, and in particular the use of semiclassical Green's function, will be well adapted to temperature ranges significantly larger than the mean level spacing Δ. They are the subject of section 2.1. The low ($T < \Delta$) temperature regime however requires a modelling of individual energies and wave-functions and are therefore better described, in the hard-chaos regime, by statistical approaches such as random-matrix theory and the random plane-wave model. The latter is introduced in section 2.2. Finally section 2.3 provides a discussion of the screening of the Coulomb interaction.

I then turn to the description of a few examples of physical systems where the physics is dominated by the interplay of interaction effects and mesoscopic fluctuations. The choice of these examples is of course quite arbitrary, and the criterion for selecting them is essentially my familiarity with the issue. Therefore, there will be a strong bias towards questions I have actually worked on, which should not be interpreted as a statement about their relative importance. I start with a discussion of the orbital magnetic response with some general considerations in section 3 followed by a few specific examples of diffusive and ballistic systems in section 4. One important difficulty to be addressed here is the renormalization of the interaction due to higher-order terms in the Cooper channel, and this issue will be discussed in detail in both the diffusive and ballistic regimes. In section 5, I wander briefly away from Fermi-liquid systems and address the mesoscopic fluctuations associated with the physics of a Kondo impurity (Kondo 1964, Hewson 1993) placed in a finite size system. The last physical example is, in section 6, the role of interactions in the fluctuation of peak spacing in Coulomb blockade (Beenakker 1991, Grabert and Devoret 1992, Weinmann *et al* 1996, Sohn *et al* 1997) experiments. After a general introduction of the universal-Hamiltonian picture, I cover the various physical effects which need to be further considered if one expects to understand experimental peak spacing and ground-state spin distributions for these systems.

Finally, the concluding section contains some general discussion and in particular comes back to the issue of non-chaotic dynamics.

2. Basic tools

2.1. Semiclassical formalism

Consider a system of indistinguishable Fermions governed by the one-particle Hamiltonian

$$H_{1p} = -\frac{\hbar^2}{2m_e}\Delta + U(\boldsymbol{r}) \tag{2.1}$$

and interacting weakly through the two-body potential $V(\boldsymbol{r}-\boldsymbol{r}')$. A systematic perturbative expansion can be constructed to arbitrary order (if necessary) in terms of the unperturbed Green's function[1]

$$G(\boldsymbol{r},\boldsymbol{r}';\epsilon) \stackrel{\text{def}}{=} \langle \boldsymbol{r}|\frac{1}{\epsilon - H_{1p}}|\boldsymbol{r}'\rangle = \sum_\kappa \frac{\varphi_\kappa(\boldsymbol{r})\varphi_\kappa^*(\boldsymbol{r}')}{\epsilon-\epsilon_\kappa}, \tag{2.2}$$

where in the last expression ϵ_κ and φ_κ are, respectively, the energies and eigenstates of H_{1p}. In a clean bulk system $U(\boldsymbol{r}) \equiv 0$ so that the eigenstates are just plane waves and the expression of Green's function becomes trivial in the momentum representation. For confined (coherent) systems however, translational invariance is lost and there is in general no simple expression for the exact eigenstates and eigenfunctions. It therefore becomes necessary to find some approximation scheme for the unperturbed Green's function itself before considering a perturbation expansion in the interaction.

2.1.1. Semiclassical Green's function. In many regimes of interest a semiclassical approach can be used to fulfil this role. This includes the case where the confining potential $U(\boldsymbol{r})$ is a smooth function on the scale of the Fermi wavelength λ_F, but also, for instance, when it contains a weak, eventually short range, disorder, as long as λ_F is much smaller than the elastic mean free path ℓ. Under these conditions, the retarded Green's function $G^R(\epsilon) \stackrel{\text{def}}{=} \lim_{\eta\to 0} G(\epsilon+\mathrm{i}\eta)$ can be written as a sum over all *classical* trajectories j joining $\boldsymbol{r}'$ to $\boldsymbol{r}$ at energy ϵ (Gutzwiller 1990, 1991):

$$\begin{aligned} G^R(\boldsymbol{r},\boldsymbol{r}';\epsilon) &\simeq \sum_{j:\boldsymbol{r}'\to\boldsymbol{r}} G_j^R(\boldsymbol{r},\boldsymbol{r}';\epsilon), \\ G_j^R(\boldsymbol{r},\boldsymbol{r}';\epsilon) &\stackrel{\text{def}}{=} \frac{2\pi}{(2\mathrm{i}\pi\hbar)^{(d+1)/2}} D_j(\epsilon) \\ &\quad \times \exp(\mathrm{i}S_j(\epsilon)/\hbar - \mathrm{i}\zeta_j\pi/2), \end{aligned} \tag{2.3}$$

with d the number of degrees of freedom,

$$S_j(\epsilon) = \int_{r'}^{r} \boldsymbol{p}\cdot \mathrm{d}\boldsymbol{r} \tag{2.4}$$

the classical action along the trajectory j and

$$D_j(\epsilon) = \left|\frac{1}{\dot r_1 \dot r_1'}\det{}'\left[-\frac{\partial^2 S}{\partial \boldsymbol{r}\partial\boldsymbol{r}'}\right]\right|^{1/2} \tag{2.5}$$

[1] All Green's functions used in this review will be unperturbed Green's functions. I shall therefore not use any subscript to distinguish them from the interacting ones.

a determinant describing the stability of trajectories near j. In (2.5) $\boldsymbol{r} = (r_1, \ldots, r_d)$, and the prime on the determinant indicates that the first component (i.e. first row $\partial^2 S/\partial r_1 \partial r_i'$ and first column $\partial^2 S/\partial r_i \partial r_1', i = 1, \cdots, d$) is omitted. Finally, the Maslov index ζ_j essentially counts the number of caustics (i.e. places where the determinant D_j is zero) on the trajectory j between $\boldsymbol{r}'$ and $\boldsymbol{r}$.[2] For two-dimensional systems ($d = 2$), the determinant takes the particularly simple form

$$D_j(\epsilon) = \left| \frac{1}{\dot{r}_\parallel \dot{r}_\parallel'} \frac{1}{\left(\partial r_\perp / \partial p_\perp'\right)_{r_\perp}} \right|^{1/2}, \tag{2.6}$$

where $r_\parallel$ and $r_\perp$ are the r-components, respectively, parallel and orthogonal to the trajectory.

2.1.2. Simple properties of the classical action. Many important characteristic features of the semiclassical Green's function, and therefore of the fermion gas, can be directly deduced from basic properties of classical action (Goldstein 1964, Arnold 1989). In particular:

(i) the variation with respect to the energy:

$$\frac{\partial S_j}{\partial \epsilon} = t_j, \tag{2.7}$$

where t_j is the time elapsed to go from $\boldsymbol{r}'$ to $\boldsymbol{r}$ along trajectory j at energy ϵ;

(ii) the variation with respect to the position:

$$\frac{\partial S_j}{\partial \boldsymbol{r}'} = -\boldsymbol{p}_j' \qquad \frac{\partial S_j}{\partial \boldsymbol{r}} = \boldsymbol{p}_j; \tag{2.8}$$

and finally

(iii) the effect of a perturbation. Indeed, let us assume that the one-particle Hamiltonian can be written as the sum of a main term H_0 and a small perturbation H_1:

$$H_{1\mathrm{p}} = H_0 + H_1, \tag{2.9}$$

and let us denote by S_j^0 the action calculated for the trajectory j, i.e. $(\boldsymbol{r}_j^0(t), \boldsymbol{p}^0(t))_j$, $t \in [0, t^0]$, joining $\boldsymbol{r}'$ to $\boldsymbol{r}$ under the Hamiltonian H_0. We then have

$$\delta S_j \stackrel{\mathrm{def}}{=} S_j - S_j^0 \simeq -\int_0^{t_0} \mathrm{d}t\, H_1(\boldsymbol{r}_j^0(t), \boldsymbol{p}_j^0(t)). \tag{2.10}$$

Note there is no need for H_1 to be small on the quantum scale, and therefore (2.10) remains applicable much beyond the limit of quantum perturbation theory[3].

To illustrate how the above properties can be used in our context, let us consider for instance the (unperturbed) local density of states,

$$\nu_{\mathrm{loc}}(\boldsymbol{r}; \epsilon) \stackrel{\mathrm{def}}{=} \sum_\kappa |\varphi_\kappa(\boldsymbol{r})|^2 \delta(\epsilon - \epsilon_\kappa) = -\frac{1}{\pi} \mathrm{Im} G^R(\boldsymbol{r}, \boldsymbol{r}; \epsilon). \tag{2.11}$$

[2] For the kind of kinetic plus potential Hamiltonian we consider here, the Maslov index increases by one at each crossing of a caustic. Note however that for a more general Hamiltonian it may however also decrease.

[3] It should be stressed that the exponential sensitivity to perturbations of chaotic trajectories does not prevent finding a perturbed trajectory following closely the unperturbed one and joining the same endpoints in configuration space (but with slightly different momenta). See for instance Cerruti and Tomsovic (2002) for a recent discussion on this (old) question.

Using (2.3), ν_{loc} can be expressed as a sum over all the closed orbits starting and ending at the point $\boldsymbol{r}$. In this process, the 'direct' orbit j_0, whose length goes to zero as $\boldsymbol{r} \to \boldsymbol{r}'$, needs however to be treated separately, as the determinant D_{j_0} diverges. On the other hand, the contribution of this orbit to Green's function can be identified to the free Green's function for a constant potential. It therefore just gives rise to the smooth (bulk-like) contribution

$$\begin{aligned} \nu_0^{(d)}(\boldsymbol{r}; \epsilon) &= \int \frac{\mathrm{d}\boldsymbol{p}}{(2\pi\hbar)^d} \delta(\epsilon - H(\boldsymbol{p}, \boldsymbol{r})) \\ &= \frac{m_{\mathrm{e}} k(\boldsymbol{r})^{d-2}}{(2\pi)^n \hbar^2} \frac{\mathrm{d}\pi^{d/2}}{\Gamma(d/2+1)}. \end{aligned} \tag{2.12}$$

($\nu_0^{(2)} = m_{\mathrm{e}}/2\pi\hbar^2$, $\nu_0^{(3)} = m_{\mathrm{e}} k/2\pi^2\hbar^2$), where d is the dimensionality and the last equality holds for the usual kinetic plus potential Hamiltonian, with $k(\boldsymbol{r}) = \sqrt{2m_{\mathrm{e}}(\epsilon - U(\boldsymbol{r}))}/\hbar$. I shall in the following use the notation $\rho(\epsilon) = \int \mathrm{d}\boldsymbol{r} \nu_{\mathrm{loc}}(\boldsymbol{r}; \epsilon)$ for the total density of states and

$$\rho_0(\epsilon) = \int \frac{\mathrm{d}\boldsymbol{p}\, \mathrm{d}\boldsymbol{r}}{(2\pi\hbar)^d} \delta(\epsilon - H(\boldsymbol{p}, \boldsymbol{r})) \tag{2.13}$$

for its Weyl (smooth) part.

The local density of states can therefore be separated into a smooth and an oscillating part

$$\nu_{\mathrm{loc}}(\boldsymbol{r}; \epsilon) = \nu_0(\boldsymbol{r}; \epsilon) + \nu_{\mathrm{osc}}(\boldsymbol{r}; \epsilon), \tag{2.14}$$

where $\nu_{\mathrm{osc}}(\boldsymbol{r}; \epsilon)$ is expressed semiclassically as a sum over all finite length closed orbits

$$\nu_{\mathrm{osc}}(\boldsymbol{r}; \epsilon) = \sum_{j \neq j_0 : \boldsymbol{r} \to \boldsymbol{r}} \nu_j(\boldsymbol{r}; \epsilon) + \mathrm{c.c.}, \tag{2.15}$$

$$\nu_j(\boldsymbol{r}; \epsilon) = \frac{-\mathrm{i}}{(2\mathrm{i}\pi\hbar)^{(d+1)/2}} D_j(\epsilon) \exp(\mathrm{i} S_j(\epsilon)/\hbar - \mathrm{i}\zeta_j \pi/2). \tag{2.16}$$

For energies ϵ close, on the classical scale, to some reference energy $\bar{\epsilon}$, one can therefore use (2.7) to write

$$\nu_j(\boldsymbol{r}; \bar{\epsilon} + \delta\epsilon) = \nu_j(\boldsymbol{r}; \bar{\epsilon}) \exp(\mathrm{i}\, \delta\epsilon\, t_j/\hbar). \tag{2.17}$$

Thus, the local density of states appears as the bulk contribution plus some oscillating terms which, with (2.7), have a period in energy $2\pi\hbar/t_j$ determined by the *travel time* of the closed orbits.

In the same way, Friedel oscillations near the boundary of the system or near an impurity can be understood as a direct consequence of (2.8), applied to the trajectory bouncing on the obstacle and coming back directly to its starting point. Quite generally one can write for the contribution of the orbit j to the local density of states

$$\nu_j(\boldsymbol{r} + \delta\boldsymbol{r}; \epsilon) = \nu_j(\boldsymbol{r}; \epsilon) \exp(\mathrm{i}(\boldsymbol{p}_j' - \boldsymbol{p}_j)\delta\boldsymbol{r}/\hbar), \tag{2.18}$$

so that locally $\nu_{\mathrm{loc}}(\boldsymbol{r}; \epsilon)$ appears as a sum of plane waves the wave-vectors of which are determined by the difference between the final and initial momenta of the corresponding returning orbits. Periodic orbits, which are such that $\boldsymbol{p}_j' = \boldsymbol{p}_j$,

have no variation locally and therefore will give rise to the dominant contribution to the total density of states $\rho(\epsilon)$ (Gutzwiller 1970, 1971). Friedel oscillations on the other hand correspond to trajectories which, after bouncing off the boundary of the system or some impurity, travel back directly to the initial point, so that $\boldsymbol{p}'_j = -\boldsymbol{p}_j$. In this case the corresponding plane-wave contribution has a wave-vector with modulus twice the wave-vector $k(\boldsymbol{r}) = \sqrt{(\epsilon - U(\boldsymbol{r}))/2m_e}/\hbar$. In the particular case of a two-dimensional system with a straight hard wall (with Dirichlet boundary condition) at $x = 0$, the direct application of (2.6) and (2.15) gives (for $kx \geqslant 1$)

$$\nu_{\rm osc}(\boldsymbol{r}=(x,y);\epsilon) = -\sqrt{2\pi}\,\nu_0^{(2)}\frac{\sin(2kx+\pi/4)}{\sqrt{2kx}}, \qquad (2.19)$$

from which the Friedel oscillations in the density of particles $n(\boldsymbol{r})$ are derived by integration over the energy. More general cases (e.g. curved boundary) are easily obtained by calculating the corresponding value of $\partial p_\perp/\partial r'_\perp$ (and eventually Maslov indices).

Finally as an illustration of the third property (2.10), let us compute the variation of the density of states under the modification of an external magnetic field $\boldsymbol{B} = \boldsymbol{\nabla}\times\boldsymbol{A}$. When the magnetic field is changed from $\boldsymbol{B} \to \boldsymbol{B} + \delta\boldsymbol{B}$ (with the corresponding change in the vector potential $\boldsymbol{A} \to \boldsymbol{A} + \delta\boldsymbol{A}$), one has

$$H_0 = \frac{1}{2m_e}(\boldsymbol{p} - e\boldsymbol{A})^2 + U(\boldsymbol{r}), \qquad (2.20)$$

and in first order in $\delta\boldsymbol{A}$

$$H_1 = -\frac{e}{m_e}(\boldsymbol{p} - e\boldsymbol{A})\cdot\delta\boldsymbol{A} = -e\boldsymbol{v}\cdot\delta\boldsymbol{A}, \qquad (2.21)$$

with $\boldsymbol{v} = \dot{\boldsymbol{r}} = (\partial H/\partial\boldsymbol{p})$ the velocity. The variation of the action along a closed trajectory $j : \boldsymbol{r}\to\boldsymbol{r}$ is therefore given by

$$\frac{1}{\hbar}\delta S_j = \frac{e}{\hbar}\oint_{j:\boldsymbol{r}\to\boldsymbol{r}} {\rm d}t\,(\delta\boldsymbol{A}\cdot\boldsymbol{v}) = \frac{e}{\hbar}\oint_{j:\boldsymbol{r}\to\boldsymbol{r}} {\rm d}\boldsymbol{l}\cdot\delta\boldsymbol{A} = \frac{2\pi\,\delta\phi_j}{\phi_0}, \qquad (2.22)$$

where $\delta\phi_j$ is the flux of δB across the trajectory j and $\phi_0 \stackrel{\rm def}{=} 2\pi\hbar/e$ is the flux quantum. The variation of the contribution of the orbit j to the local density of states can therefore be written as

$$\nu_j(\boldsymbol{r};\epsilon;\boldsymbol{B}+\delta\boldsymbol{B}) = \nu_j(\boldsymbol{r};\epsilon;\boldsymbol{B})\exp(i\delta\phi_j/\phi_0). \qquad (2.23)$$

2.1.3. Sum rule for the determinant D_j. The computation of the contribution of some orbit j to the semiclassical Green's function for a given geometry implies in practice the determination of the action of the orbit, which is usually not too difficult, but also of the stability determinant D_j and the Maslov index ζ_j which for generic systems may involve some technicalities (see, e.g. Bogomolny (1988) for an illustration on the examples of the stadium and elliptic billiards and Creagh *et al* (1990) for a detailed discussion about the Maslov indices). It turns out that in practice a large number of results can be obtained without an explicit calculation of these quantities, but can be derived from a sum rule (M-formula) for the determinants D_j, analogous in spirit to the Hannay–Ozorio de Almeida sum rule (Hannay and Ozorio de Almeida 1984, Ozorio de Almeida 1988), and which in a similar way expresses the conservation of the Liouville measure by the classical flow. The M-formula can be expressed as (Argaman 1996)

$$\sum_{j:\boldsymbol{r}'\to\boldsymbol{r}}\frac{|D_j(\epsilon)|^2}{(2\pi\hbar)^d}\delta(t-t_j) = \nu_0^{(d)}(\boldsymbol{r}')P_{\rm cl}^{\epsilon}(\boldsymbol{r},\boldsymbol{r}',t), \qquad (2.24)$$

where $\nu_0^{(d)}(\boldsymbol{r}')$ is the bulk density of states per unit area (and spin) (see (2.12)) for the local value of $k_{\rm F}$ and $P_{\rm cl}^{\epsilon}(\boldsymbol{r},\boldsymbol{r}',t)$ is the classical (density of) probability that a trajectory launched in $\boldsymbol{r}'$ is in the neighbourhood of $\boldsymbol{r}$ at time t.

The sum rule (2.24) is particularly useful for diffusive systems, for which $P_{\rm cl}^{\epsilon}(\boldsymbol{r},\boldsymbol{r}',t)$ is the solution of a diffusion equation (with diffusion coefficient D)

$$(\partial_t + D\Delta_{\boldsymbol{r}})P_{\rm cl}^{\epsilon}(\boldsymbol{r},\boldsymbol{r}',t) = \delta(\boldsymbol{r}-\boldsymbol{r}')\delta(t) \qquad (2.25)$$

with boundary conditions $\partial_{\vec{n}}P_{\rm cl} = 0$ at the boundary of the system (if any). We shall see in the next subsection that it can be also applied usefully for ballistic chaotic systems.

2.1.4. Thouless energy. When considering a confined system of (for now) non-interacting particles, one might first, before any actual calculation, try to understand what energy scales are affected by the confinement. On the low-energy side, this is clearly bounded by the mean level spacing, the finiteness of which is the most obvious consequence of the fact that the system is bounded. On the high-energy end, a direct implication of (2.17) is that if the Green's function is smoothed on an energy scale ϵ, only the contributions of trajectories with a time of travel $t < \hbar/\epsilon$ survive the averaging process. Therefore the minimal time $t_{\rm min}$ such that a classical particle feels the presence of the boundary, determines the maximal energy scale $E_{\rm Th}$ such that the quantum system is affected by the latter. This energy scale, $E_{\rm Th}$, is referred to as the Thouless energy.

For ballistic systems, $t_{\rm min}$ is essentially the time of flight $t_{\rm fl}$ across the system, which is also the time scale of the shortest closed orbit for a generic point $\boldsymbol{r}$ inside the system. As a consequence $E_{\rm Th}$ is also in this case the energy scale beyond which no fluctuations exist.

For diffusive systems $t_{\rm min}$ is the time necessary to diffuse to the boundary of the system, the time at which the solution of the diffusion equation (2.25) starts to differ from free space diffusion. In this case however, the scale is different (and usually significantly larger) than the time associated with the shortest closed orbit, which is rather of the order of the momentum randomization time $t_{\rm tr}$.

As I shall illustrate below, a significant number of results can be derived for singly connected chaotic or diffusive quantum dots using the sum rule (2.24) in conjunction with a simple approximation for the probability $P_{\rm cl}^{\epsilon}(\boldsymbol{r},\boldsymbol{r}',t)$. Indeed, for time shorter than $t_{\rm min}$ the presence of boundaries can be ignored and the free flight (free diffusion) expression can be used for the ballistic (diffusive) case. On the other

hand, the classical probability $P^{\epsilon}_{\rm cl}(\boldsymbol{r},\boldsymbol{r}',t)$ can usually be taken as being independent of the initial condition for time larger than $t_{\rm min}$ and simply proportional to the phase-space volume $\int {\rm d}\boldsymbol{p}\delta(\epsilon - H(\boldsymbol{p},\boldsymbol{r}))$. For a billiard system of volume $\mathcal{A}$ this gives, for instance, for the return probability

$$P^{\epsilon}_{\rm cl}(\boldsymbol{r},\boldsymbol{r},t) = 0 \qquad t < t_{\rm min}, \tag{2.26}$$

$$P^{\epsilon}_{\rm cl}(\boldsymbol{r},\boldsymbol{r},t) = 1/\mathcal{A} \qquad t > t_{\rm min} \tag{2.27}$$

for the chaotic system and in the diffusive case

$$P^{\epsilon}_{\rm cl}(\boldsymbol{r},\boldsymbol{r},t) = (4\pi Dt)^{-d/2} \qquad t < t_{\rm min}, \tag{2.28}$$

$$P^{\epsilon}_{\rm cl}(\boldsymbol{r},\boldsymbol{r},t) = 1/\mathcal{A} \qquad t > t_{\rm min}. \tag{2.29}$$

2.2. Random-matrix and random-plane-wave models in the hard-chaos regime

The semiclassical approach introduced in the previous subsection is a natural tool to describe energy scales significantly larger than the mean level spacing Δ. It is however not convenient, if only because it is usually not convergent, when the properties of a single wave-function are considered and more generally when quantum properties are investigated on the scale not larger than a few mean level spacings (see however Tomsovic *et al* (2007) in this respect).

In the hard-chaos regime (and quite often in the diffusive regime), it is however possible to use an alternative route, based on the statistical description of the eigenstates' and eigenfunctions' fluctuations.

2.2.1. Random matrices. The most basic model is to assume that the fluctuations of physical quantities for the quantum system under consideration are well described by ensembles of random matrices, such as the Gaussian orthogonal, unitary or symplectic ensembles. These ensembles have been introduced by Wigner in the context of nuclear physics to account for the complex (i.e. large number of degrees of freedom, large and complicated interactions) characteristics of the nuclei. Studies of billiard systems have however led Bohigas, Giannoni and Schmit (Bohigas *et al* 1984a, 1984b) to conjecture that even 'simple' (i.e. low-dimensional, with innocent looking Hamiltonians) systems would display the spectral fluctuations of these Gaussian ensembles as long as they have a chaotic dynamics. This conjecture, although still not formally proven, is supported by recent semiclassical calculations showing that the form factor (the Fourier transform of the two-point correlation function) predicted by the random-matrix ensembles can be recovered in all orders of a perturbation expansion within a periodic orbit theory (Berry 1985, Richter and Sieber 2002, Muller *et al* 2004, 2005, Heusler and Haake 2004). It has furthermore been verified numerically on a large variety of systems, giving a kind of experimental demonstration that classical chaos, rather than complexity, is the origin of these characteristic fluctuation properties.

Wigner Gaussian ensembles are constructed by first considering the set of $N \times N$ (in the limit $N \to \infty$) Hamiltonian matrices corresponding to the symmetries with respect to time reversal of the physical systems. These are Hermitian matrices $H = H^{(0)} + {\rm i}H^{(i)}$ for time-reversal non-invariant systems (Gaussian unitary ensemble (GUE)), real symmetric matrices $H = H^{(0)}$ for spinless time-reversal invariant systems (Gaussian orthogonal ensemble (GOE)) and quaternion real matrices $H = H^{(0)} \otimes \mathbf{1} + H^{(1)} \otimes \sigma_x + H^{(2)} \otimes \sigma_y + H^{(3)} \otimes \sigma_z$ for spin 1/2 time-reversal invariant but non-rotationally invariant systems (Gaussian symplectic ensemble (GSE)). ($H^{(0)}$ is a real symmetric matrix, and the $H^{(\alpha)}$, $\alpha > 0$ are real antisymmetric matrices.) The associated probability is then constructed (i) assuming that each matrix element $h^{(\alpha)}_{ij}$ ($i \leqslant j$) is independent and (ii) in such a way that the probability is invariant under the group transformation corresponding to a change in basis (unitary transformations for GUE, orthogonal transformations for GOE and symplectic transformations for GSE). This leads to (Mehta 1991)

$$P_{\beta_{\rm RMT}}(H)\,{\rm d}H = K_{N\beta_{\rm RMT}} \exp[-{\rm Tr}(H^2)/4v^2]\,{\rm d}H, \tag{2.30}$$

where $K_{N\beta_{\rm RMT}}$ is a normalization constant, $\beta_{\rm RMT}$ indexes the symmetry class ($\beta_{\rm RMT} = 1, 2, 4$ corresponding, respectively, to GOE, GUE and GSE), v is an energy scale determined in practice by the physical mean level spacing and ${\rm d}H$ is the natural measure

$${\rm d}H = \prod_{i\leqslant j}\prod_{\alpha} {\rm d}h^{(\alpha)}_{ij}. \tag{2.31}$$

From the probability distribution (2.30) various spectral correlation functions can be derived (Mehta 1991). For instance, the distribution of the (scaled) nearest neighbour $s = (\epsilon_{n+1} - \epsilon_n)/\Delta$ can be shown to be well approximated by the Wigner-surmise distribution

$$P_{\rm nns}(s) = a_{\beta_{\rm RMT}} s^{\beta_{\rm RMT}} \exp(-c_{\beta_{\rm RMT}} s^2), \tag{2.32}$$

with the numbers $(a_{\beta_{\rm RMT}}, c_{\beta_{\rm RMT}})$ fixed by the constraints on the normalization and on the mean[4].

The main content of (2.30) is its universal character. Indeed beyond the scale v and the symmetries of the system, the resulting distributions are completely independent of the particular feature of the physical problem under consideration, as long as the corresponding classical dynamics is chaotic. This makes it possible to obtain quantitative predictions for various physical configurations without a precise knowledge of the system's specific details. This is presumably one of the reasons why so much focus has been put, both theoretically and experimentally, on the hard chaotic regime.

2.2.2. Random-plane-wave model. As far as spectral statistics are concerned, and when energy scales much shorter than the Thouless energy are considered, the random-matrix models have been shown to be extremely reliable. The situation is however more ambiguous when one considers wave-function statistics. On the one hand, some

[4] The parameters $(a_{\beta_{\rm RMT}}, c_{\beta_{\rm RMT}})$ are equal to $(\pi/2, \pi/4)$ for $\beta_{\rm RMT} = 1$, $(32/\pi^2, 4/\pi)$ for $\beta_{\rm RMT} = 2$ and $(2^{18}/3^6\pi^3, 64/9\pi)$ for $\beta_{\rm RMT} = 4$ (see, e.g. appendix A of Bohigas (1991)).

properties, such as the Porter–Thomas characteristic (Brody *et al* 1981)

$$P(u = |\varphi_n(\boldsymbol{r})|^2/\langle|\varphi|^2\rangle) = \exp(-u) \quad \text{GOE} \tag{2.33}$$

$$= \frac{1}{\sqrt{2\pi u}}\exp(-u/2) \quad \text{GUE} \tag{2.34}$$

of the fluctuations around the mean value $\langle|\varphi|^2\rangle$ of the eigenstates probability at a given position, are well observed in numerical calculations and can be derived straightforwardly from a random matrix description. On the other hand, some other wave-function statistics clearly cannot be addressed within a simple random-matrix model. Consider, for instance, a billiard-like quantum dot, which is therefore characterized by a constant (in space) Fermi wave-vector k_F. Wave-function correlations are then characterized by a length scale $\lambda_F = 2\pi/k_F$, which is clearly absent in the random-matrix description.

To introduce this scale in the wave-function statistics let us consider, for an arbitrary wave-function $\varphi(\boldsymbol{r})$, its Wigner transform defined as

$$[\varphi]_W(\boldsymbol{r},\boldsymbol{p}) \stackrel{\text{def}}{=} \int \mathrm{d}\boldsymbol{x}\exp(-\mathrm{i}\boldsymbol{p}\boldsymbol{x}/\hbar)\varphi^*(\boldsymbol{r}+\boldsymbol{x}/2)\varphi(\boldsymbol{r}-\boldsymbol{x}/2). \tag{2.35}$$

The normalization of the wave-function implies $(2\pi\hbar)^{-d}\int \mathrm{d}\boldsymbol{r}\,\mathrm{d}\boldsymbol{p}[\varphi_n]_W = 1$. If φ is an eigenstate with energy ϵ, it can be shown (Berry 1977, Voros 1979) that for chaotic systems $[\varphi]_W(\boldsymbol{r},\boldsymbol{p})$ converges in probability in the semiclassical limit towards the micro-canonical distribution

$$\mu_{mc}(\boldsymbol{r},\boldsymbol{p}) = \rho_0^{-1}\delta(\epsilon_n - H(\boldsymbol{r},\boldsymbol{p})). \tag{2.36}$$

(ρ_0 is the Weyl density of states (2.13).) Definition (2.35) can be inverted into

$$\varphi^*(\boldsymbol{r})\varphi(\boldsymbol{r}') = \frac{1}{(2\pi\hbar)^d}\int \mathrm{d}\boldsymbol{p}\exp(\mathrm{i}\boldsymbol{p}\cdot(\boldsymbol{r}-\boldsymbol{r}')/\hbar)[\varphi]_W(\boldsymbol{r},\boldsymbol{p}). \tag{2.37}$$

Replacing on average $[\varphi]_W$ by μ_{mc} one immediately obtains an explicit expression for the two-point correlation function $\langle\varphi^*(\boldsymbol{r})\varphi(\boldsymbol{r}')\rangle$. For instance, for the usual kinetic plus potential Hamiltonian $H = \boldsymbol{p}^2/2m + U(\boldsymbol{r})$ and for a distance short enough such that the variation of the potential (and therefore of $k(\boldsymbol{r})$) can be neglected

$$\langle\varphi^*(\boldsymbol{r})\varphi(\boldsymbol{r}')\rangle = \frac{\nu_0(\boldsymbol{r})}{\rho_0}\int_0^{2\pi}\frac{\mathrm{d}\theta}{2\pi}\exp(\mathrm{i}k|\boldsymbol{r}-\boldsymbol{r}'|\cos(\theta))$$

$$= \frac{\nu_0(\boldsymbol{r})}{\rho_0}J_0(k|\boldsymbol{r}-\boldsymbol{r}'|) \qquad (d=2), \tag{2.38a}$$

$$\langle\varphi^*(\boldsymbol{r})\varphi(\boldsymbol{r}')\rangle = \frac{\nu_0(\boldsymbol{r})}{\rho_0}\int_0^{+\pi}\frac{\sin\theta\mathrm{d}\theta}{2}\exp(\mathrm{i}k|\boldsymbol{r}-\boldsymbol{r}'|\cos\theta)$$

$$= \frac{\nu_0(\boldsymbol{r})}{\rho_0}\frac{\sin(k|\boldsymbol{r}-\boldsymbol{r}'|)}{(k|\boldsymbol{r}-\boldsymbol{r}'|)} \qquad (d=3). \tag{2.38b}$$

This equation is obviously valid only for $|\boldsymbol{r}-\boldsymbol{r}'| \ll L$, with L the typical size of the system.

More generally, (2.37) with the notion that on average $[\varphi]_W(\boldsymbol{r},\boldsymbol{p}) = \mu_{mc}(\boldsymbol{r},\boldsymbol{p})$ makes it natural to model the statistical properties of an eigenstate φ_i close (on the scale of L) to some point $\boldsymbol{r}$, by a superposition of a large number M of plane waves

$$\varphi_i(\boldsymbol{r}') = \sum_{\mu=1,M} a_{i\mu}\exp(\mathrm{i}\boldsymbol{p}_\mu\cdot(\boldsymbol{r}'-\boldsymbol{r})/\hbar), \tag{2.39}$$

where $\boldsymbol{p}_\mu$ are uniformly distributed with the probability $\delta(\epsilon_n - H(\boldsymbol{r},\boldsymbol{p}))$ and, for time-reversal non-invariant systems, a_i are complex random numbers such that

$$\langle a_{i\mu}a^*_{i'\mu'}\rangle = \frac{1}{M}\frac{\nu_0(\boldsymbol{r})}{\rho_0}\delta_{ii'}\delta_{\mu\mu'}. \tag{2.40}$$

Time-reversal invariance can be taken into account by having $2M$ plane waves ($\mu = \pm1,\ldots,\pm M$) with $\boldsymbol{p}_{-\mu} = -\boldsymbol{p}_\mu$, $a_{-\mu} = a^*_\mu$, and $\langle a_{i\mu}a^*_{i'\mu'}\rangle = (\nu_0(\boldsymbol{r})/2\rho_0 M)\delta_{ii'}\delta_{|\mu||\mu'|}$.

I shall for instance use this approach in section 6 to include the residual interactions into the fluctuations of Coulomb-blockade peak spacings. In that case, the leading-order terms in an expansion in $1/g$, where $g = E_{Th}/\Delta$ is the dimensionless conductance, can be derived straightforwardly from the model (2.39)–(2.40), supplemented only, following a kind of 'minimum information hypothesis', by the assumption that $a_{i\mu}$ form a Gaussian vector.

Sub-leading terms are however 'aware' of the finiteness of the system. One then needs to further modify the description of the wave-function fluctuations so that it also includes the typical scale L of the system under consideration. A simple way to do this is to use only plane waves fulfilling the quantization condition

$$\boldsymbol{p}_\mu = 2\pi\hbar\boldsymbol{n}_\mu/L \tag{2.41}$$

with the set of integers $\boldsymbol{n}_\mu = (n_1,\ldots,n_d)$. While doing so, one needs to give a width $\simeq \hbar/L$ to the Fermi surface and to include in the modelling of the eigenstates all the plane waves with the kinetic energy in a band $\delta\epsilon = \alpha E_{Th}$ around the Fermi energy, with α a constant of order one. For the $M = \alpha g$ basis vector in this shell, one can then use a random-matrix description. To leading order in $1/M$, the eigenstates ϕ_i then fulfil (2.39)–(2.40), as well as the Gaussian character of the coefficient $a_{i\mu}$, but some correlations of order $1/M$ are induced by orthonormalization constraints (Brody *et al* 1981). More importantly however, the width $\delta p \sim \hbar/L$ of the Fermi surface modifies the wave-function correlations at distances of order L (for instance, the two-point correlation function decreases more rapidly than what is expressed by (2.38*a*) and (2.38*b*)). Time-reversal symmetry can here be taken into account using a real basis ($(\cos(\boldsymbol{p}_\mu\cdot\boldsymbol{r}), \sin(\boldsymbol{p}_\mu\cdot\boldsymbol{r}))$ instead of $(\exp(\pm\mathrm{i}\boldsymbol{p}_\mu\cdot\boldsymbol{r}))$ and a GOE matrix.

This model, which is defined both by the choice of the basis vectors and by the use of random matrices, is what I will refer to as the random-plane-wave (RPW) model. It has to be borne in mind that this is a model, justified by physical considerations, but that should be in principle validated by comparing the fluctuations derived within this model with those obtained for the eigenfunctions of actual chaotic systems such as quantum billiards (see for instance in this respect McDonald and Kaufman (1988), Kudrolli *et al* (1995), Pradhan and Sridhar (2002), Urbina and

Richter (2003), Miller *et al* (2005)). In particular, relatively delicate questions concerning the normalization of the wavefunctions may be important for some statistical quantities, which then requires further modifications of the random-plane-wave model described above (Urbina and Richter 2004, 2007, Tomsovic *et al* 2007).

2.3. Screening of the Coulomb interaction in quantum dots

For a degenerate electron gas, the 'strength' of the Coulomb interaction

$$V_{\rm coul}(\boldsymbol{r}-\boldsymbol{r}') = \frac{e^2}{|\boldsymbol{r}-\boldsymbol{r}'|} \tag{2.42}$$

between particles is usually expressed in terms of the gas parameter $r_s = r_0^{(d)}/a_0$, where $a_0 \stackrel{\rm def}{=} \hbar^2/m_{\rm e}e^2$ is the $(3d)$ Bohr radius and $r_0^{(d)}$ is the radius of a d-dimensional sphere containing on average one particle. Expressing, for instance for $d = 2$ or 3, the density of particle $n_0^{(d)} \equiv (2\pi\hbar)^{-d} g_{\rm s} \int {\rm d}\boldsymbol{p}\Theta(\epsilon - \boldsymbol{p}^2/2m)$ as ($g_{\rm s} = 2$ is the spin degeneracy and Θ the Heaviside function)

$$n_0^{(2)} \stackrel{\rm def}{=} \frac{1}{\pi r_0^{(2)}} = \frac{g_{\rm s}k_{\rm F}^2}{4\pi}, \tag{2.43}$$

$$n_0^{(3)} \stackrel{\rm def}{=} \frac{1}{\frac{4}{3}\pi r_0^{(3)}} = \frac{g_{\rm s}k_{\rm F}^3}{6\pi^2}, \tag{2.44}$$

we see that, up to a constant of order one, $r_0^{(d)}$ is essentially the inverse of the Fermi wave-vector $k_{\rm F}$. As a consequence, r_s is, again up to a constant of order one, proportional to the ratio $(e^2/r_0^{(d)})/(\hbar^2k_{\rm F}^2/2m_{\rm e})$ of the Coulomb energy between two electrons at the typical inter-particle distance and the kinetic energy. The parameter r_s therefore actually measures the relative strength of the Coulomb interaction.

Even for small r_s, $V_{\rm coul}(\boldsymbol{r}-\boldsymbol{r}')$ is long ranged and for this reason large, in the sense that it cannot be taken into account by a low-order expansion. When physical properties are considered at an energy scale much smaller than the Fermi energy, it is however known (and well understood) that, for bulk systems, this interaction is renormalized because of screening into a much weaker effective interaction $V_{\rm sc}(\boldsymbol{r}-\boldsymbol{r}')$. Approximations for $V_{\rm sc}(\boldsymbol{r}-\boldsymbol{r}')$ can be obtained using for instance the random phase approximation (RPA) (Fetter and Walecka 1971) giving in the zero-frequency low-momentum limit

$$V_{\rm sc}(\boldsymbol{r}) = \int \frac{{\rm d}\boldsymbol{q}}{(2\pi)^2}\hat{V}_{\rm sc}(\boldsymbol{q})\exp[{\rm i}\boldsymbol{q}\cdot\boldsymbol{r}], \tag{2.45}$$

$$\hat{V}_{\rm sc}(\boldsymbol{q}) = \frac{2\pi e^2}{|\boldsymbol{q}| + \kappa_{(2)}} \quad (d=2), \tag{2.46}$$

$$\hat{V}_{\rm sc}(\boldsymbol{q}) = \frac{4\pi e^2}{\boldsymbol{q}^2 + \kappa_{(3)}^2} \quad (d=3), \tag{2.47}$$

with $\kappa_{(2)} = (2\pi e^2)(g_{\rm s}\nu_0^{(2)})$ and $\kappa_{(3)}^2 = (4\pi e^2)(g_{\rm s}\nu_0^{(3)})$ the screening wave vectors[5]. One way to understand the screening mechanism is to view it in the spirit of the renormalization-group approach, where the effective Coulomb interaction that should be used for low-energy processes is produced by the integration of the 'fast modes' (high-energy degrees of freedom) of the electron gas (Shankar 1994).

For finite systems, the situation is slightly more complicated because the renormalization process which transforms the bare interaction (2.42) into the screened one (2.46) or (2.47) also produces a mean-field potential $U_{\rm mf}(\boldsymbol{r})$ which modifies the one-particle part of the electron's Hamiltonian. Since both processes (screening and creation of the mean-field potential) take place at the same time, their interplay is *a priori* not completely obvious.

In the semiclassical limit, and more precisely whenever the screening length κ^{-1} is much smaller than the typical size L of the system, the common wisdom—that I shall follow here whenever necessary—is however simply to state that since the characteristic scales of variation of $V_{\rm sc}$ and of $U_{\rm mf}$ are parametrically different (the former κ^{-1} is a quantum scale, when the latter L is classical), one could nevertheless use the same screened interaction as for the bulk and furthermore assume that $U_{\rm mf}(\boldsymbol{r})$ is correctly approximated by a Thomas–Fermi approximation. This latter amounts to minimizing, with a fixed number of particles, the density functional

$$\mathcal{F}_{\rm TF}[n] = \mathcal{T}_{\rm TF}[n] + \mathcal{E}_{\rm ext}[n] + \mathcal{E}_{\rm coul}[n], \tag{2.48}$$

where

$$\mathcal{E}_{\rm coul}[n] = \frac{e^2}{2}\int {\rm d}\boldsymbol{r}\,{\rm d}\boldsymbol{r}'\frac{n(\boldsymbol{r})n(\boldsymbol{r}')}{|\boldsymbol{r}-\boldsymbol{r}'|},$$

$$\mathcal{E}_{\rm ext}[n] = \int {\rm d}\boldsymbol{r}U_{\rm ext}(\boldsymbol{r})n(\boldsymbol{r})$$

($U_{\rm ext}(\boldsymbol{r})$ is the external confining potential) and the kinetic energy term, originating from the Pauli exclusion principle, is given by

$$\mathcal{T}_{\rm TF}[n] \equiv \int {\rm d}\boldsymbol{r}\,t_{\rm TF}(n(\boldsymbol{r})),$$

$$t_{\rm TF}(n) \equiv \int_0^n {\rm d}n'\,{\rm e}(n'), \tag{2.49}$$

with ${\rm e}(n)$ the inverse of the function $n({\rm e})$ defined as

$$n({\rm e}) \equiv g_{\rm s}\int \frac{{\rm d}\boldsymbol{p}}{(2\pi\hbar)^d}\Theta({\rm e} - \boldsymbol{p}^2/2m_{\rm e}). \tag{2.50}$$

In particular ${\rm e}(n) = (\hbar^2/2m_{\rm e})(4\pi n/g_{\rm s})^2$ for $d = 2$ and ${\rm e}(n) = (\hbar^2/2m_{\rm e})(6\pi^2 n/g_{\rm s})^{2/3}$ for $d = 3$.

The self-consistent equations obtained by minimizing the Thomas–Fermi functional then read

$$U_{\rm mf}(\boldsymbol{r}) = U_{\rm ext}(\boldsymbol{r}) + \int {\rm d}\boldsymbol{r}'n(\boldsymbol{r}')V_{\rm coul}(\boldsymbol{r},\boldsymbol{r}'), \tag{2.51}$$

$$n(\boldsymbol{r}) = \int \frac{{\rm d}\boldsymbol{p}}{(2\pi\hbar)^d}\Theta(\mu - U_{\rm mf}(\boldsymbol{r}) - \boldsymbol{p}^2/2m_{\rm e}). \tag{2.52}$$

Note, however, that currently there is no general microscopic derivation of the above picture. More precisely, our confidence in having the Thomas–Fermi approximation as a correct starting point for the computation of $U_{\rm mf}$ is due to the fact that this approximation can be derived in a

[5] Equations (2.46) and (2.47) are actually the expression of the screened interaction in the Thomas–Fermi approximation. To avoid confusion with the Thomas–Fermi approximation for the mean-field potential, I will nevertheless refer to them, although slightly improperly, as the RPA-screened interaction.

quite general framework starting from a density functional description (in, e.g. the local density approximation) and neglecting the effect of interferences (Ullmo *et al* 2001, 2004). The 'common wisdom' prescription given above therefore essentially amounts to trusting the density functional approach on the classical scale L (although it might be less reliable on the quantum scale λ_F ; cf for instance the discussion in Ullmo *et al* (2004)), keeping the usual (bulk) form of the screened interaction on the quantum scale and assuming that the two scales are not going to interfere in any significant way. That there is no microscopic derivation of this 'common wisdom' prescription is presumably not too much of an issue as far as qualitative or statistical descriptions are concerned, but might become a limitation when accurate simulation tools are required to quantitatively describe the particular behaviour of a specific mesoscopic system.

In this respect, one should note that there is a class of systems (namely billiards with weak disorder) for which it is possible to perform a renormalization procedure (Blanter *et al* 1997, Aleiner *et al* 2002) where the fast modes are integrated out so that only the interesting low-energy physics remains. It is then possible to see how both the mean field and the screened interaction emerge from this procedure. The generalization to a more general case, for which $U_{\rm mf}(\boldsymbol{r})$ is not well approximated by a constant, is however not completely straightforward and is still an open problem. A relatively extensive discussion of this question is given in appendix A.

3. Orbital magnetism: general formalism

As a first illustration of physical systems where the interrelation between interference effects and interactions plays a fundamental role, we shall consider in this section the orbital part—in opposition to the Zeeman part, associated with the coupling of the magnetic field to the spin degrees of freedom—of the magnetic response at finite temperature $k_{\rm B}T = \beta^{-1}$ of mesoscopic objects in the ballistic or the diffusive regime.

Since the Bohr–van Leeuwen theorem (Leeuwen 1921), it has been known that the magnetic response of a system of classical charged particles is exactly zero. This is a simple consequence of the fact that when writing the classical partition function $Z_{\rm cl} = \int {\rm d}\boldsymbol{p}\,{\rm d}\boldsymbol{r}\exp(-\beta H_{\rm cl}(\boldsymbol{r},\boldsymbol{p}))$ with $H_{\rm cl}(\boldsymbol{r},\boldsymbol{p}) = (\boldsymbol{p} - e\boldsymbol{A}(\boldsymbol{r}))^2/2m + U(\boldsymbol{r})$, the vector potential $\boldsymbol{A}(\boldsymbol{r})$, and thus any dependence in the magnetic field, can be eliminated by a change in the origin of $\boldsymbol{p}$ in the integral over momentum. The same holds true for the Weyl density of states since, up to an irrelevant multiplicative constant, it is derived from $Z_{\rm cl}$ by an inverse Laplace transform. As a consequence, whatever is measured has to be related to quantum effects[6], and, in the case of bounded fully coherent systems such as disordered systems, more specifically interference effects.

In the early nineties, progress made in the design and probe of micrometre scale electronic systems, such as small metallic grains or quantum dots patterned in semiconductor hetero-structures, made it technically feasible to measure the magnetic response of coherent electronic structures. As orbital magnetism is a particularly well-adapted probe of interference effects in these coherent structures, this motivated a series of experimental works for (disordered/diffusive) metallic grains (Lévy *et al* 1990, Chandrasekhar *et al* 1991) as well as, slightly later, ballistic quantum dots (Lévy *et al* 1993, Mailly *et al* 1993).

All these experiments were able to give convincing evidence—in particular the magnetic field scale—that the measured magnetic response was indeed related to quantum interferences. Moreover it was relatively soon realized that although the magnetic response of a single ring or dot can be dominated by terms for which the interactions are irrelevant, the dominant non-interacting contribution to the magnetic response varied very rapidly with the size or chemical potential of the system. As a consequence, after averaging, the mean response of an ensemble of micro-structures is, most probably, driven by the contribution of the interactions. In other words, the magnetic response of ensembles of coherent electronic micro-structures is due to the interplay between interference effects and interactions.

I stress however that 'most probably' is the best that could be said here. Indeed, after the first series of experiments (Lévy *et al* 1990, Chandrasekhar *et al* 1991, Lévy *et al* 1993, Mailly *et al* 1993), which has sparked a host of theoretical works[7], enough puzzles remain to indicate that a full understanding of the experimental data is lacking. I shall come back in more detail to this point at the end of section 4. It should be borne in mind however that what follows should not be understood as the final 'theory' of orbital magnetism in mesoscopic systems, but merely as the predictions that can be obtained for the equilibrium properties within a perturbative/Fermi-liquid description.

In practice, I shall therefore consider a model of particles confined by some potential $U(\boldsymbol{r})$, which is already assumed to contain the smooth part of the Coulomb interaction within some self-consistent scheme, interacting through the (residual) screened interaction (2.45), and subject either to a uniform magnetic field $\boldsymbol{B}$ or, in the case of a ring, to a flux line Φ. Spin will be included only as a degeneracy factor (i.e. Zeeman coupling will not be considered). I shall furthermore limit the discussion to two-dimensional systems, but no drastically new effect is expected for $d = 3$.

Within the grand canonical formalism, our goal will be to compute perturbatively in the interactions the field dependent part of the grand potential

$$\Omega = -\frac{1}{\beta}\ln Z_{\rm G.C} \tag{3.1}$$

with $Z_{\rm G.C} = {\rm Tr}\exp(-\beta(\hat{H} - \mu\hat{N}))$ the grand canonical partition function and from there, for instance in the uniform

[6] For instance, as discussed in Richter *et al* (1996b), the Landau diamagnetism can be understood as originating from quantum corrections to the Weyl term in the smooth density of states.

[7] See for instance Bouchiat and Montambaux (1989), Ambegaokar and Eckern (1990a, 1990b), Eckern (1991), Oh *et al* (1991), Schmid (1991), von Oppen and Reidel (1991, 1993), Argaman *et al* (1993), Gefen *et al* (1994), von Oppen (1994), Ullmo *et al* (1995, 1997, 1998), Montambaux (1996), Richter *et al* (1996b, 1996c) and von Oppen *et al* (2000).

field case, the magnetization

$$\langle \hat{M}_z \rangle = -\frac{\partial \Omega}{\partial B_z} \tag{3.2}$$

(for completeness, equation (3.2), as well as its analogue (4.26) for persistent current, is re-derived briefly in appendix B) or the susceptibility

$$\chi = \frac{1}{\mathcal{A}} \left(\frac{\partial \langle \hat{M}_z \rangle}{\partial B} \right)_{\mathrm{T},\mu} \tag{3.3}$$

($\mathcal{A}$ is the area of the micro-structure).

In the bulk, and more precisely when the cyclotron radius is larger than the coherence length L_ϕ or the thermal length L_T (to be defined more precisely below), the magnetic response is given by the (diamagnetic) Landau susceptibility $\chi_\mathrm{L} = -g_\mathrm{s} e^2/24\pi m_\mathrm{e}$. The latter originates from higher order in $\hbar$ corrections to the Weyl (smooth) density of states (Kubo 1964, Prado *et al* 1994) (see also the discussion in section 3 of Richter *et al* (1996b)), and I will use it below as the reference scale for the susceptibility.

3.1. First order perturbations.

As mentioned in section 2.3, the effective strength of the screened interaction is related to the parameter r_s characterizing the density of the electron gas. In most experimentally relevant cases, r_s is of order one and the high-density expansion is just a convenient way to order the various contributions, but some re-summation of a series of higher-order diagrams is necessary in order to get an accurate result. On the other hand, it is interesting and pedagogical to start with the genuine high-density asymptotics of small r_s. Then, provided the momenta involved are of the order of the Fermi momentum p_F (which will be the case, except for the notable exception of *periodic* orbits, see discussion below) $\hat{V}_\mathrm{sc}(q)$ will be of order r_s/ν_0 and the diagrammatic development of the thermodynamic potential is indeed a development in r_s. In that case we are interested in the first order (or Hartree–Fock) correction in the screened interaction, which can be evaluated without drawing any Feynman diagram.

3.1.1. First order perturbations. Working in the grand canonical ensemble at temperature $k_\mathrm{B}T = \beta^{-1}$, one can express the first correction to the thermodynamic potential as a direct (Hartree) plus an exchange (Fock) contribution in terms of the eigenfunctions φ_u and eigenenergies ϵ_u of the non-interacting problem (Fetter and Walecka 1971),

$$\begin{aligned}\Delta\Omega^{(1)} &= g_\mathrm{s}^2 \mathcal{H} - g_\mathrm{s} \mathcal{F} \\ &= \frac{1}{2} \sum_{u,v} f_u f_v [g_\mathrm{s}^2 \langle \varphi_u \varphi_v | V | \varphi_u \varphi_v \rangle - g_\mathrm{s} \langle \varphi_u \varphi_v | V | \varphi_v \varphi_u \rangle],\end{aligned} \tag{3.4}$$

with $f_v = f(\epsilon_v - \mu) = [1 + \exp[\beta(\epsilon_v - \mu)]]^{-1}$ the Fermi occupation factor. For sake of clarity, the spin degeneracy factor $g_\mathrm{s} = 2$ is made explicit.

Introducing

$$\begin{aligned}n(\boldsymbol{r}, \boldsymbol{r}') &\equiv \sum_v f_v \langle \boldsymbol{r}' | \varphi_v \rangle \langle \varphi_v | \boldsymbol{r} \rangle \\ &= -\frac{1}{2\mathrm{i}\pi} \int \mathrm{d}\epsilon f(\epsilon - \mu) [G^R(\boldsymbol{r}, \boldsymbol{r}'; \epsilon) - G^A(\boldsymbol{r}, \boldsymbol{r}'; \epsilon)],\end{aligned} \tag{3.5}$$

($n(\boldsymbol{r}) \equiv n(\boldsymbol{r}, \boldsymbol{r})$ is the local electron density in the non-interacting problem), one can re-express the direct and indirect contributions as

$$\mathcal{H} = \frac{1}{2} \int \mathrm{d}\boldsymbol{r}\, \mathrm{d}\boldsymbol{r}' n(\boldsymbol{r}) V(\boldsymbol{r} - \boldsymbol{r}') n(\boldsymbol{r}'), \tag{3.6a}$$

$$\mathcal{F} = \frac{1}{2} \int \mathrm{d}\boldsymbol{r}\, \mathrm{d}\boldsymbol{r}' n(\boldsymbol{r}, \boldsymbol{r}') V(\boldsymbol{r} - \boldsymbol{r}') n(\boldsymbol{r}', \boldsymbol{r}). \tag{3.6b}$$

As discussed in section 2.1, $G^R(\boldsymbol{r}, \boldsymbol{r}'; \epsilon)$ can be semiclassically approximated as a sum over classical trajectories travelling from $\boldsymbol{r}'$ to $\boldsymbol{r}$ at energy ϵ. The advanced Green's function can be written in terms of the retarded one as

$$G^A(\boldsymbol{r}, \boldsymbol{r}'; \epsilon) = [G^R(\boldsymbol{r}', \boldsymbol{r}; \epsilon^*)]^* \tag{3.7}$$

and can therefore be interpreted as a sum running over all the trajectories going backward in time from $\boldsymbol{r}$ to $\boldsymbol{r}'$.

Using equation (2.7) which relates the variation in energy of the action with the time of travel t_j of the trajectory j, we understand the integral in (3.5) as the convolution between a function oscillating with a period $2\pi\hbar/t_j$ and the Fermi function which varies from one to zero on a scale $\beta^{-1} = k_\mathrm{B}T$. Introducing the characteristic time (or length) associated with temperature

$$t_\mathrm{T} = \frac{L_\mathrm{T}}{v_\mathrm{F}} = \frac{\hbar\beta}{\pi}, \tag{3.8}$$

(v_F is the Fermi velocity), we see that the contribution of a trajectory j will be exponentially damped as soon as $t_j \gg t_\mathrm{T}$. More precisely (see for instance appendix A of Richter *et al* (1996b)), if G_j^R is the contribution of the trajectory j to the sum (2.3), one has

$$\int \mathrm{d}\epsilon f(\epsilon - \mu) G_j^R(\boldsymbol{r}, \boldsymbol{r}') = \left(-\frac{\mathrm{i}\hbar}{t_j} R(t_j/t_\mathrm{T}) G_j^R(\boldsymbol{r}, \boldsymbol{r}') \right), \tag{3.9}$$

with $R(x) \stackrel{\mathrm{def}}{=} x/\sinh(x)$. To proceed in the evaluation of equations (3.6*a*) and (3.6*b*), let us introduce the coordinates $\bar{\boldsymbol{r}} = (\boldsymbol{r} + \boldsymbol{r}')/2$ and $\delta\boldsymbol{r} = (\boldsymbol{r} - \boldsymbol{r}')$. Since the interaction between electrons is taken to be short ranged, one can assume the relevant $\delta\boldsymbol{r}$ to be small and, using $(\partial S_j/\partial \boldsymbol{r}') = \boldsymbol{p}_j^\mathrm{f}$, $(\partial S_j/\partial \boldsymbol{r}) = -\boldsymbol{p}_j^\mathrm{i}$, with $\boldsymbol{p}_j^\mathrm{i}, \boldsymbol{p}_j^\mathrm{f}$ the initial and final momenta of the trajectory j, one can approximate

$$\begin{aligned}&G_j^R(\bar{\boldsymbol{r}} \pm \delta\boldsymbol{r}/2, \bar{\boldsymbol{r}} \pm \delta\boldsymbol{r}'/2) \\ &\quad = G_j^R(\bar{\boldsymbol{r}}, \bar{\boldsymbol{r}}) \exp\left[\frac{\mathrm{i}}{2\hbar} (\pm \boldsymbol{p}_j^\mathrm{f} \cdot \delta\boldsymbol{r}' \mp \boldsymbol{p}_j^\mathrm{i} \cdot \delta\boldsymbol{r}) \right].\end{aligned} \tag{3.10}$$

The integral over $\delta\boldsymbol{r}$ therefore yields the Fourier transform of $V_\mathrm{sc}(\boldsymbol{r} - \boldsymbol{r}')$ and, neglecting the terms $G^A G^A$ and $G^R G^R$ which will eventually average to zero, one can semiclassically express

the first order correction to the thermodynamic potential as a sum over all pairs (k,l) of *closed* orbits

$$\mathcal{H}=\frac{1}{(2\pi)^3\hbar}\times\int \mathrm{d}\boldsymbol{r}\sum_{kl} Q_k Q_l \cos(\psi_k-\psi_l)\hat{V}_{\mathrm{sc}}((\boldsymbol{p}_k^{\mathrm{f}}-\boldsymbol{p}_k^{\mathrm{i}}+\boldsymbol{p}_l^{\mathrm{f}}-\boldsymbol{p}_l^{\mathrm{i}})/2\hbar), \tag{3.11a}$$

$$\mathcal{F}=\frac{1}{(2\pi)^3\hbar}\times\int \mathrm{d}\boldsymbol{r}\sum_{kl} Q_k Q_l \cos(\psi_k-\psi_l)\hat{V}_{\mathrm{sc}}((\boldsymbol{p}_k^{\mathrm{f}}-\boldsymbol{p}_k^{\mathrm{i}}+\boldsymbol{p}_l^{\mathrm{f}}-\boldsymbol{p}_l^{\mathrm{i}})/2\hbar), \tag{3.11b}$$

where $Q_j = R(t_j/t_{\mathrm{T}})D_j/t_j$ and $\psi_j = (S_k/\hbar-\zeta_j\pi/2)$. The field dependence of the above expression can then be obtained from (cf (2.22))

$$\frac{\partial S_j}{\partial B} = 2\pi \mathrm{a}_j/\phi_0, \tag{3.12}$$

with a_j the area enclosed by the orbit j.

For a generic pair of trajectories (k,l) the term $\cos[(S_k \pm S_l)/\hbar]$ will be a highly oscillating function of the coordinate $\boldsymbol{r}$. Performing the integration over position, the stationary phase condition reads $(\boldsymbol{p}_k^{\mathrm{f}}-\boldsymbol{p}_k^{\mathrm{i}})\pm(\boldsymbol{p}_l^{\mathrm{f}}-\boldsymbol{p}_l^{\mathrm{i}})=0$, and unless k and l are related by a symmetry, this will correspond to isolated points, each of which yields a contribution $\hbar^{1/2}$ smaller than the original prefactor. On the other hand, special pairings where $S_k = S_l$ will kill the oscillating phase. Such a condition is trivially satisfied when $k=l$ but this also kills any field dependence. A second possibility is to pair a given trajectory with its time reversed. This is a non-trivial pairing since the resulting term is field dependent. Keeping only these contributions the direct and exchange terms can be written as

$$\mathcal{H}_{(D)} = \frac{1}{(2\pi)^3\hbar}\int \mathrm{d}\boldsymbol{r}\sum_j \left(\frac{\hbar R(t_j/t_{\mathrm{T}})}{t_j}\right)^2 |D_j|^2 \times \cos\left(\frac{4\pi \mathrm{a}_j B}{\phi_0}\right)\hat{V}_{\mathrm{sc}}\left(\frac{\boldsymbol{p}'_j-\boldsymbol{p}_j}{\hbar}\right), \tag{3.13a}$$

$$\mathcal{F}_{(D)} = \frac{1}{(2\pi)^3\hbar}\int \mathrm{d}\boldsymbol{r}\sum_j \left(\frac{\hbar R(t_j/t_{\mathrm{T}})}{t_j}\right)^2 |D_j|^2 \times \cos\left(\frac{4\pi \mathrm{a}_j B}{\phi_0}\right)\hat{V}_{\mathrm{sc}}\left(\frac{\boldsymbol{p}'_j+\boldsymbol{p}_j}{\hbar}\right), \tag{3.13b}$$

where the sub-index (D) indicates the *diagonal* approximation, with sums running over *individual* trajectories j (and not pairs as in (3.11*a*) and (3.11*b*)). A third possible pairing appears when we can match the actions of k and l, even if the trajectories are not the same or time reversed of each other. Such a situation arises in integrable systems with families of trajectories degenerate in action and is discussed in detail in Ullmo *et al* (1998).

3.1.2. The high-density limit. The sums in equations (3.13*a*) and (3.13*b*) run over all *closed* (not necessarily periodic) trajectories (more precisely, we have twice the sum over all time-reversed pairs). Therefore *a priori*, and in contrast to non-interacting theory, periodic orbits do not play any particular role. It is interesting to note however that if the high-density limit is to be taken seriously (i.e. $r_s \to 0$), then again periodic orbits are singled out. Indeed, in this case $\hat{V}_{\mathrm{sc}}((\boldsymbol{p}'_j-\boldsymbol{p}_j)/\hbar)$ is of order $r_s\nu_0^{-1}$ except when $\boldsymbol{p}'_j-\boldsymbol{p}_j=0$, that is when the orbit is periodic, in which case $\hat{V}_{\mathrm{sc}}(0)=\nu_0^{-1}$. Note that $\boldsymbol{p}'_j+\boldsymbol{p}_j=0$ implies that the trajectory j is self-retracing and thus has a zero enclosed area. As a consequence for the exchange term all contributions to the magnetic response are of order r_s.

Therefore in the high-density limit, the integrand in (3.13*a*) is significantly larger in the neighbourhood of periodic orbits. For chaotic systems this will be compensated by the fact that these orbits are isolated. As a consequence the relative weight of their neighbourhood may depend on the particular system under consideration. For integrable systems however, for which periodic orbits come in families whose projection on the configuration space has a non-zero measure, the magnetic response induced by electron–electron interactions will be dominated by periodic orbits when $r_s \ll 1$ and will reach a finite limit as $r_s \to 0$.

3.2. Correlations effects

As discussed at the beginning of this section, realistic values of the parameter r_s (appropriate for metals or GaAs/AlGaAs hetero-structures) force us to consider high-order effects in the diagrammatic expansion of the thermodynamic potential. Therefore, correlation effects are important and need to be taken into account.

A value of $r_s \simeq 1$ means that the range of the screened potential is of the order of the Fermi wavelength. In other words, the screened interaction has a local character and can be written as

$$V(\boldsymbol{r}-\boldsymbol{r}') = \frac{\lambda_0}{g_{\mathrm{s}}\nu_0}\delta(\boldsymbol{r}-\boldsymbol{r}'), \tag{3.14}$$

where $g_{\mathrm{s}}\nu_0$ is the total density of states (i.e. including the spin degeneracy factor g_{s}) and λ_0 is a constant of order one that will also serve to label the order of perturbation.

The perturbative expansion of the thermodynamic potential can be represented in the usual way (cf for instance section 15 of Abrikosov *et al* (1963)) by Feynman diagrams, with straight lines standing for the finite temperature (Matsubara) Green's functions and the wavy lines for the interaction V. In the same way as in the theory of superconductivity, it turns out that it is essential to consider the full Cooper series whose associated diagrams are represented in figure 1 (Abrikosov *et al* 1963, Aslamazov and Larkin 1975). One way to see this is to realize that, since r_s is actually not a small parameter, what is done here is more a semiclassical expansion (i.e. in powers of $\hbar$) than one in the strength of the interaction. Therefore, one should perform a simple counting of the powers of $\hbar$ of such contributions. The Cooper diagram of order k implies k

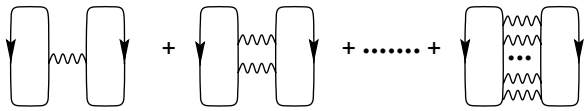

Figure 1. Direct terms of the Cooper series for the perturbative expansion of the thermodynamic potential Ω. Reprinted with permission from Ullmo *et al* 1998. Copyright 1998 by the American Physical Society.

interaction lines (each of which yields a factor ν_0^{-1}), k pairs of Green's functions and $(k+1)$ summations of Matsubara frequencies (each of them associated with a factor β^{-1}). As far as powers of $\hbar$ are concerned, $|G|^2 \sim \nu_0/\hbar$ (whatever the dimension). Therefore, the only delicate point here is to realize that each temperature factor β^{-1} should be accounted for as an $\hbar$, since in the mesoscopic regime considered here, the time $t_T = \hbar\beta/\pi$ introduced above should be of the order of some characteristic time t_c of the system (say the time of flight), and thus $\beta^{-1} \sim \hbar/t_c \propto \hbar$ (again as far as powers of $\hbar$ are concerned). The kth term of the Cooper series is therefore of order $[1/\nu_0]^k[\nu_0/\hbar]^k[\hbar]^{k+1} \sim \hbar$ and thus scales as $\hbar$ independently of k. The RPA series can be seen, in the same way, to be of order $\hbar$, but the corresponding terms turn out to have negligible magnetic field dependence and can therefore be omitted from the calculation of the magnetic response. Moreover one can convince oneself that all other diagrams would, at some given order k, have either a smaller number of Green's functions or a larger number of frequency summations and therefore are of higher order in $\hbar$.

Noting that, because interaction (3.14) is local, the direct and exchange Cooper diagrams differ only by their sign and by a spin degeneracy factor, the magnetic response can be derived from the Cooper series contribution to the thermodynamic potential[8]:

$$\Omega^C = \frac{g_s^2 - g_s}{2\beta} \times \sum_{k=1}^{\infty} \frac{\lambda_0^k}{k} \sum_{\omega_m<\epsilon_F} \int d\boldsymbol{r}_1 \ldots d\boldsymbol{r}_k \Sigma(\boldsymbol{r}_1,\boldsymbol{r}_k;\omega_m)\ldots\Sigma(\boldsymbol{r}_2,\boldsymbol{r}_1;\omega_m) = \frac{g_s^2 - g_s}{2\beta} \sum_{\omega_m<\epsilon_F} \mathrm{Tr}\{\ln[1+\lambda_0\Sigma(\boldsymbol{r},\boldsymbol{r}';\omega_m)]\}, \tag{3.15}$$

where $\omega_m = 2\pi m/\beta$ are (bosonic) Matsubara frequencies,

$$\Sigma(\boldsymbol{r},\boldsymbol{r}';\omega_m) = \frac{1}{\beta g_s \nu_0} \sum_{\epsilon_n<\epsilon_F} \mathcal{G}(\boldsymbol{r},\boldsymbol{r}';\epsilon_n)\mathcal{G}(\boldsymbol{r},\boldsymbol{r}';\omega_m-\epsilon_n) \tag{3.16}$$

is the (free) particle–particle propagator and the finite range $\sim \lambda_F$ of the interaction introduces a cutoff on the summation over Matsubara frequencies at the corresponding energy scale ϵ_F.

The trace over the space coordinates is a short way of expressing the expansion in all orders in $\lambda_0\Sigma$. The concept of the particle–particle propagator, as well as the Cooper series contribution, comes from the Cooper pairs in the theory of superconductivity. The main difference in our case is that now the interaction is repulsive (thus the plus sign in the trace) and that we have lost translational invariance (therefore we cannot trade the operators for ordinary functions by going to the momentum representation).

3.2.1. Semiclassical evaluation of the particle–particle propagator. To proceed further with our semiclassical formalism, it is useful to write the finite temperature Green's function between points $\boldsymbol{r}$ and $\boldsymbol{r}'$ for a fermionic Matsubara frequency (or rather energy) $\epsilon_n = (2n+1)\pi/\beta$ in terms of the retarded and advanced Green's functions as

$$\mathcal{G}(\boldsymbol{r},\boldsymbol{r}';\epsilon_n) = \Theta(\epsilon_n)G^R(\boldsymbol{r},\boldsymbol{r}';\epsilon_F+i\epsilon_n) + \Theta(-\epsilon_n)G^A(\boldsymbol{r},\boldsymbol{r}';\epsilon_F+i\epsilon_n), \tag{3.17}$$

with ϵ_F the Fermi energy. The retarded and advanced Green's functions are related through (3.7) and expressed, in a semiclassical approach, as expansions over all trajectories j joining $\boldsymbol{r}'$ and $\mathbf{r}$ at energy ϵ (see (2.3)). The complex energy-arguments of (3.17) force us to perform some analytic continuation. However, if the Matsubara energies are much smaller than ϵ_F, one can expand the classical action and use (2.7) to obtain

$$G_j^R(\boldsymbol{r},\boldsymbol{r}';\epsilon_F+i\epsilon_n) = G_j^R(\boldsymbol{r},\boldsymbol{r}';\epsilon_F)\times\exp\left[-\frac{\epsilon_n t_j}{\hbar}\right]. \tag{3.18}$$

Note that, as in (3.8), temperature introduces the time scale $t_T = \hbar\beta/\pi$ which exponentially suppresses the contributions of long paths through the term $\epsilon_n t_j/\hbar = (2n+1)t_j/t_T$. Therefore, only small Matsubara frequencies need to be considered, and the assumption used for the perturbative treatment of the energy is consistent.

To compute the magnetic susceptibility at $B=0$, the field dependent part of the semiclassical Green's function can also be treated perturbatively, and using (3.12) one can write

$$G_j^R(\boldsymbol{r},\boldsymbol{r}';\epsilon_F+i\epsilon_n;B) = G_j^R(\boldsymbol{r},\boldsymbol{r}';\epsilon_F;B=0) \times\exp\left[-\frac{\epsilon_n t_j}{\hbar}\right]\times\exp\left[i2\pi\frac{Ba_j}{\phi_0}\right], \tag{3.19}$$

where a_j is the effective area enclosed by the orbit (circulation of the vector potential between $\boldsymbol{r}'$ and $\boldsymbol{r}$) and ϕ_0 the flux quantum. The weak-field semiclassical approximation to (3.17) is then given by

$$\mathcal{G}(\boldsymbol{r},\boldsymbol{r}';\epsilon_n,B) = \theta(\epsilon_n)\sum_{j:\boldsymbol{r}'\to\boldsymbol{r}}\frac{D_j}{\sqrt{-2i\pi\hbar^3}}e^{iS_j/\hbar-i\pi\zeta_j/2} \times\exp\left[-\frac{\epsilon_n t_j}{\hbar}\right]\times\exp\left[i2\pi\frac{Ba_j}{\phi_0}\right] + \theta(-\epsilon_n)\sum_{j':\boldsymbol{r}\to\boldsymbol{r}'}\frac{D_{j'}}{\sqrt{-2i\pi\hbar^3}}e^{-iS_{j'}/\hbar+i\pi\zeta_{j'}/2} \times\exp\left[\frac{\epsilon_n t_{j'}}{\hbar}\right]\times\exp\left[-i2\pi\frac{Ba_{j'}}{\phi_0}\right], \tag{3.20}$$

where trajectories j and j' travel from $\boldsymbol{r}'$ to $\boldsymbol{r}$ in opposite directions, at energy ϵ_F, and in the absence of a magnetic field.

Note the usefulness of (3.20) goes beyond the problem of orbital magnetism discussed here, as it provides a calculational

[8] Note that the diagrammatic rules for Ω differ slightly from the ones for correlation functions. There is in particular a factor $1/k$ associated with each term of order k, thus the log.

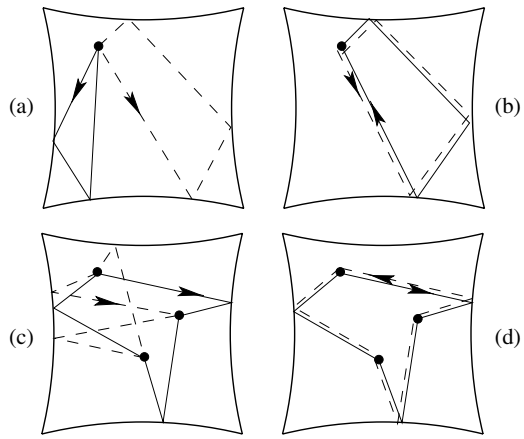

Figure 2. Pairs of orbits contributing to Ω^{C} (see (3.15) for a (non-integrable) billiard. Top row: first order contributions. Bottom row: third order contributions (there are therefore three pairs of orbits connected at interaction points in both (c) and (d)). Left column: generic case. Right column: pairing of time-reversed trajectories (diagonal contribution), for which the dynamical phases cancel. (Courtesy of Harold Baranger.)

approach to any perturbative problem where the single-particle classical dynamics is known.

The particle–particle propagator $\Sigma(\boldsymbol{r},\boldsymbol{r}';\omega_m)$ can now be evaluated semiclassically from (3.20) and (3.16). In general this involves a sum over all pairs of classical trajectories joining $\boldsymbol{r}'$ to $\boldsymbol{r}$. An illustration is shown in figure 2. As in section 3.1, however, most of these pairs yield highly oscillating contributions which average to zero when integrated over position, and one should only consider the non-oscillating terms which maintain a field dependence. One way to do this is, again, to pair time-reversed trajectories, which implies that in the sum over the fermionic Matsubara frequencies in (3.16), only the ϵ_n such that $\epsilon_n(\omega_m-\epsilon_n)<0$ should be kept. This diagonal part $\Sigma^{(D)}$ of the particle–particle propagator can then be written as

$$\Sigma^{(D)}(\boldsymbol{r},\boldsymbol{r}';\omega_m)\simeq\frac{k_{\mathrm{B}}T}{g_{\mathrm{s}}\hbar}\sum_{j:\boldsymbol{r}\to\boldsymbol{r}'}\frac{|D_j|^2}{m_{\mathrm{e}}}\exp\left[\mathrm{i}4\pi\frac{Ba_j}{\phi_0}\right]\times\sum_{\epsilon_n(\omega_m-\epsilon_n)<0}^{\epsilon_n<\epsilon_{\mathrm{F}}}\exp\left[-\frac{(|\epsilon_n|+|\omega_m-\epsilon_n|)t_j}{\hbar}\right]. \tag{3.21}$$

Summing over ϵ_n in the contribution of trajectory j, one gets

$$\sum_{\epsilon_n(\omega_m-\epsilon_n)<0}^{\epsilon_n<\epsilon_{\mathrm{F}}}\exp\left[-\frac{(|\epsilon_n|+|\omega_m-\epsilon_n|)t_j}{\hbar}\right]=\exp\left[-\frac{\omega_m t_j}{\hbar}\right]\frac{R(2t_j/t_{\mathrm{T}})}{2t_j/t_{\mathrm{T}}}\left(1-\exp\left[-\frac{(\epsilon_{\mathrm{F}}-\omega_m)t}{\hbar}\right]\right), \tag{3.22}$$

where the function R and the temperature time t_{T} were introduced in the discussion of (3.9). The last factor $(1-\exp[-(\epsilon_{\mathrm{F}}-\omega_m)t/\hbar])$ originates from the upper bound ϵ_{F} of the Matsubara sum. If one assumes $\omega_m\ll\epsilon_{\mathrm{F}}$, this factor removes from $\Sigma^{(D)}(\boldsymbol{r},\boldsymbol{r}')$ all the contributions of trajectories of length smaller than $\Lambda_0=\lambda_{\mathrm{F}}/\pi$, thus preventing the particle–particle propagator from diverging as $\boldsymbol{r}\to\boldsymbol{r}'$. Replacing it by a hard cutoff at Λ_0 one obtains

$$\Sigma^{(D)}(\boldsymbol{r},\boldsymbol{r}';\omega_m)\simeq\frac{k_{\mathrm{B}}T}{g_{\mathrm{s}}\hbar}\sum_{\substack{j:\boldsymbol{r}\to\boldsymbol{r}'\\ L_j>\Lambda_0}}\frac{|D_j|^2}{m_{\mathrm{e}}}\frac{R(2t_j/t_{\mathrm{T}})}{2t_j/t_{\mathrm{T}}}\times\exp\left[\mathrm{i}4\pi\frac{Ba_j}{\phi_0}\right]\exp\left[-\frac{\omega_m t_j}{\hbar}\right]. \tag{3.23}$$

The semiclassical form for $\Sigma^{(D)}(\boldsymbol{r},\boldsymbol{r}';\omega_m)$ shares with $\mathcal{H}_D$ and $\mathcal{F}_D$ (equations (3.13a) and (3.13b)) the property of being a semiclassical expansion which does not oscillate rapidly (on the scale of λ_{F}) as a function of the coordinates, as would be the case for the Green's functions (3.20).

4. Orbital magnetism: diffusive and ballistic systems

4.1. Diffusive systems

The semiclassical approach described above does not rely on any assumption concerning the character of the underlying classical dynamics. It is therefore applicable to (integrable or chaotic) ballistic structures (Ullmo *et al* 1998, von Oppen *et al* 2000) as well as to diffusive systems (Montambaux 1996, Ullmo *et al* 1997). Because diffusive motion is in some sense relatively simple, it is natural to consider first the orbital magnetism of interacting systems whose non-interacting classical dynamics is diffusive. More specifically, I will discuss the interaction contributions to the persistent current of metal rings and to the susceptibility of singly connected two-dimensional diffusive systems. We shall see that in this case, the semiclassical approach recovers, in a very transparent and intuitive way, results previously obtained by quantum diagrammatic calculations (Aslamazov and Larkin 1975, Altshuler *et al* 1983, Ambegaokar and Eckern 1990b, Eckern 1991, Oh *et al* 1991). Applied to diffusive dynamics, the semiclassical approach is indeed on the same level of approximation. Moreover, by making the connection with the classical dynamics, it provides a physically intuitive picture of the interplay between disorder and interactions.

We assume here that the Fermi wavelength λ_{F} is the shortest length scale, in particular $\lambda_{\mathrm{F}}<\ell$ with ℓ the elastic mean free path, and that the magnetic field is classically weak, i.e. the cyclotron radius at the Fermi energy is such that $R_{\mathrm{c}}\gg\ell$. Then the paths entering into (3.23) can be approximated by those of the system at zero field, but include the presence of the disorder potential.

For diffusive systems it proves convenient to relate $\Sigma^{(D)}$ to the (classical) conditional probability $P^{\epsilon}_{\mathrm{cl}}(\boldsymbol{r},\boldsymbol{r}';t|A)$ to propagate from $\boldsymbol{r}'$ to $\boldsymbol{r}$ in a time t and enclosing an area A since this probability satisfies a simple diffusion equation. For this purpose let us introduce an additional time and area integration $1=\int\mathrm{d}t\delta(t-t_j)\int\mathrm{d}\mathrm{A}\delta(\mathrm{A}-\mathrm{a}_j)$ in (3.23) in order to make use of the sum rule (2.24), which, for a two-dimensional kinetic plus potential Hamiltonian, and including the constraint on the area, reads

$$\sum_{j:\boldsymbol{r}'\to\boldsymbol{r}}\frac{|D_j(\epsilon)|^2}{m_{\mathrm{e}}}\delta(t-t_j)\delta(\mathrm{A}-a_j)=2\pi\,P^{\epsilon}_{\mathrm{cl}}(\boldsymbol{r},\boldsymbol{r}',t|A). \tag{4.1}$$

One therefore obtains

$$\Sigma^{(D)}(\boldsymbol{r},\boldsymbol{r}';\omega_m) \simeq \frac{2\pi}{g_s}\frac{k_B T}{\hbar}\int \mathrm{d}A \int_{t>\Lambda_0/v_F} \mathrm{d}t\; P^{\epsilon}_{cl}(\boldsymbol{r},\boldsymbol{r}',t|A)\frac{R(2t/t_T)}{2t/t_T} \times \exp\left[\mathrm{i}4\pi\frac{BA}{\phi_0}\right]\exp\left[-\frac{\omega_m t}{\hbar}\right]. \quad (4.2)$$

In the same way the nth order (diagonal) contribution to the thermodynamic potential in (3.15) can then be expressed through the joint return probability $P(\boldsymbol{r}_1,\boldsymbol{r}_n,\ldots,\boldsymbol{r}_1;t_n,\ldots,t_1|A)$ to visit the n points $\boldsymbol{r}_i$ under the conditions that t_i is the time elapsed during propagation from $\boldsymbol{r}_i$ to $\boldsymbol{r}_{i+1}$ and that the total enclosed area is A. For diffusive motion the probability is multiplicative, namely,

$$\int \mathrm{d}\boldsymbol{r}_1\ldots\mathrm{d}\boldsymbol{r}_n P(\boldsymbol{r}_1,\boldsymbol{r}_n,\ldots,\boldsymbol{r}_1;t_n,\ldots,t_1|A) = \int \mathrm{d}\boldsymbol{r}P(\boldsymbol{r},\boldsymbol{r};t_{tot}|A) \quad (4.3)$$

with $t_{tot}=\sum t_i$. Upon inserting the sum rule (4.1) and the relation (4.3) into (3.23), the contribution from the diagonal terms $\Sigma^{(D)}$ to Ω (see (3.15)) yields

$$\Omega^{(D)} = \sum_n \Omega_n^{(D)} = \frac{1}{\beta}\int \mathrm{d}\boldsymbol{r}\int \mathrm{d}t\coth\left(\frac{t}{t_T}\right)K(t)\mathcal{A}(\boldsymbol{r},t;B). \quad (4.4)$$

The factor $\coth(t/t_T)$ (with t_T defined by (3.8)) arises from the ω-sum in (3.15) which can be performed here explicitly. In (4.4) the functions K and $\mathcal{A}$ are defined as

$$K(t)\equiv\sum_n K_n(t);$$

$$K_n(t)\equiv\frac{(-\lambda_0)^n}{n}\left\{\int\prod_{i=1}^{n}\left[\frac{\mathrm{d}t_i R(2t_i/t_T)}{g_s t_i}\right]\delta(t-t_{tot})\right\}, \quad (4.5)$$

$$\mathcal{A}(\boldsymbol{r},t;B)\equiv\int \mathrm{d}A\cos\left(\frac{4\pi BA}{\phi_0}\right)P(\boldsymbol{r},\boldsymbol{r};t|A). \quad (4.6)$$

$K(t)$ accounts for temperature effects while $\mathcal{A}(\boldsymbol{r},t;B)$ contains the field dependence and the classical return probability.

4.1.1. Renormalization scheme for diffusive systems. This semiclassical approach allows us further to obtain the renormalization of the coupling constant (Altshuler *et al* 1983, Altshuler and Aronov 1985, Eckern 1991, Ullmo *et al* 1997) for diffusive systems by resuming the higher-order diagrams of the Cooper series. To this end let us first introduce the Laplace transform of $K_1(t)$,

$$\hat{f}(p)=\frac{4\lambda_0}{g_s}\sum_{n=0}^{n_F}\frac{1}{pt_T+2(2n+1)}, \quad (4.7)$$

where

$$n_F=\frac{\beta\epsilon_F}{2\pi}=\frac{k_F L_T}{4}. \quad (4.8)$$

The full kernel $K(t)$ is given by the inverse Laplace transform

$$K(t)=\frac{1}{2\pi\mathrm{i}}\int_{-i\infty}^{+i\infty}\mathrm{d}p\,\mathrm{e}^{+pt}\ln[1+\hat{f}(p)]. \quad (4.9)$$

To evaluate the above integral, let us define

$$\hat{g}(p)\equiv 1+\hat{f}(p) \quad (4.10)$$

and furthermore denote the singularities of $\hat{g}(p)$ by

$$p_n=-\frac{2(2n+1)}{t_T} \quad (4.11)$$

with $n=0,\ldots,n_F$. Let $\tilde{p}_n$ be the corresponding zeros ($\tilde{p}_n$ is assumed to lie between p_n and p_{n+1}). On the real axis, $\hat{g}$ is a real function which is negative within each interval $[\tilde{p}_n,p_n]$ (with the notation $\tilde{p}_{n_F}=-\infty$) and positive elsewhere. As a consequence, $\ln\hat{g}(p)$ is analytic everywhere in the complex plane except for the branch cut $[\tilde{p}_n,p_n]$. The phase jump across the branch cuts is 2π, since the imaginary part of $\hat{g}(p)$ is positive above and negative below the real axis. Deforming the contour of integration as sketched in figure 3, one therefore finds

$$K(t)=\lim_{\epsilon\to 0}\int_{-\infty}^{0}\frac{\mathrm{d}p}{2\mathrm{i}\pi}(\ln[\hat{g}(p-\mathrm{i}\epsilon)]-\ln[\hat{g}(p+\mathrm{i}\epsilon)])\mathrm{e}^{pt} \quad (4.12)$$

$$=\sum_{n=0}^{n_F}\int_{\tilde{p}_n}^{p_n}\mathrm{d}p\mathrm{e}^{pt} \quad (4.13)$$

$$=\frac{1}{t}\sum_{n=0}^{n_F}[\mathrm{e}^{p_n t}-\mathrm{e}^{\tilde{p}_n t}]. \quad (4.14)$$

For $n\ll n_F$ one has $\delta_n\equiv t_T(p_n-\tilde{p}_n)\ll 1$ and thus to first order in δ_n:

$$1+\frac{\lambda_0}{g_s}\sum_{n'\neq n}^{n_F}\frac{1}{n'-n}-\frac{4\lambda_0}{g_s}\frac{1}{\delta_n}=0\,. \quad (4.15)$$

The above condition gives

$$\delta_n=\frac{4}{g_s/\lambda_0+\Psi(n_F+1)-\Psi(2n+1)} \quad (4.16)$$

with Ψ the digamma function.

In the *high temperature regime* $t_T\leqslant t$, all the ns actually contributing to the sum (4.14) are such that the denominator in (4.16) is dominated by $\Psi(n_F+1)\simeq\ln(n_F)$. One obtains in this case

$$K(t)=\frac{1}{t}\sum_{n=0}^{n_F}\mathrm{e}^{p_n t}[1-\mathrm{e}^{-\delta_n t/t_T}] \quad (4.17)$$

$$\simeq\frac{1}{t_T}\frac{4}{\ln(k_F L_T/4)}\sum_{n=0}^{n_F}\mathrm{e}^{p_n t}. \quad (4.18)$$

In the *low temperature regime* $t_T/t\gg 1$, the typical n contributing to (4.14) is $n_0\equiv t_T/4t$ (that is still assumed to be much smaller than n_F). Because of the slow variation of the logarithm, one can in this case replace n by n_0 in (4.16).

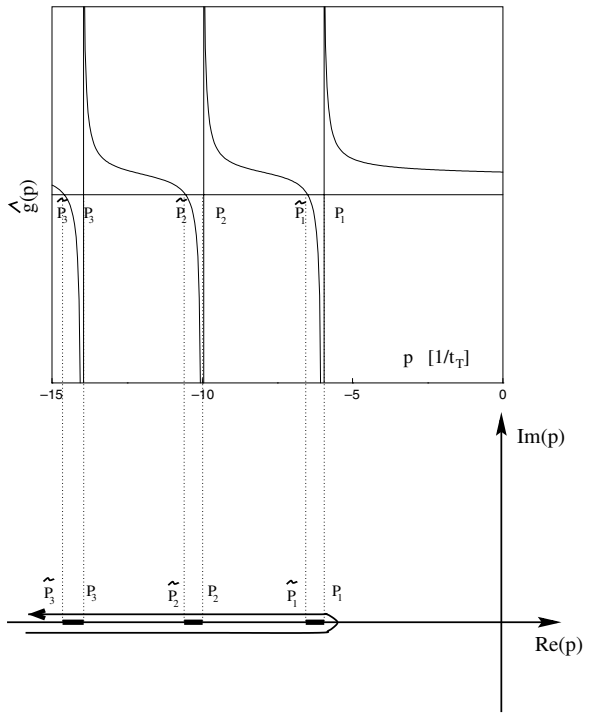

Figure 3. Top: graph of the function $\hat{g}(p)$ (for $n_f = 200$). Bottom: integration path for the inverse Laplace transform (4.13) in the complex p plan.

(A formal derivation would consist of replacing sum (4.14) by an integral, changing to the variable $\ln(n)$ and using the stationary phase approximation.) This gives

$$\delta_n \simeq \frac{4}{\ln(n_f) - \ln(2n_0)} = \frac{4}{\ln(2k_F v_F t)}, \tag{4.19}$$

and in the same way as above

$$K(t) \simeq \frac{1}{t_T} \frac{4}{\ln(2k_F v_F t)} \sum_{n=0}^{n_F} e^{p_n t}. \tag{4.20}$$

Noting that

$$K_1(t) = \frac{4\lambda_0}{g_s t_T} \sum_{n=0}^{n_F} e^{p_n t}, \tag{4.21}$$

one identifies

$$K(t) \simeq \frac{g_s}{\lambda_0 \ln(k_F L^*)} K_1(t) \tag{4.22}$$

with

$$L^* = \min(2v_F t, L_T/4). \tag{4.23}$$

This relation is valid when $\ln k_F L^* \gg 1$. It is certainly satisfied when $\ln k_F l \gg 1$ which may be regarded as a semiclassical approximation in the diffusive regime. Equation (4.22) shows that the higher-order terms in $K(t)$ merely lead to a renormalization of the first order contribution $K_1(t)$: the coupling constant $\lambda_0 = 1$, entering into $K_1(t)$, is renormalized to $g_s/\ln(k_F L^*)$.

In first order one has from (4.5)

$$K_1(t) = \lambda_0 \frac{R(2t/t_T)}{2t}, \tag{4.24}$$

so that K reduces to

$$K(t) \simeq \frac{R(2t/t_T)}{t \ln(k_F L^*)}. \tag{4.25}$$

Equations (4.4)–(4.6) together with (4.25) may serve as a general and convenient starting point to compute the orbital response of disordered mesoscopic systems. The specific character of the geometry enters into $\Omega^{(D)}$ solely through the Fourier transform (4.6) of the return probability $P(\boldsymbol{r}, \boldsymbol{r}, t|A)$. In the following I shall apply this approach to compute the magnetic response of two important types of mesoscopic structures.

4.1.2. Persistent current of disordered rings. While the magnetic response of a singly connected system is usually described in terms of its susceptibility, the response of a ring-type structure threaded by a flux ϕ is related to the persistent current

$$I \equiv -\frac{\partial \Omega}{\partial \phi} \tag{4.26}$$

(see appendix B for a derivation of this equation). To make contact with previous approaches (Ambegaokar and Eckern 1990b, Montambaux 1996) let us start with the computation of the contribution of the first order interaction term, $\Omega_1^{(D)}$, to I which will be denoted by I_1.

Consider a (thin) disordered ring of width b, cross section σ and circumference L. For $L \gg l, b$ the motion of particles around the ring effectively follows a law for one-dimensional diffusion. The total area enclosed by a path is given in terms of the number m of windings around the ring. One thus has

$$P(\boldsymbol{r}, \boldsymbol{r}; t|A) = \sum_{m=-\infty}^{+\infty} \frac{1}{\sigma} \frac{1}{\sqrt{4\pi D t}} \times \exp\left(-\frac{m^2 L^2}{4Dt}\right) \delta\left(A - \frac{mL^2}{4\pi}\right), \tag{4.27}$$

where $D = v_F l/d$ is the diffusion constant in d dimensions and v_F the Fermi velocity. Note that due to the disorder average, the classical return probability does not depend on $\boldsymbol{r}$.

Combining the expression (4.24) for $K_1(t)$ with the coth function in (4.4) one obtains

$$\Omega_1^{(D)} = \frac{\lambda_0}{g_s} \frac{2L\hbar}{2\pi} \sum_{m=-\infty}^{+\infty} \cos\left(\frac{4\pi m\phi}{\phi_0}\right) g_m(T) \tag{4.28}$$

with

$$g_m(T) = \int_0^\infty dt \frac{R^2(t/t_T)}{t^2} \frac{\exp\left[-(mL)^2/(4Dt)\right]}{\sqrt{4\pi Dt}}. \tag{4.29}$$

After taking the flux derivative according to (4.26), one recovers the first order interaction contribution to the persistent current (Ullmo *et al* 1997),

$$I_1 = \frac{\lambda_0}{g_s} \frac{2Le}{\pi} \sum_{m=-\infty}^{+\infty} m \sin\left(\frac{4\pi m\phi}{\phi_0}\right) g_m(T). \tag{4.30}$$

This first order result was first obtained by purely diagrammatic techniques by Ambegaokar and Eckern (1990b) and semiclassically by Montambaux (1996).

However, higher-order terms are essential for an appropriate computation of the interaction contribution. As shown in the preceding subsection, these higher-order terms merely lead to a renormalization of the coupling constant according to (4.22). Thus the persistent current from the entire interaction contribution is reduced to (Ullmo *et al* 1997)

$$I = \frac{2Le}{\pi \ln(k_F L^*)} \sum_{m=-\infty}^{+\infty} m \sin\left(\frac{4\pi m\phi}{\phi_0}\right) g_m(T). \tag{4.31}$$

For diffusive rings the length scale $v_F t$, entering in (4.23) for L^*, is given by $L_m = v_F(mL)^2/4D$, the average length of a trajectory diffusing m times around the ring. Hence one gets at a low temperature ($L_T \gg L_m$) a (renormalized) prefactor $\sim 2/\ln(k_F L_m)$ for I. At a high temperature, $L_T \ll L_m$, the prefactor includes $2/\ln(k_F L_T/4)$. These two limits agree with the quantum results obtained diagrammatically by Eckern (1991). The functional form of the temperature dependence (exponential T-damping (Ambegaokar and Eckern 1990b)) is in line with experiments (Lévy *et al* 1990, Chandrasekhar *et al* 1991, Mohanty *et al* 1996). However, the amplitude of the full persistent current with renormalized coupling constant is a factor ~3–5 to small compared with experiments.

4.1.3. Susceptibility of two-dimensional diffusive systems. In ring geometries the exponential temperature dependence of I is related to the existence of a minimal length, the circumference of the ring, for the shortest flux-enclosing paths. In singly connected systems the geometry does not constrain returning paths to have a minimal length, and therefore one expects a different temperature dependence of the magnetic response.

Consider a two-dimensional singly connected quantum dot with diffusive dynamics. If one makes use of the general renormalization property of diffusive systems, expressed by (4.25), the diagonal part of the thermodynamic potential (see (4.4)), including the entire Cooper series, reads

$$\Omega^{(D)} = \frac{1}{\beta} \int \mathrm{d}\boldsymbol{r} \int_{\tau_{el}}^{\infty} \mathrm{d}t \frac{1}{\ln(k_F v_F t)} \frac{t_T}{t^2} R^2\left(\frac{t}{t_T}\right) \mathcal{A}(\boldsymbol{r}, t; B). \tag{4.32}$$

The parameter L^* appearing in (4.22) has been here replaced by $v_F t$ since the factor R^2 ensures that the main contribution to the integral comes from $t < t_T$. In the above time integral the elastic scattering time $\tau_{el} = l/v_F$ enters as a lower bound. This cutoff must be introduced since for backscattered paths with times shorter than τ_{el} the diffusion approximation (4.33) no longer holds. Short paths with $t < \tau_{el}$, which may arise from higher-order interaction events, contribute to the clean bulk magnetic response (Aslamazov and Larkin 1975, von Oppen *et al* 2000). This latter term is, however, negligible compared with the disorder induced interaction contributions considered here.

To evaluate the integral for $\mathcal{A}$, the conditional return probability in two dimensions is conveniently represented in terms of the Fourier transform (Argaman *et al* 1993)

$$P(\boldsymbol{r}, \boldsymbol{r}, t|A) = \frac{1}{8\pi^2} \int \mathrm{d}k|k| \frac{\mathrm{e}^{\mathrm{i}kA}}{\sinh(|k|Dt)}. \tag{4.33}$$

Introducing the magnetic time

$$t_B = \frac{\phi_0}{4\pi BD} = \frac{L_B^2}{4\pi D} \tag{4.34}$$

(t_B is related to the square of the magnetic length L_B^2 which can be regarded as the area enclosing one flux quantum (assuming diffusive dynamics)), one obtains

$$\mathcal{A}(\boldsymbol{r}, t; B) = \frac{1}{4\pi D} \frac{R(t/t_B)}{t}. \tag{4.35}$$

The function R occurring in (4.35) has a different origin than in (4.32).

The magnetic susceptibility (3.3) is obtained after including the expression (4.35) in (4.32) and taking the second derivative with respect to the magnetic field. One finds, after normalization to the Landau susceptibility of non-interacting particles in a clean system,

$$\frac{\chi^{(D)}}{|\chi_L|} = -\frac{12}{\pi}(k_F l) \int_{\tau_{el}}^{\infty} \frac{\mathrm{d}t}{t \ln(k_F v_F t)} R^2\left(\frac{t}{t_T}\right) R''\left(\frac{t}{t_B}\right). \tag{4.36}$$

Here, $D = v_F l/2$, and R'' denotes the second derivative of R.

The above equation (4.36) holds true only as long as the effective upper cutoff time $t^* \equiv \min(t_T, t_B)$, introduced through the R-functions, remains smaller than the Thouless time $t_c = L^2/D$ with L being the system size. For times larger than t_c the two-dimensional diffusion approximation is no longer valid since the dynamics begins to behave ergodically.

Assuming $\tau_{el} \ll t^* < t_c$, the integral in (4.36) can be approximately evaluated by replacing the upper bound by t^* and by replacing $R(t/t_T)$ and $R''(t/t_B)$ by $R(0) = 1$ and $R''(0) = -1/3$, respectively. The averaged magnetic susceptibility of a diffusive two-dimensional quantum system reads under these approximations (Ullmo *et al* 1997)

$$\frac{\chi^{(D)}}{|\chi_L|} \simeq \frac{4}{\pi}(k_F l) \ln\left\{\frac{\ln[k_F v_F \min(t_T, t_B)]}{\ln(k_F l)}\right\}. \tag{4.37}$$

The magnetic response of diffusive systems is paramagnetic and enhanced by a factor $k_F l$ compared with the clean Landau susceptibility χ_L.

Contrary to the exponential temperature dependence of the ring geometry discussed in the previous section one finds a log–log temperature dependence for $t_T < t_B$ as well as a log–log B dependence for $t_T > t_B$. The log–log form of the result is produced by the $1/t \ln t$ dependence of the integral in (4.36). It results from the wide distribution of path-lengths in the system—there are flux-enclosing paths with lengths ranging from about $v_F \tau_{el}$ up to $v_F t^*$.

Expression (4.37) agrees with results from Aslamazov and Larkin (1975), Altshuler *et al* (1983) and Oh *et al* (1991) which are obtained with quantum diagrammatic perturbation theory. The equivalence between the semiclassical and diagrammatic

approaches, demonstrated here as well as in the preceding section for diffusive rings, may be traced back to the fact that 'quantum' diagrammatic perturbation theory relies on the use of the small parameter $1/k_F\ell$ and can therefore also be viewed as a semiclassical approximation.

4.2. Ballistic systems

We turn now to the magnetic response of ballistic mesoscopic objects. This problem has attracted considerably less attention than the diffusive regime, partly because of the experimental difficulties involved, but also presumably because from the theoretical point of view, ballistic systems cannot be addressed with the more traditional approaches of solid state physics. Indeed, for diffusive systems, the main virtue of the 'quantum-chaos' based approach presented in this review was to provide an alternative, maybe more intuitive, way to get known results. In contrast, the ballistic regime represents one example for which it is actually the only way to get an understanding of the physics involved.

The ballistic character of the underlying classical dynamics brings about some important differences, especially since one no longer talks about probabilistic concepts (like the return probability), but one needs to input the information about specific trajectories. Depending on the geometry of the confining potential, one can have chaotic or integrable motion, and the structure of the semiclassical expansions differs in some respects in these two cases. In particular, the existence of families of trajectories for integrable dynamics will translate into a larger magnetic response.

4.2.1. Renormalization scheme for ballistic systems. As for diffusive systems, (3.15) and (3.23) form the basic expressions from which the magnetic response can be computed. We just saw that in this latter case, they allow quite straightforwardly to express the magnetic susceptibility of dots or persistent current of rings in closed form. For ballistic systems on the other hand, even when the classical dynamics is simple enough to yield $\Sigma^{(D)}(\boldsymbol{r},\boldsymbol{r}';\omega_m)$ explicitly, taking the logarithm of this operator as implied by (3.15) will require proceeding numerically. It should be borne in mind however that this numerical calculation is significantly simpler than the one we would have faced had we decided to start directly with a numerical approach. This can be understood for instance by considering that the original operator $\Sigma(\boldsymbol{r},\boldsymbol{r}';\omega_m)$, because of its quantal nature, has a scale of variation determined by λ_F. Discretizing this operator on a grid would therefore require using a mesh containing at least a few points per λ_F, which would make any computation rapidly intractable as the size of the problem increases. On the other hand, within the semiclassical approach, the operator one has to deal with is $\Sigma^{(D)}(\boldsymbol{r},\boldsymbol{r}')$ which, up to one exception to which I shall return below, varies only on a *classical* scale. $\Sigma^{(D)}(\boldsymbol{r},\boldsymbol{r}')$ is therefore what one may call a 'classical operator'. It permits the use of a grid mesh whose scale is fixed by the classical dynamics within the system and is therefore much larger than λ_F.

As mentioned above $\Sigma^{(D)}(\boldsymbol{r},\boldsymbol{r}')$ is not yet completely classical. Indeed, there is still, in (3.23), the scale $\Lambda_0 = \lambda_F/\pi$ which specifies that trajectories shorter than Λ_0 should be excluded from the sum over trajectories joining $\boldsymbol{r}'$ to $\boldsymbol{r}$. This last quantum scale can be removed using a simple renormalization scheme where integration over short trajectories yields a decreased effective coupling constant. To this end consider a new cutoff Λ larger than Λ_0 but much smaller than any other characteristic lengths (a, L_T, or $\sqrt{\phi_0/B}$). For each path j joining $\boldsymbol{r}'$ to $\boldsymbol{r}$ with $L_j > \Lambda$, let $\Sigma_j(\boldsymbol{r},\boldsymbol{r}')$ denotes its contribution to $\Sigma^{(D)}(\boldsymbol{r},\boldsymbol{r}')$ and define

$$\tilde{\Sigma}_j(\boldsymbol{r},\boldsymbol{r}') \equiv \Sigma_j(\boldsymbol{r},\boldsymbol{r}') - \lambda_0 \int \mathrm{d}\boldsymbol{r}_1\, \Sigma_j(\boldsymbol{r},\boldsymbol{r}_1)\hat{\Sigma}(\boldsymbol{r}_1,\boldsymbol{r}') + \lambda_0^2 \int \mathrm{d}\boldsymbol{r}_1\,\mathrm{d}\boldsymbol{r}_2\, \Sigma_j(\boldsymbol{r},\boldsymbol{r}_2)\hat{\Sigma}(\boldsymbol{r}_2,\boldsymbol{r}_1)\hat{\Sigma}(\boldsymbol{r}_1,\boldsymbol{r}') + \cdots, \tag{4.38}$$

where the $\boldsymbol{r}_i$ integration is over $\Lambda_0 < |\boldsymbol{r}_{i-1} - \boldsymbol{r}_i| < \Lambda$ (with $\boldsymbol{r}_0 \equiv \boldsymbol{r}'$). $\hat{\Sigma}(\boldsymbol{r}_1,\boldsymbol{r}')$ is defined by (3.23) but with the sum restricted to 'short' trajectories with lengths in the range $[\Lambda_0, \Lambda]$; $\Sigma_j(\boldsymbol{r},\boldsymbol{r}_1)$ is obtained from $\Sigma_j(\boldsymbol{r},\boldsymbol{r}')$ by continuously deforming trajectory j. To avoid the awkward ln in (3.15), let us introduce

$$\Gamma = \frac{1}{\beta}\sum_{\omega_m} \mathrm{Tr}\left[\frac{1}{1+\lambda_0\Sigma^{(D)}(\boldsymbol{r},\boldsymbol{r}';\omega_m)}\right], \tag{4.39}$$

from which $\Omega^{(D)}$ can be derived through

$$\Omega^{(D)}(\lambda_0) = \int_0^{\lambda_0} \frac{\mathrm{d}\lambda_0'}{\lambda_0'}\,\Gamma(\lambda_0'). \tag{4.40}$$

The replacement Σ by $\tilde{\Sigma}$ in Γ amounts to a reordering of the perturbation expansion of Γ in which short paths are gathered into lower-order terms. Moreover, if $L_j \gg \Lambda$, small variations in the spatial arguments do not noticeably modify the characteristics of Σ_j. Approximating $\Sigma_j(\boldsymbol{r},\boldsymbol{r}_1)$ by $\Sigma_j(\boldsymbol{r},\boldsymbol{r}')$ in (4.38) and using $\hat{\Sigma}(\boldsymbol{r}_1,\boldsymbol{r}') \simeq 1/4\pi|\boldsymbol{r}_1 - \boldsymbol{r}'|^2$ valid for short paths, one obtains

$$\lambda_0\tilde{\Sigma}_j(\boldsymbol{r},\boldsymbol{r}') \simeq \frac{\lambda_0\Sigma_j(\boldsymbol{r},\boldsymbol{r}')}{1+\lambda_0\int \mathrm{d}\boldsymbol{r}_1\hat{\Sigma}(\boldsymbol{r}_1,\boldsymbol{r}')} \simeq \lambda(\Lambda)\,\Sigma_j(\boldsymbol{r},\boldsymbol{r}'), \tag{4.41}$$

where the running coupling constant is defined by

$$\lambda(\Lambda) = \frac{\lambda_0}{1+(\lambda_0/g_s)\ln(\Lambda/\Lambda_0)}. \tag{4.42}$$

Therefore, these successive steps amount to a change in both the coupling constant and the cutoff (since now trajectories shorter than Λ must be excluded) without changing Γ; that is,

$$\Gamma(\Lambda_0,\lambda_0) = \Gamma\left(\Lambda,\lambda(\Lambda)\right). \tag{4.43}$$

Through (4.40), this renormalization scheme can be applied to $\Omega^{(D)}$ and so to the average susceptibility.

In this way, we have eliminated the last 'quantum scale' Λ_0 from the definition of $\Sigma^{(D)}$: Λ can be made much larger than λ_F while remaining smaller than all classical lengths. This will serve two purposes. From a quantitative point of view, it means that discretizing the operator $\Sigma^{(D)}$ can be done on a relatively coarse grid, and therefore operations such as taking

the trace logarithm of $1+\Sigma^{(D)}$ that may be necessary to get the magnetic response can be done numerically much more easily.

Furthermore, it is qualitatively reasonable that the perturbation series of $\Omega^{(D)}$ becomes convergent when Λ is of order of the typical size L of the system, since by this point the spread in length scales causing the divergence has been eliminated. Of course the renormalization scheme given above assumes Λ to be much smaller than all the classical scales of the system, and using $\Lambda \simeq L$ is beyond the range for which a reliable quantitative answer can be obtained. At a qualitative level however, this implies that higher-order terms in the diagonal contribution mainly renormalize the coupling constant λ_0 into

$$\lambda(L) = \frac{\lambda_0}{1 + (\lambda_0/g_s)\ln(k_F L)}. \tag{4.44}$$

In the deep semiclassical limit $\ln(k_F L) \gg 1$, the original coupling constant λ_0 drops from the final results and is replaced by $g_s/\ln(k_F L)$.

For integrable systems in which non-diagonal channels exist, a simple inspection shows that the latter are not renormalized. Indeed the corresponding higher-order terms in the perturbation expansion are highly oscillatory. The non-diagonal contributions are therefore of order λ_0 rather than $g_s/\ln(k_F L)$ and will as a consequence dominate the magnetic response in the deep semiclassical regime.

4.2.2. Ballistic squares. As an illustration, let us consider square quantum dots. The choice of squares is motivated first because this is the geometry used experimentally (Lévy *et al* 1993) and secondly because squares are particularly amenable to a semiclassical treatment, since it is very easy to enumerate all the classical trajectories[9]. To be more specific, I will consider a square billiard model, of size L, with free motion (i.e. just a kinetic energy term) inside the the billiard and Dirichlet boundary conditions on its border. An illustration of the shortest (with non-zero area) closed orbit and of the shortest periodic orbit, for the classical version of the billiard, is given in figure 4.

Let us first discuss the diagonal contribution $\Omega^{(D)}$ (3.15) to the thermodynamic potential. Because of the simplicity of the geometry, the explicit expression of $\Sigma_j(\boldsymbol{r}, \boldsymbol{r}'; \omega)$ for any orbit j joining $\boldsymbol{r}'$ to $\boldsymbol{r}$ can be obtained quite straightforwardly (though the resulting expressions might be a bit cumbersome and will thus not be given). At a given temperature T, the operator $\Sigma^{(D)}(\boldsymbol{r}, \boldsymbol{r}'; \omega)$ is then constructed by summing all such contributions for orbits of lengths shorter than the thermal length L_T (see (3.8)). A numerical computation of $\Omega^{(D)}$ (and therefore, after derivation with respect to the magnetic field, of the magnetic susceptibility) can then be obtained by representing $\Sigma^{(D)}(\boldsymbol{r}, \boldsymbol{r}'; \omega)$ on a grid, then going to a diagonal representation, and in this diagonal representation taking the log and performing the trace. The temperature dependence of the resulting contribution to the susceptibility, for a number of particles corresponding to $k_F L = 50$, is shown as a dotted line in figure 5.

[9] As a consequence of the two previous facts, orbital magnetism in ballistic squares has been thoroughly studied within non-interacting models (Gefen *et al* 1994, VonOppen 1994, Ullmo *et al* 1995, Richter *et al* 1996a, 1996b, 1996c).

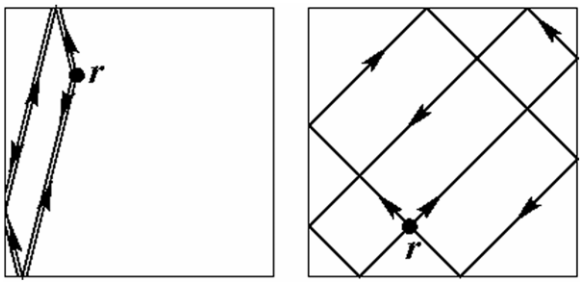

Figure 4. Typical pairs of real-space trajectories that contribute to the average susceptibility to first order in the interaction in the diagonal channel (left) and the non-diagonal channel (right). Reprinted with permission from Ullmo *et al* (1998). Copyright 1998 by the American Physical Society.

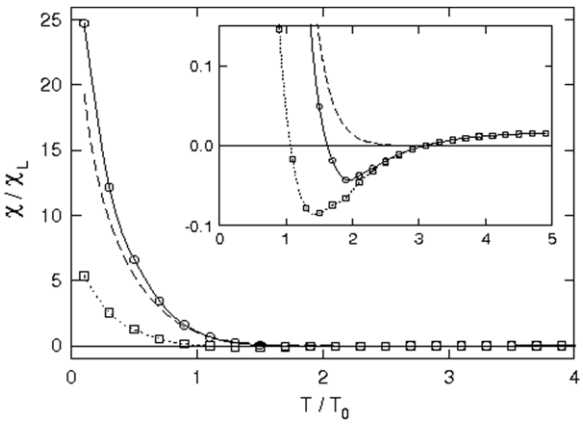

Figure 5. Temperature dependence of the zero-field susceptibility (solid line) for an ensemble of squares at $k_F L = 50$. The contribution of the non-diagonal channel (dashed, family (11) and repetitions) exceeds that of the diagonal Cooper channel (dotted) at low temperatures. Temperatures are expressed in units of $k_B T_0 = \hbar v_F/2\pi L$. Inset: same, but with a different scale for the vertical axis. Reprinted with permission from Ullmo *et al* (1998). Copyright 1998 by the American Physical Society.

In this way, one can further check that the renormalization process described above actually works for the square geometry. For instance, figure 6 shows the value of the magnetic susceptibility at zero field, and for a temperature such that $L_T = 4L$, as a function of the cutoff Λ. As long as $\Lambda \ll L$, the diagonal part of the susceptibility is clearly independent of the cutoff if the renormalized interaction $\lambda(\Lambda)$ given by (4.42) is used.

Let us finally compare the diagonal and non-diagonal contributions. This latter is built from pairs of orbits with the same action (i.e. for a billiard, same length) but different geometry, overlapping at a given point. These may occur quite generically for integrable systems for which families of periodic orbits exist and two members of the same family may intersect in the configuration space. An illustration of such an intersection is given in the right panel of figure 4 for the family (labelled (1, 1)) of shortest periodic orbits (with non-zero enclosed area) of this system. In the square billiard,

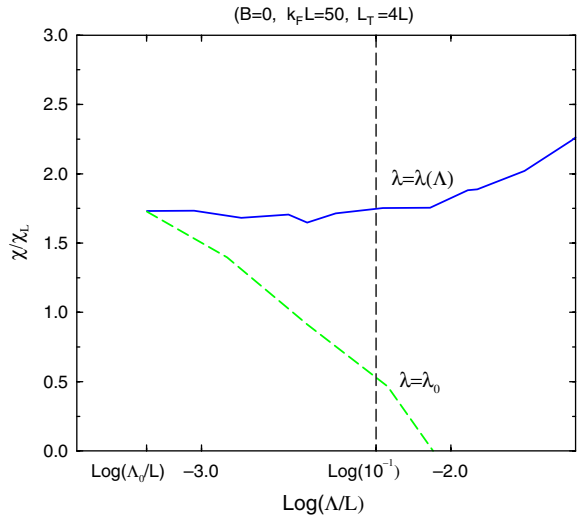

Figure 6. Diagonal part of the interacting contribution to the magnetic susceptibility as a function of the cutoff Λ used to define the particle–particle propagator Σ. The data correspond to zero magnetic field, $k_F L = 50$, and a temperature T such that $L_T = 4L$. Solid line: computation for which the coupling constant λ varies as a function of Λ following (4.42). Dashed line: λ is kept fixed ($= \lambda_0$). The vertical (dashed) line corresponds to the limit of the range for which the condition $\Lambda \ll L$ is fulfilled.

for a given closed orbit j of length L_j and enclosing an area a_j, the action in the absence of magnetic field is given by $S_j^0/\hbar = k_F L_j$, its derivative with respect to the magnetic field by $dS_j/dB = 2\pi a_j/\phi_0$ and the stability determinant (cf (2.5)) by $D_j = m/\sqrt{\hbar k_F L_j}$. The contribution $\chi_{(1,1)}$ of the pairs of orbits from the family (1, 1) can for instance be derived quite straightforwardly from equations (3.11*a*) and (3.11*b*) noting that $L_{11} = 2\sqrt{2}L$ and $a_{11} = 2x_0(L - x_0)$ (x_0 is the abscissa of the intersection of the orbit with the bottom border of the billiard and can be used to label an individual orbit within the family (1, 1)). One obtains in this way (Ullmo *et al* 1998)

$$\frac{\langle \chi_{(1,1)}^{\text{non-diag}} \rangle}{|\chi_L|} = -\frac{3k_F L}{2(\sqrt{2}\pi)^3} \frac{d^2\mathcal{C}^2(\varphi)}{d\varphi^2} R^2\left(\frac{L_{11}}{L_T}\right). \qquad (4.45)$$

The temperature dependence is governed by the function $R(x) = x/\sinh(x)$ and the field dependence by $\mathcal{C}(\varphi) = (2\varphi)^{-1/2}[\cos(\pi\varphi)C(\sqrt{\pi\varphi}) + \sin(\pi\varphi)S(\sqrt{\pi\varphi})]$, with $\varphi = BL^2/\phi_0$ and C and S being Fresnel functions.

As seen in figure 5, because the non-diagonal contribution is not renormalized by higher-order terms, it dominates the magnetic response as soon as the temperature is low enough not to suppress it.

4.3. Discussion

After this overview of some of the results that can be derived for the magnetic response of mesoscopic rings or dots within a Fermi-liquid, at equilibrium, description, it is worthwhile to come back to how well existing experiments can be understood within this framework. Since the typical response for a single system (Mailly *et al* 1993, Chandrasekhar *et al* 1991) may in some cases be dominated by the non-interacting contribution, which is not addressed here, I will however limit this discussion to experiments done on ensembles of micro-structures.

Ballistic and diffusive systems differ with respect to the comparison between experimental measurements and theoretical predictions, but for both cases there is clearly not complete adequacy.

In the case of ballistic systems (Lévy *et al* 1993), the amplitude of the magnetic response in the low temperature range, as well as the scale of the field dependence, is well in line with the predictions (von Oppen 1994, Ullmo *et al* 1995, Richter *et al* 1996b). However, the temperature dependence, and in particular the fact that a magnetic response is observed even when the thermal length L_T is smaller than the size of the system, seems very difficult to interpret within the Fermi-liquid framework used here (Ullmo *et al* 1995, 1998). There is, up to now, no real suggestion to explain how a significant magnetic response, with a field scale unambiguously associated with interference effects, could survive at such high temperatures.

For diffusive rings (Lévy *et al* 1990), the temperature dependence seems to be less of an issue than in the ballistic case. However the magnitude of the average persistent current appears to be quite a bit larger (a factor 3 to 5) than what is expected theoretically (Ambegaokar and Eckern 1990a). It has been suggested that this large magnetic response might be related to non-equilibrium effects, such as the coupling to a phonon or photon bath (Mohanty 1999, Kravtsov and Altshuler 2000, Entin-Wohlman *et al* 2003). In later experiments (Jariwala *et al* 2001) (see also Reulet *et al* (1995) and Deblock *et al* (2002) in this context), a further, and presumably more dramatic, discrepancy is that the sign of the magnetic response—which has not been determined in Lévy *et al* (1990)—was furthermore not the one expected for a repulsive interaction. This has motivated consideration of whether a BCS interaction, weak enough to be compatible with the absence of an observed superconducting state for the considered materials, could be responsible for both the change in sign (which would be an immediate consequence of having an attractive interaction) and the increase in the magnitude of the observed signal (Schechter *et al* 2003, 2004, Eckern *et al* 2004). It is not clear however that such a range of attractive interactions actually exist in practice.

In the end, it is remarkable that on the one hand a good part of the experimental findings has a simple and natural interpretation within the 'confined electron gas with weak interaction' picture developed here, while on the other hand no consensus has emerged as yet concerning the interpretation of other significant experimental findings. One of the limiting factors in this respect is presumably the imbalance between the large number of theoretical works and the much sparser character of experimental studies on these questions. In particular, only one group has measured the magnetic response of an ensemble of micro-structures in the ballistic regime (Lévy *et al* 1993). In this case the low temperature data agree very well with the theoretical description when there is little hope to interpret what is observed in the high temperature regime without introducing some new physical mechanisms. However, the lack of experimental indications of what these other mechanisms could be is making any theoretical progress

difficult. In the same way, for diffusive systems, a complete understanding would be made easier if one knew how much the sign of the magnetization observed in Jariwala *et al* (2001) is material dependent.

Obviously, it would be very non-trivial to improve on the existing experiments, in particular because it is necessary to deal properly with very weak magnetic fields. However, there are enough indications that some deep physics might be involved to motivate further experimental work in this field.

5. Mesoscopic Kondo effect

Turning now to another context where the interrelation between interferences and interactions plays an important role, I shall wander briefly away from Fermi liquids and consider some (limited) aspects of the problem of a Kondo impurity within a mesoscopic conductor.

5.1. A quick background

The term 'Kondo effect' refers to the physics of an impurity with some internal degree of freedom, interacting with a gas of otherwise non-interacting electrons. It represents one of the simplest models in condensed matter physics for which *correlations* play a central role (Hewson 1993).

In its simplest version, the *s–d* model, the impurity is just treated as a spin one half interacting locally with the electron gas. The corresponding Hamiltonian then reads

$$H_{\rm K} = \sum_{\alpha\sigma} \epsilon_\alpha \hat{c}^\dagger_{\alpha\sigma}\hat{c}_{\alpha\sigma} + H_{\rm int}, \tag{5.1}$$

where $\hat{c}^\dagger_{\alpha\sigma}$ creates a particle with energy ϵ_α, spin σ and wave-function $\varphi_\alpha(\boldsymbol{r})$, and the interaction with the impurity is expressed as

$$H_{\rm int} = \frac{J_0}{\hbar^2}\boldsymbol{S}\cdot\boldsymbol{s}(0), \tag{5.2}$$

with J_0 the coupling strength, $\boldsymbol{S} = (S_x, S_y, S_z)$ a spin operator ($\hbar^{-1}S_i$ is half of the Pauli matrix σ_i), $\boldsymbol{s}(0) = \frac{\hbar}{2}\hat{\Psi}^\dagger_\sigma(0)\boldsymbol{\sigma}_{\sigma\sigma'}\hat{\Psi}_\sigma(0)$ the spin density of the electron gas at the impurity position $\boldsymbol{r} \equiv 0$ and $\hat{\Psi}^\dagger_\sigma(0) = \sum_\alpha \varphi_\alpha(0)\hat{c}^\dagger_\alpha$.

Originally, physical realizations of the Kondo Hamiltonian corresponded to actual impurities (e.g. Fe) in a bulk metal (e.g. Cu). The wave-functions φ_α could then be taken as plane waves, and one could assume a constant spacing Δ between the ϵ_α, so that the electron gas could be characterized by only two quantities: the local density of states $\nu_0 = (\mathcal{A}\Delta)^{-1}$ ($\mathcal{A}$ is the volume of the sample) and the bandwidth D_0 of the spectrum.

What gave (and still gives) to the Kondo problem its particular place in condensed matter physics is that it is the simplest problem for which the physics is dominated by renormalization effects. Indeed, assuming the dimensionless constant $J_0\nu_0 \ll 1$, it can be shown using the one-loop renormalization-group analysis (Fowler and Zawadowzki 1971) or equivalent earlier approaches such as Anderson's poor man's scaling (Anderson 1970) or Abrikosov's parquet diagrams re-summation (Abrikosov 1965) that the low energy physics remains unchanged by the simultaneous modification of both J_0 and D_0 into new values $J_{\rm eff}$ and $D_{\rm eff}$ provided they are related by

$$J_{\rm eff}(D_{\rm eff}) = \frac{J_0}{1 - J_0\nu_0\ln(D_0/D_{\rm eff})}. \tag{5.3}$$

The renormalization procedure should naturally be stopped when $D_{\rm eff}$ becomes of the order of the temperature T of the system. Equation (5.3) defines an energy scale, the Kondo temperature

$$T_{\rm K} = D_0\exp(-1/(J_0\nu_0)), \tag{5.4}$$

which specifies the crossover between the weakly and strongly interacting regime. For $T \gg T_{\rm K}$, the impurity is effectively weakly coupled to the electron gas, and the properties of the system can be computed within a perturbative approach provided the renormalized interaction $J_{\rm eff}(T)$ is used. The regime $T \ll T_{\rm K}$ is characterized by an effectively very strong interaction (in spite of the bare coupling value $J_0\nu_0$ being small), in such a way that the spin of the impurity is almost completely screened by the electron gas. Perturbative renormalization analysis (and thus (5.3) itself) can obviously not be applied in this regime, but (for a bulk system) a rather complete description has been obtained by a variety of approaches, including numerical renormalization group (Wilson 1975), Bethe anzatz techniques (Andrei 1980, Wiegmann 1980) and in the very low temperature regime Nozières' Fermi-liquid description (Nozières 1974).

One important consequence of the scaling law (5.3) is that physical quantities can be described by universal functions, which can be understood by a simple counting of the number of parameters defining the *s–d* model in the bulk. I will illustrate this discussion with a particular physical quantity, namely, the local susceptibility

$$\chi_{\rm loc} = \int_0^\beta {\rm d}\tau\,\langle S_z(\tau)S_z(0)\rangle, \tag{5.5}$$

which is the variation of the impurity spin magnetization to a field applied only to the impurity. The electron gas is characterized by its local density of states ν_0 and its bandwidth D_0, and the impurity by the coupling constant J_0. Therefore, for a given temperature T, $\chi_{\rm loc}$, as any physical quantity, can depend only on these four parameters. Furthermore, only two dimensionless parameters can be constructed from them, the ratio T/D_0 and the product $J_0\nu_0$. However, because of the scaling law (5.3), we see that these two parameters turn out to be eventually redundant. A dimensionless quantity can therefore be expressed as a function of a single parameter, which can be chosen to be $T/T_{\rm K}$ so that we have for instance

$$T\chi_{\rm loc} = f_\chi(T/T_{\rm K}), \tag{5.6}$$

with $f_\chi(x)$ a universal function which has been computed by Wilson (1975) using his numerical renormalization-group approach. Note finally that within the one-loop approximation (5.3) and (5.4),

$$T/T_{\rm K} = \exp(J_{\rm eff}(T)\nu_0), \tag{5.7}$$

so that another way to express the universal character of physical quantities is to say that they depend only on the dimensionless quantity $J_{\rm eff}(T)\nu_0$.

5.2. Mesoscopic fluctuations

We see that the universal character of the Kondo physics is a direct consequence of the fact that the local density of states is flat and featureless and can therefore be characterized by two parameters, ν_0 and D_0. There are many situations however for which the variation in energy (and position actually) of the local density of states $\nu_{\rm loc}(\boldsymbol{r};\epsilon)$ might be significantly more complex, and it is natural to ask in which way this would modify the description given above in the bulk (flat band) case.

The origin of fluctuations in the density of states can be of different nature, but they are always in the end associated with interference or finite size effects. One possibility is the presence of disorder in a bulk material (Dobrosavljević *et al* 1992, Kettemann 2004, Kettemann and Mucciolo 2006, 2007, Zhuravlev *et al* 2007), in either the metallic or the localized regime. Another is the proximity of some boundary in the host material (Ujsaghy *et al* 2001), for instance, in the case of a narrow point contact (Zaránd and Udvardi 1996) or for thin films (Crépieux and Lacroix 2000). Finally the class of systems where a Kondo impurity is placed within a fully coherent, finite size electron sea, as has been realized for instance in the context of 'quantum corrals' (Fiete *et al* 2001), has been also considered (Thimm *et al* 1999, Affleck and Simon 2001, Cornaglia and Balseiro 2002a, 2002b, 2003, Simon and Affleck 2002, Franzese *et al* 2003, Kaul *et al* 2005, 2006, Lewenkopf and Weidenmuller 2005, Simon *et al* 2006).

One important recent development which has made very natural the idea that a magnetic impurity could be connected to a finite size electron gas is the realization that Kondo physics was actually relevant to transport properties of quantum dots (Glazman and Pustilnik 2005). Indeed, as was pointed out by Glazman and Raikh (1988) and simultaneously by Ng and Lee (1988), a quantum dot in the deep Coulomb-blockade regime (so that particle number fluctuations are suppressed) containing an odd number of electrons, and sufficiently small such that the temperature can be made much smaller than the mean level spacing between orbitals, can be described by an Anderson impurity model, which, up to a Schrieffer–Wolff transformation, is essentially equivalent to a Kondo impurity. When the dot is weakly coupled to leads, the latter play the role of the electron gas. In the low temperature regime $T \ll T_{\rm k}$, a correlated state is formed which mixes the quantum dots and both drain and source wave-functions, leading to a large conductance ($\simeq e^2/h$) in spite of the dot being in the deep Coulomb-blockade regime. These predictions have been observed by Goldhaber-Gordon *et al* (1998) a decade after they were formulated, some later experimental realizations even reaching the unitarity limit (van der Wiel *et al* 2000).

The great flexibility in the design and control of nanoscopic systems further motivated the study of many new configurations involving more exotic Kondo effects. One can cite for instance the theoretical design (Oreg and Goldhaber-Gordon 2003) and experimental observation (Potok *et al* 2007) of the 2-channel Kondo, which has proved to be elusive in bulk systems, the possible occurrence of $SU(4)$ Kondo (Borda *et al* 2003, Le Hur and Simon 2003, Le Hur *et al* 2004, Galpin *et al* 2005, Hur *et al* 2007) and its relevance to carbon nanotubes (Choi *et al* 2005, Makarovski *et al* 2007a, 2007b) or the double dot system where Kondo physics might be in competition with RKKY interactions (Craig *et al* 2004, Simon *et al* 2005, Vavilov and Glazman 2005, Martins *et al* 2006).

The subject of Kondo physics and quantum dots is a very vast, and still rapidly developing, field. It is clearly not realistic to cover it in any reasonable way here, and I will only consider in more detail the, admittedly rather specific, aspects more closely related to the subject of this review. Indeed most of the more exotic designs imply at some point that a small quantum dot playing the role of a quantum impurity is connected to a larger mesoscopic object, for which Kondo physics in itself is irrelevant, but such that finite size effects may become important. In other words, the context of Kondo physics and quantum dots makes it almost unavoidable to consider situations where the 'quantum impurity' is connected to an electron gas for which finite size effects are important.

As a consequence, for each such mesoscopic electron reservoir connected to the quantum impurity, two new energy scales enter into the description of the Kondo problem: the corresponding mean level spacing Δ_R and Thouless energy $E_{\rm Th}$. The existence of a finite mean level spacing of the electron reservoir will, for instance, clearly modify the Kondo physics drastically for low temperature $T \ll \Delta_R$. This will affect the conductance (Thimm *et al* 1999, Simon and Affleck 2002, Cornaglia and Balseiro 2003) as well as thermodynamic properties (Cornaglia and Balseiro 2002a, Franzese *et al* 2003, Kaul *et al* 2005), and considerable insight can be gained by considering the properties of the ground states and first few excited states of the system (Kaul *et al* 2006, 2008).

The range of energy between Δ_R and $E_{\rm Th}$ is further characterized by the presence of mesoscopic fluctuations (at all scales in this range) in the local density of states of the reservoir's electron and thus by the fact that the density of states is not flat and featureless. In particular, one may wonder whether a (eventually fluctuating) Kondo temperature can be defined and if physical quantities remain a universal function of the ratio $T/T_{\rm K}$.

To fix the ideas, let us consider the s–d Hamiltonian (5.1) with a local density of states at the impurity site $\nu(\boldsymbol{r}=0;\epsilon) \stackrel{\rm def}{=} \sum_i |\varphi_i(0)|^2 \delta(\epsilon-\epsilon_i)$. In the semiclassical regime, $\nu(\boldsymbol{r}=0;\epsilon)$ can be written as the sum

$$\nu(\epsilon) = \nu_0 + \nu_{\rm fl}(\epsilon), \tag{5.8}$$

where ν_0 is the bulk-like contribution (2.12) (one should of course include here either a realistic band dispersion relation or a cutoff at D_0 to account for the finite bandwidth), and the fluctuating term $\nu_{\rm fl}(\epsilon)$ is a quantum correction associated with the interfering closed orbit contributions (2.15). Because $\nu_{\rm fl}(\epsilon)$ is the sum of rapidly oscillating terms, it will fluctuate not only with respect to the energy ϵ, but also with respect to the position $\boldsymbol{r}$ of the quantum impurity or with respect to the variation of any external parameter that may affect the classical actions S_j (2.4) on the scale $\hbar$. As a consequence, one may think of $\nu_{\rm fl}(\epsilon)$ as a statistical quantity with different realizations corresponding

to various locations of $\boldsymbol{r}$ or obtained by varying an external parameter in such a way that the classical dynamics remains unmodified, but that the phases $\exp(\mathrm{i}S_j/\hbar)$ are randomized.

Let us denote T_{K}^0 the Kondo temperature of the associated bulk system for which $\nu(\epsilon)$ is replaced by ν_0. For $T \gg T_{\mathrm{K}}^0$ it is possible to use a perturbative renormalization-group approach in the same way as in the bulk, but including the mesoscopic fluctuations of the density of states. Following Zaránd and Udvardi (1996), this gives in the one-loop approximation

$$J_{\mathrm{eff}}(D_{\mathrm{eff}}) = \frac{J_0}{1 - J_0 \int_{D_{\mathrm{eff}}}^{D_0} (\mathrm{d}\omega/\omega)\, \nu_\beta(\omega)}, \tag{5.9}$$

with

$$\nu_\beta(\omega) = \frac{\omega}{\pi} \int_{-\infty}^{\infty} \mathrm{d}\epsilon \frac{\nu_{\mathrm{loc}}(\epsilon)}{\omega^2 + \epsilon^2} \tag{5.10}$$

the temperature smoothed density of states (note that the renormalization up to order two loops was given by Zaránd and Udvardi (1996)).

There are two different ways to use the above renormalization-group equation. For some physical realizations, the fluctuations of the local density of states may be very significant, yielding an even larger variation of the Kondo properties because of the exponential dependence in (5.4). In this case, one is mainly interested in the fluctuations of the Kondo temperature (which is now a functional of the local density of states) defined as the *energy scale* separating the weak and strong coupling regimes. One can then use the same approach as in the bulk and define $T_{\mathrm{K}}[\nu_\beta]$ as the temperature at which the one-loop effective interaction diverges, giving the implicit equation

$$J_0 \int_{T_{\mathrm{K}}^*[\nu_\beta]}^{D_0} \frac{\mathrm{d}\omega}{\omega} \nu_\beta(\omega) = 1. \tag{5.11}$$

Examples of systems for which the fluctuations of the density are large enough to justify that one is mainly interested in the fluctuation of the scale T_{K}^* defined by (5.11) include, for instance, the case of 'real' (chemical) impurities in a geometry such that one dimension is not much larger than the Fermi wavelength. This may be either a quantum point contact in a two-dimensional electron gas (Zaránd and Udvardi 1996) or a thin three-dimensional film (Crépieux and Lacroix 2000). In this case there is a high probability that the impurity is located at a place at which the Friedel oscillations (i.e. the term in the oscillating part of the density of states associated with the trajectory bouncing back on the boundary and returning directly to its starting point) are large. In this case, the impurities located at a distance from the boundary such that the interference of the returning orbit is constructive have a significantly larger Kondo temperature. Disordered metals near or beyond the localization transition provide another kind of system with large fluctuations of the local density of states and can lead in this particular case to a finite density of 'free moments' for which the $T_{\mathrm{K}}^*[\nu_\beta]$ corresponding to the space location is actually zero (Kettemann and Mucciolo 2007, Zhuravlev *et al* 2007).

In a typical ballistic or disordered-metallic mesoscopic system with all dimensions much larger than the Fermi wavelength, the fluctuating part of the local density of states ν_{fl} is a quantum correction to the secular term ν_0 and is therefore parametrically smaller. As a consequence the fluctuations of $T_{\mathrm{K}}[\nu_\beta(\omega)]$ defined by (5.11) are not very large compared with T_{K}^0, which if it is taken only as an energy scale is somewhat meaningless.

In the bulk case, T_{K} has however, beyond being an energy scale, another meaning which is to be the parameter entering into universal functions such as f_χ in (5.6). Within this framework, T_{K} is directly (and quantitatively) related to physical observables, and its fluctuations need not be large to be relevant.

In the mesoscopic case, however, there is *a priori* no reason for any physical observable to be a universal function, since the number of 'parameters' defining the problem can be considered as infinite (in the sense that one needs an infinite number of parameters to define the function $\nu(\epsilon)$). For a given temperature $T > T_{\mathrm{K}}^0$ however, it is possible to perform the perturbative renormalization-group analysis leading to the effective interaction strength $J_{\mathrm{eff}}(T)$, (5.9), which amounts to integrating out all degrees of freedom corresponding to energies larger than T. One can assume moreover that the features of the density of states at energies smaller than T will not affect the observables at temperature T. As a consequence, after renormalization, physical quantities can depend only on the parameters T, $J_{\mathrm{eff}}(T)$ and $\nu_\beta(T)$. Dimensional analysis then implies that dimensionless quantities such as $T\chi_{\mathrm{loc}}(T)$ can depend only on one single parameter, the product $\mathcal{J}(T) = \nu_\beta(T) J_{\mathrm{eff}}(T)$. In particular $T\chi_{\mathrm{loc}}(T)$ should be equal for an arbitrary mesoscopic realization and for some bulk system with, at temperature T, the same value of the parameter $\mathcal{J}(T)$. This implies that if one defines the *realization and temperature dependent* Kondo temperature $T_{\mathrm{K}}[\nu_\beta](T)$ by the generalization of (5.7) to the mesoscopic case, namely,

$$T_{\mathrm{K}}[\nu_\beta](T) = \frac{T}{\exp(J_{\mathrm{eff}}(T)\nu_\beta(T))}, \tag{5.12}$$

one obtains, within the one-loop approximation, a quantitative prediction for physical quantities in the mesoscopic case. For instance, one has for the local susceptibility

$$T\chi_{\mathrm{loc}}(T) = f_\chi(T/T_{\mathrm{K}}[\nu_\beta](T)) = f_\chi(1/\exp(J_{\mathrm{eff}}(T)\nu_\beta(T)), \tag{5.13}$$

which relates the universal function f_χ, *computed for the bulk*, to the impurity susceptibility in the mesoscopic case.

From a practical point of view, however, one may first note that with definition (5.12), $T_{\mathrm{K}}[\nu_\beta](T_{\mathrm{K}}^0) = T_{\mathrm{K}}^*[\nu_\beta]$ is the same as the one obtained from (5.11). Furthermore, one finds that there is in general little difference between $f_\chi(T/T_{\mathrm{K}}[\nu_\beta](T))$ and $f_\chi(T/T_{\mathrm{K}}^*[\nu_\beta])$ in a large range of temperatures above T_{K}^0. Therefore, although only (5.13) can be formally justified, I will continue the discussion assuming that in the high temperature regime $T \geqslant T_{\mathrm{K}}^0$, the susceptibility can be described by the universal form $f_\chi(T/T_{\mathrm{K}}^*)$ with a realization (but not temperature) dependent T_{K}^* defined by (5.11).

It turns out that this approach gives a very precise prediction, provided T_{K}^0 is computed from a fit or the two-loop

approximation, and one uses $T_K^* = T_K^0 + \delta T_K$ with δT_K defined by

$$J_0 \int_{T_K^0+\delta T_K}^{D_0} \frac{d\omega}{\omega}(\nu_0 + \delta\nu_\beta(\omega)) = J_0 \int_{T_K^0}^{D_0} \frac{d\omega}{\omega}\nu_0. \qquad (5.14)$$

Kaul *et al* (2005) and Yoo *et al* (2005) showed, by comparison with the exact numerical quantum Monte-Carlo calculations, that, even if one neglects the temperature variation of $T_K[\nu_\beta]$, the predictions from (5.13) are quantitatively extremely precise, even up to temperatures somewhat below T_K^0. This approach therefore provides a simple and quantitative way to discuss the mesoscopic fluctuations of the Kondo properties in the temperature regime $T \geqslant T_K^0$.

The nice thing here is that in this form, all the fluctuations of physical quantities in this regime are expressed in terms of the local density of states that we know how to relate to classical closed orbits. Indeed, (5.14) can be rewritten for $\delta T_K \ll T_K^0$ as

$$\frac{\delta T_K}{T_K^0} = \nu_0^{-1} \int_{T_K^0}^{} \frac{d\omega}{\omega}\nu_\beta(\omega). \qquad (5.15)$$

Furthermore using that $\nu_\beta(\omega) = \nu_{\rm loc}(\epsilon_F + i\omega)$ and the analytical continuation of (2.3) for complex energies in the same way as in (3.18), one can immediately relate the realization dependent Kondo temperature $T_K^*[\nu_\beta]$ to a sum over orbits starting and ending at the impurity site $\boldsymbol{r}_0 = 0$

$$\frac{\delta T_K}{T_K^0} \simeq \frac{1}{\sqrt{2\pi^3\hbar^3}\,\nu_0} \sum_{j:\boldsymbol{r}_0\to\boldsymbol{r}_0} D_j \sin\left[\frac{1}{\hbar}S_j(\epsilon) - \zeta_j\frac{\pi}{2} + \frac{\pi}{4}\right] \times \int_{T_K^0}^{\infty} \frac{d\omega}{\omega}\exp(-t_j\omega/\hbar). \qquad (5.16)$$

The last integral can be approximated by $\log(\frac{T_K^0 t_j}{\hbar})\times \exp(-t_j T_K^0/\hbar)$, thus providing a cutoff for trajectories with a time of return t_j larger than $\hbar/T_K^0$. From this result, the variance of the Kondo temperature can then be obtained. Pairing a trajectory only with itself and, if the electron gas is time-reversal invariant, with its time-reversal symmetric, and using the sum rule (2.24), one has

$$\frac{\langle \delta T_K{}^2\rangle}{T_K^{0\,2}} \simeq \frac{\beta_{\rm RMT}}{\pi\hbar\nu_0}\int_{T_K^0}^{D_{\rm cut}} \frac{d\omega_1'}{\omega_1'}\frac{d\omega_2'}{\omega_2'}\int_0^\infty dt\, P_{\rm cl}^\epsilon(t) e^{-(\omega_1'+\omega_2')t/\hbar}, \qquad (5.17)$$

with $P_{\rm cl}^\epsilon(t)$ the classical probability of return and $\beta_{\rm RMT} = 1$ for a time-reversal non-invariant and 2 for a time-reversal invariant electron gas.

For chaotic systems, using the model (2.26) and (2.27) for the classical probability of return then immediately gives

$$\frac{\langle \delta T_K{}^2\rangle}{T_K^{0\,2}} \simeq \frac{(2\beta_{\rm RMT}\ln 2)}{\pi}\frac{\Delta}{T_K^0}. \qquad (5.18)$$

Interestingly, the same result can be derived from a random-matrix description (Kettemann 2004, Kaul *et al* 2005). Indeed, using (5.15), the variance of δT_K can be expressed in terms of the correlator

$$R_2(\omega_1,\omega_2) \stackrel{\rm def}{=} \frac{1}{\nu_0^2}\int_{\omega_1}\int_{\omega_2} d\omega_1' d\omega_2' \frac{\langle \nu_\beta(\omega_1')\nu_\beta(\omega_2')\rangle}{\omega_1'\omega_2'} \qquad (5.19)$$

$$= \frac{1}{\pi^2\nu_0^2}\int_{\omega_1}\int_{\omega_2} d\omega_1' d\omega_2' \times \sum_{\alpha_1\alpha_2} \frac{\langle(|\varphi_{\alpha_1}|^2 - 1/\mathcal{A})(|\varphi_{\alpha_2}|^2 - 1/\mathcal{A})\rangle}{[(\mu-\epsilon_{\alpha_1})^2 + {\omega_1'}^2][(\mu-\epsilon_{\alpha_2})^2 + {\omega_2'}^2]}. \qquad (5.20)$$

Within the random-matrix model, the wave-functions have a Porter–Thomas distribution ((2.33) or (2.34)), and, neglecting the correlations between eigenstates, which introduce only $1/g$ corrections, one has $\langle(|\varphi_{\alpha_1}|^2 - 1/\mathcal{A})(|\varphi_{\alpha_2}|^2 - 1/\mathcal{A})\rangle = \delta_{\alpha_1\alpha_2}(\beta_{\rm RMT}/\mathcal{A}^2)$. Neglecting the fluctuations of the eigenergies ϵ_α and performing the integral, one then gets

$$R_2(\omega_1,\omega_2) = \frac{\beta_{\rm RMT}\Delta}{\pi}\left(\frac{1}{\omega_2}\ln\frac{\omega_1+\omega_2}{\omega_1} + \frac{1}{\omega_1}\ln\frac{\omega_1+\omega_2}{\omega_2}\right),$$

and thus $R_2(T_K^0, T_K^0) = 2\ln 2(\beta_{\rm RMT}\Delta/\pi T_K^0)$, from which (5.18) derives immediately (Kaul *et al* 2005). Within the random-matrix description, the full distribution of T_K has been obtained by Kettemann (2004).

To conclude this section, we see that the mesoscopic fluctuations of Kondo properties provide an example of physical systems where relatively non-trivial information is eventually encoded in the classical trajectories. Moreover through the sum rule (2.24) and the model (2.26) and (2.27) for the classical probability of return $P_{\rm cl}^\epsilon(t)$, a connection with random-matrix theory can be made.

It should be stressed however that the most interesting aspect of this mesoscopic Kondo problem, namely, the fluctuations of physical properties in the deep Kondo regime ($\Delta <) T \ll T_K^0$, is still an open problem. This regime should be characterized by much larger fluctuations, which should be therefore easier to observe experimentally, as well, as has already been seen in exact numerical Monte-Carlo calculations (Kaul *et al* 2005), as a lack of universality. The perturbative renormalization-group point of view used in the high temperature regime will clearly not be applicable at those temperatures, but Fermi-liquid descriptions based on mean-field slave-boson techniques should nevertheless be able to shed some light on the physics dominating the mesoscopic fluctuations in this regime (Burdin 2007).

6. Coulomb-blockade peak spacing and ground-state spin of ballistic quantum dots

I will turn now to a third (and last) illustration of physical systems for which the interplay between interference and interactions plays a dominant role, namely Coulomb blockade in ballistic quantum dots. Coulomb blockade in itself is an essentially classical effect. It can for instance take place when a small metallic grain is weakly connected to electrical contacts and maintained at a temperature low compared with its charging energy $E_c = e^2/C$ (C is the total capacitance of the grain). In this case, in the lowest order in the grain–leads coupling, the conductance through the grain can be seen as a

succession of transitions between states with different number of electrons N within the grain. Because of the Coulomb interaction between the electrons, these various states will have an energy difference of order E_c, and in general the conservation of the total energy cannot be fulfilled. As a consequence, the transport through the grain is blocked. If, however, the grain is capacitively coupled to an external gate, the latter will also affect in a different way the energy of the states with a different number of electrons. The potential of the gate, V_g, can therefore be tuned so as to adjust the energies of the various states. Thus, as a function of V_g, the conductance through the grain will display an alternation of valleys and peaks (for reviews see Grabert and Devoret (1992) and Kouwenhoven *et al* (1997)).

The Coulomb-blockade process described above does not imply a quantum mechanical effect and can in particular be observed if the mean level spacing, or even the Thouless energy, is much smaller than the temperature. Using very small systems, such as ballistic quantum dots built in GaAs/AlGaAs, one can nevertheless sufficiently increase the one-particle mean level spacing Δ so that $\Delta > T$, and the transport in the dot takes place through a single (or a few) levels. In this regime, one observes fluctuations in both spacings and heights of the conductance peaks, fluctuations which encode non-trivial information about the many-body ground states (with various particle numbers) and possibly a few excited states.

6.1. Constant-interaction model and experimental distributions

As far as the peak-height fluctuations are concerned, predictions (Jalabert *et al* 1992) based on the so-called 'constant-interaction model' appeared to fit the distributions measured in the earlier set of experiments (Chang *et al* 1996, Folk *et al* 1996). In this model, beyond a classical charging term $(Ne)^2/2C$, interactions among the electrons are completely neglected, and Porter–Thomas (i.e. RMT-like) fluctuations are assumed for the one-particle wave-functions. Even at this early stage, however, the presence of correlations between successive peak heights appeared incompatible with a simple RMT description and pointed to the role of short periodic orbits (Narimanov *et al* 1999, 2001, Kaplan 2000). Furthermore, more recent experiments (Patel *et al* 1998) showed a decreased probability of having either very large or very small heights. Several suggestions have been put forward to interpret these deviations, among which are the effects of inelastic scattering (Rupp *et al* 2002), of spin orbit (Held *et al* 2003) or of interactions (Usaj and Baranger 2003). It remains that for peak-height distributions, the constant-interaction model seems to capture a good part of the relevant physics.

The status of the peak-spacing fluctuations, however, is very different. For this quantity, the constant-interaction model gives very striking predictions, since, because of spin degeneracy, the alternation between singly and doubly occupied orbitals, as the number of electrons N in the dot increases, is associated with a strongly bimodal distribution (Sivan *et al* 1996). Indeed, in the zero temperature limit, the position V_g^* of a conduction peak is determined by the energy conservation condition

$$\mathcal{E}^N(V_g^*) + \mu = \mathcal{E}^{N+1}(V_g^*) \tag{6.1}$$

(μ is the chemical potential in the leads). Writing $\mathcal{E}^N(V_g)$, the ground-state energy of the dot with N electrons, as the sum of some 'intrinsic' part E_0^N plus a term $-(C_g/C)eNV_g$ due to the capacitive coupling with the control gate (C_g is the capacitance of the gate to the dot), one obtains that the spacing in V_g between two successive peaks is proportional to the second (discrete) energy difference

$$(V_g^*)_{N\to N+1} - (V_g^*)_{N-1\to N} \propto \delta^2 E_0^N \stackrel{\text{def}}{=} E_0^{N+1} + E_0^{N-1} - 2E_0^N. \tag{6.2}$$

In the constant-interaction model, the ground-state energy of the dot with N electrons is written as

$$E_0^N = \frac{(eN)^2}{2C} + \sum_{\text{occupied } i\sigma} \epsilon_i, \tag{6.3}$$

where the last term is simply the one-particle energy of a system of non-interacting fermions (i and σ are, respectively, the orbital and spin index and ϵ_i the corresponding one-particle energy). One obvious prediction of this model is that the ground-state spin of the dot can be only 0 (for N even) or 1/2 (for N odd). Furthermore, because of spin degeneracy, one gets

$$\delta^2 E_0^N = e^2/C \qquad \text{for odd N,} \tag{6.4}$$

$$\delta^2 E_0^N = e^2/C + (\epsilon_{N/2+1} - \epsilon_{N/2}) \qquad \text{for even N,} \tag{6.5}$$

and the peak spacing is the superposition of a Dirac delta function (corresponding to odd N, referred below as 'odd spacings') and of the nearest neighbour distribution $P_{\text{nns}}(s)$ of ϵ_i (corresponding to even N, referred below as 'even spacings'). For a chaotic system, this is described by random-matrix theory, giving (2.32).

The distributions observed experimentally have very little resemblance to this prediction. The first set of experimental results (Sivan *et al* 1996, Simmel *et al* 1997, 1999) not only did not show any trace of bi-modality, but the width of the distributions seemed to be on a scale of the charging energy rather than on the one of the mean level spacing (as $P_{\text{nns}}(s)$ was expected to be). It was soon realized that these very large distributions were dominated by switching events, that is, by the displacement of trapped charges located between the quantum dot and the control gate. Further experiments (Patel *et al* 1998, Lüscher *et al* 2001, Ong *et al* 2001) were then performed which took care of maintaining the level of the noise associated with switching events well below the mean-level spacing.

In the work of Patel *et al* (1998), seven dots of different sizes (and two different densities) have been investigated for finite as well as zero magnetic field. Measures were taken at an electron temperature of 100 mK, which corresponded to a ratio T/Δ ranging from 20% for the smallest dot (largest Δ) to 60% for the largest dot (smallest Δ). The noise level, estimated by

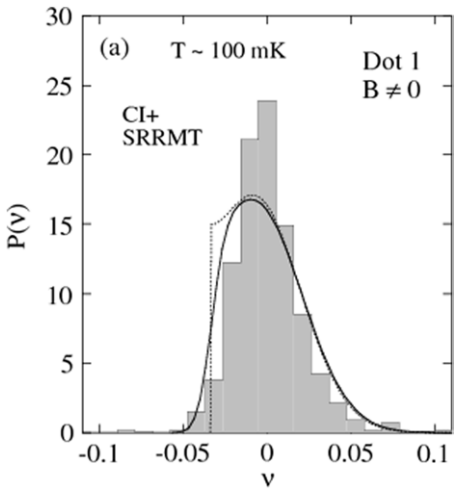

Figure 7. Histogram of the peak-spacing data for dot 1 of Patel *et al* (1998). The noise level and temperature correspond, respectively, to 8% and 20% of the mean level spacing Δ. The electronic density $n_s = 2 \times 10^{11}\,\mathrm{cm}^{-2}$ corresponds to a gas parameter $r_s \simeq 1.24$. Reprinted with permission from Patel *et al* (1998). Copyright 1998 by the American Physical Society. The dotted and solid lines correspond to predictions from the constant interaction plus spin resolved RMT model (CI+SRRMT) presented in this reference.

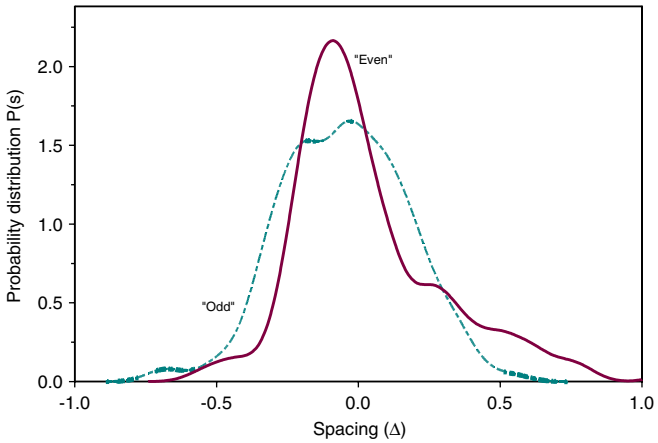

Figure 8. Probability distributions of even (solid line) and odd (dashed line) peak spacings. The data correspond to dot 1 of Patel *et al* (1998), but for a different gate configuration which is such that, in spite of the slightly lower temperature $T = 90\,\mathrm{mK}$, the ratio T/Δ is about 30%. Some visible difference is seen between the odd and even distributions, but the latter clearly do not correspond to the constant-interaction model predictions (6.4) and (6.5). This figure is taken from Ong *et al* (2001).

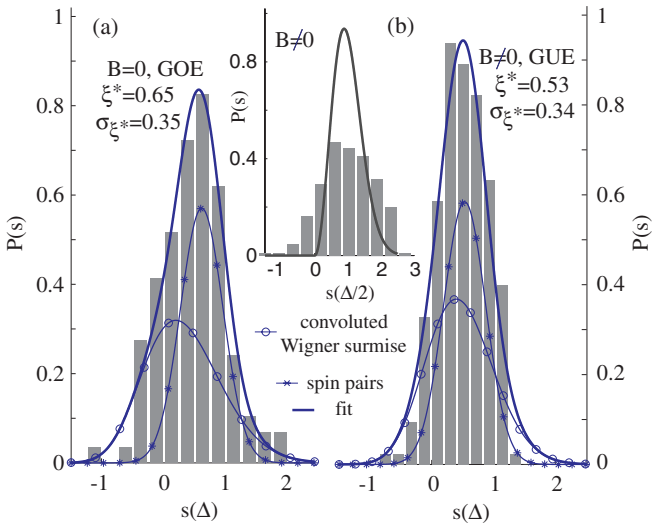

Figure 9. Histogram of the peak-spacing distribution for $B = 0$ (*a*) and $B \neq 0$ (*b*) for the quantum dot studied by Lüscher *et al* (2001). The various solid curves are fit to theoretical predictions discussed in this reference. Inset: the histogram is the same as (b), but with a different scale. Reprinted with permission from Lüscher *et al* (2001). Copyright 2001 by the American Physical Society.

comparing the data when reversing the sign of the magnetic field, ranged from 8% to 94% of the mean level spacing. The peak-spacing distribution obtained for the smallest dot, which turns out to be the one showing less noise ($T/\Delta = 20\%$, noise $= 8\%$ of Δ), is reproduced in figure 7. As seen there, this distribution remains essentially uni-modal and Gaussian, and therefore clearly incompatible with the constant-interaction model predictions.

Data from the same series of dots have been re-analysed by Ong *et al* (2001). In the latter work, special emphasis has been laid on the study of the difference between odd and even spacings predicted by the constant-interaction model. Some odd–even effect could actually be observed for the dots exhibiting the least amount of noise and the smallest T/Δ ratio. This is illustrated in figure 8 which shows separately the distributions of odd and even peak spacings for the same dot as in figure 7, but with a slightly different gate configuration so that the effective area and thus the ratio T/Δ are somewhat larger ($T \simeq 30\%\Delta$). In this case, some differences are seen between the odd and even distributions. They remain however clearly incompatible with the constant-interaction model predictions (6.4)–(6.5). In particular, the total peak-spacing distribution that would be obtained by summing the two curves would, as the one shown in figure 7, be uni-modal and essentially Gaussian.

The same kind of distributions were obtained by Lüscher *et al* (2001) for a dot defined by local oxidation with an atomic-force microscope (rather than electrostatic gating as in (Patel *et al* 1998)). The steepest confining potential obtained in this way made it possible: (i) to limit the shape variation of the dot as the lateral gate voltage V_g is changed; (ii) to use a back gate to increase the electronic density ($n_s \simeq 5.9 \times 10^{11}\,\mathrm{cm}^{-2}$) and thus reduce the gas parameter to a value $r_s \simeq 0.72$; and furthermore (iii) to define a smaller quantum dot so that the electronic temperature $T = 120\,\mathrm{mK}$ used amounts to a significantly smaller ratio $T/\Delta \simeq 5\%$. As illustrated in figure 9 the peak-spacing distributions nevertheless remained uni-modal and essentially Gaussian.

Other experimental evidence that the constant-interaction model does not properly account for the ground-state properties of quantum dots can be obtained by considering their total spin. Indeed, as already mentioned, this model implies a 'naive' occupation of the orbitals, and therefore, for the ground state, a total spin zero for even or one-half for odd number of

particles, respectively. Already in Lüscher *et al* (2001), the parametric variation of the Coulomb-blockade peak position as a function of a weak perpendicular magnetic field, and in particular the existence of kinks (Baranger *et al* 2000), pointed to the existence of ground states with spin one. Such spin-one ground states were further used to observe the Kondo effect in small dots with even number of particles (Kogan *et al* 2003). More systematic studies of ground-state spins were later performed using a stronger in-plane magnetic field coupled to the spin of the electrons through the Zeeman effect (Rokhinson *et al* 2001, Folk *et al* 2001, Lindemann *et al* 2002). Not enough data have been collected in this way to obtain an experimental distribution of ground-state spins. Folk *et al* (2001) have nevertheless obtained clear evidence of the existence of non-trivial (i.e. different from zero or one-half) ground-state spins for semiconductor quantum dots similar to the ones used for figures 7 and 8.

6.2. The universal Hamiltonian

These discrepancies between the constant-interaction model predictions and what was observed pointed clearly to the role played by the residual interactions (i.e. beyond simple charging energy) in these systems and motivated a large number of works ranging from exact numerical calculations on a small system (Sivan *et al* 1996, Berkovits 1998) to various kinds of self-consistent approximations[10]. In the end, however, it seems that, even if not all aspects of the experimental data can as yet be explained, the main features are compatible with a relatively simple Fermi-liquid description provided the role of the spins is properly taken into account (Blanter *et al* 1997, Brouwer *et al* 1999, Baranger *et al* 2000, Ullmo and Baranger 2001, Aleiner *et al* 2002). Once the consequences of a finite temperature are included (Usaj and Baranger 2001, 2002), the predictions for the distributions of Coulomb-blockade peak spacing are actually in very decent agreement with at least some of the experimental data.

What is meant by 'Fermi-liquid' description here is the picture given in section 2.3: an effective 'mean-field' one-particle Hamiltonian $H_{\rm MF}$ which, for a specific system, could be in principle obtained by minimizing the Thomas–Fermi functional (2.48) (see for instance the discussions given in Ullmo *et al* (2001, 2004)) and a weak residual interaction well approximated by the RPA-screened Coulomb interaction, or even its long wave length zero-frequency limit (2.46) and (2.47). As pointed out in section 2.3 there is up to now, for a generic system, no real derivation of this picture from basic principles. The point here is thus not to define an approximation scheme to predict quantitatively the energies of a few specific realizations, but rather to have a model which, once supplemented by some modelling for the fluctuations of the one-particle eigenstates φ_i and energies ϵ_i, typically RMT for chaotic systems, gives correct predictions for statistical properties such as the peak-spacing distribution.

[10] Such as for instance Hartree–Fock (Ahn *et al* 1999, Cohen *et al* 1999, Walker *et al* 1999a, 1999b) or density functional theory (Stopa 1993, 1996, Koskinen *et al* 1997, Lee *et al* 1998, Hirose and Wingreen 1999, 2002, Jiang *et al* 2003a, 2003b).

6.2.1. Time-reversal non-invariant systems. As for orbital magnetism (see section 3.2), time-reversal invariance introduces a slight complication in the discussion because of the Cooper series for which, at $r_s \simeq 1$, high-order terms need to be included and eventually renormalize the effects of the interactions. I shall therefore start the discussion assuming the presence of a magnetic field strong enough to break time-reversal invariance, but nevertheless small enough not to qualitatively change the classical dynamics within the system (and in particular so that it remains in the chaotic regime). In this case, the screened interaction can be treated at the first order of the perturbation.

In the limit where the residual interactions are neglected, the many-body eigenstates are Slater determinants characterized by the occupation numbers $n_{i\sigma} = 0, 1$ of the mean-field Hamiltonian's wave-functions φ_i. For the states such that all singly occupied orbitals have the same spin polarization (which as we shall see are the only ones that can be the ground state of the system), the usual non-degenerate perturbation theory can be used: in first order the eigenstates are unmodified and have an energy (Ullmo and Baranger 2001)

$$E\{n_{i\sigma}\} = E_{\rm sm}(N) + \sum_{i\sigma} n_{i\sigma}\epsilon_i + E^{\rm RI}\{n_{i\sigma}\}, \tag{6.6}$$

$$E^{\rm RI}\{n_{i\sigma}\} = \frac{1}{2}\sum_{i\sigma,j\sigma'} n_{i\sigma}\mathrm{M}_{ij}n_{j\sigma'} - \frac{1}{2}\sum_{i,j,\sigma} n_{i\sigma}\mathrm{N}_{ij}n_{j\sigma}. \tag{6.7}$$

Here $E_{\rm sm}(N)$ is a smooth contribution containing essentially the electrostatic energy $(Ne)^2/2C$, so that the first two terms of (6.6) correspond to the constant-interaction model. The residual-interaction term $E^{\rm RI}\{n_{i\sigma}\}$ is then expressed in terms of

$$\mathrm{M}_{ij} = \int \mathrm{d}\boldsymbol{r}\,\mathrm{d}\boldsymbol{r}'|\varphi_i(\boldsymbol{r})|^2 V_{\rm sc}(\boldsymbol{r}-\boldsymbol{r}')|\varphi_j(\boldsymbol{r}')|^2, \tag{6.8a}$$

$$\mathrm{N}_{ij} = \int \mathrm{d}\boldsymbol{r}\,\mathrm{d}\boldsymbol{r}'\varphi_i(\boldsymbol{r})\varphi_j^*(\boldsymbol{r})V_{\rm sc}(\boldsymbol{r}-\boldsymbol{r}')\varphi_j(\boldsymbol{r}')\varphi_i^*(\boldsymbol{r}'). \tag{6.8b}$$

We shall see below (see section 6.3) that the fluctuations of the M_{ij} and N_{ij} are parametrically smaller than their mean values $\langle\mathrm{M}_{ij}\rangle$ and $\langle\mathrm{N}_{ij}\rangle$. We shall therefore for a moment neglect the former. The quantities $\langle\mathrm{M}_{ij}\rangle$ and $\langle\mathrm{N}_{ij}\rangle$ can be derived by different methods, in particular from the knowledge of the two-point correlation function (2.38*a*) and a Gaussian hypothesis for the higher-order correlation functions (Srednicki 1996, Hortikar and Srednicki 1998). This can also be done directly from the random-plane-wave model. For instance, for a billiard system with only a kinetic energy term in a region of space of volume (or area) $\mathcal{A}$, the insertion of (2.39) in (6.8*a*) gives

$$\langle\mathrm{M}_{ij}\rangle = \int \mathrm{d}\boldsymbol{r}\mathrm{d}\boldsymbol{r}' \sum_{\mu,\mu',\eta,\eta'} \langle a_{i\mu}a^*_{i\mu'}a_{j\eta}a^*_{i\eta'}\rangle \times \exp\left(\frac{\mathrm{i}}{\hbar}[\boldsymbol{r}(\boldsymbol{p}_{i\mu}-\boldsymbol{p}_{i\mu'}) + \boldsymbol{r}'(\boldsymbol{p}_{j\mu}-\boldsymbol{p}_{j\mu'})]\right). \tag{6.9}$$

The Gaussian character of the $a_{i\mu}$ and (2.40) imply $\langle a_{i\mu}a^*_{i\mu}a_{j\eta}a^*_{j\eta'}\rangle = \langle a_{i\mu}a^*_{i\mu'}\rangle\langle a_{j\eta}a^*_{j\eta'}\rangle + \delta_{ij}\langle a_{i\mu}a^*_{i\eta'}\rangle\langle a_{i\eta}a^*_{i\mu'}\rangle = (\mathcal{A}M)^{-1}(\delta_{\mu\mu'}\delta_{\eta\eta'} + \delta_{ij}\delta_{\mu\eta'}\delta_{\eta\mu'})$. One obtains in this way

$$\langle \mathrm{M}_{ij}\rangle = \langle \mathrm{M}_{i\neq j}\rangle + \delta_{ij}\,\delta\langle \mathrm{M}_{ii}\rangle,$$

$$\langle \mathrm{M}_{i\neq j}\rangle = \frac{1}{\mathcal{A}}\hat{V}_{\mathrm{sc}}(0), \tag{6.10}$$

$$\delta\langle \mathrm{M}_{ii}\rangle = \frac{1}{\mathcal{A}}\langle \hat{V}_{\mathrm{sc}}\rangle_{\mathrm{f.s.}}, \tag{6.11}$$

where $\langle \hat{V}_{\mathrm{sc}}\rangle_{\mathrm{f.s.}}$ is the average of $\hat{V}_{\mathrm{sc}}(\boldsymbol{q})$ for $\boldsymbol{q} = \boldsymbol{p} - \boldsymbol{p}'$, $\boldsymbol{p}$ and $\boldsymbol{p}'$ being uniformly distributed on the Fermi surface. For two and three dimensions:

$$\langle \hat{V}_{\mathrm{sc}}\rangle_{\mathrm{f.s.}} = \frac{1}{2\pi}\int \mathrm{d}\theta\, \hat{V}_{\mathrm{sc}}(k_{\mathrm{F}}\sqrt{2(1+\cos\theta)}) \quad (d=2), \tag{6.12}$$

$$= \frac{1}{4\pi}\int \sin(\theta)\mathrm{d}\theta\mathrm{d}\varphi\, \hat{V}_{\mathrm{sc}}(k_{\mathrm{F}}\sqrt{2(1+\cos\theta)}) \quad (d=3). \tag{6.13}$$

A direct calculation gives similarly

$$\langle \mathrm{N}_{i\neq j}\rangle = \delta\langle \mathrm{M}_{ii}\rangle = \frac{1}{\mathcal{A}}\langle \hat{V}_{\mathrm{sc}}\rangle_{\mathrm{f.s.}}. \tag{6.14}$$

The equality between $\langle \mathrm{N}_{i\neq j}\rangle$ and $\delta\langle \mathrm{M}_{ii}\rangle$, which may seem somewhat surprizing at first sight, can be understood as taking root in the invariance of the residual-interaction energy under a change in the spin quantization axis. Finally $\mathrm{N}_{ii} = \mathrm{M}_{ii}$ and thus compensates the corresponding $\sigma = \sigma'$ contribution.

Using the approximation (2.46) and (2.47) for the screened interaction one gets

$$\frac{1}{\mathcal{A}}\hat{V}_{\mathrm{sc}}(0) = \frac{\Delta}{g_{\mathrm{s}}}, \tag{6.15}$$

$$\frac{1}{\mathcal{A}}\langle \hat{V}_{\mathrm{sc}}\rangle_{\mathrm{f.s.}} = J_{\mathrm{RPA}}\Delta, \tag{6.16}$$

where Δ is the mean level spacing between the ϵ_is and $g_{\mathrm{s}} = 2$ the spin degeneracy. The last equation actually defines the dimensionless constant J_{RPA}, which, according to (2.46) and (2.47), is seen to be of order r_s in the high-density ($r_s \to 0$) limit but of order one (although always smaller than 0.5) as r_s becomes of order one. More properly however, $-\langle \hat{V}_{\mathrm{sc}}\rangle_{\mathrm{f.s.}}/\Delta$ should be interpreted as the parameter f_a^0 of Fermi-liquid theory (Pines and Nozieres 1966). This ratio has been computed, as a function of r_s, in a variety of ways. Figure 10 shows for instance, for two-dimensional systems, a comparison between the value J_{RPA} obtained from the RPA (actually Thomas–Fermi) expression (2.46) and the numerical Monte-Carlo evaluation from Tanatar and Ceperley (1989). For $r_s = 1$ for instance, we see that the Monte-Carlo result $\simeq$0.34 is slightly larger than $\langle \hat{V}_{\mathrm{sc}}\rangle_{\mathrm{f.s.}}/\mathcal{A} = 0.28$ obtained from RPA.

A few remarks are in order here. First, we note that, as expected, the mean value of the interaction contribution to the total energy is much smaller than the mean value of the non-interacting contributions (whether the electrostatic term $E_{\mathrm{sm}}(N) \simeq (eN)^2/2C$ or the smooth part of the one-particle energy $\sum n_{i\sigma}\epsilon_i$). In the same way, we shall see below that the fluctuations of the interaction contributions are parametrically smaller than that of the non-interacting term. However, *the mean values* of the M_{ij}s and N_{ij}s are on the same scale (Δ) as *the fluctuations* of the one-particle energies ϵ_i. In the end, it is the interplay between these fluctuations of a large term and the mean value of a smaller one which makes possible a qualitative change from the interactions although they can be treated perturbatively.

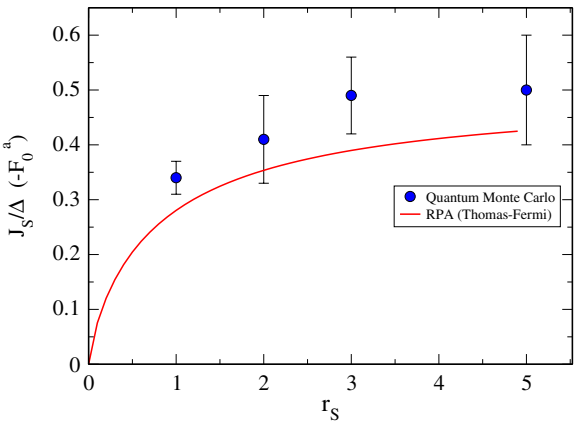

Figure 10. Comparison between the value J_{RPA} obtained from the RPA (actually Thomas–Fermi) expression (2.46) and the numerical Monte-Carlo evaluation of f_a^0 from Tanatar and Ceperley (1989). (Courtesy of Gonzalo Usaj.)

The second point that should be stressed is that, since the variation with the orbital indices of the N_{ij}s and M_{ij}s is neglected, the residual-interaction term (6.7) depends only on the number of same-spin and different-spin pairs of particles, which themselves can be expressed in terms of the total number of particle N and of the difference $(N_+ - N_-)$ between the numbers of majority and minority spins. We consider here only the states such that all singly occupied orbitals have the same-spin polarization: hence $(N_+ - N_-)$ is just twice the total spin S of the system. Keeping in mind that $\delta\langle \mathrm{M}_{ii}\rangle = \langle \mathrm{N}_{ij}\rangle$, we get from simple algebra that

$$E^{\mathrm{RI}}(N,S) = \frac{N(N-1)}{2}\langle \mathrm{M}_{i\neq j}\rangle - \frac{N(N-4)}{4}\langle \mathrm{N}_{ij}\rangle/2 - S(S+1)\langle \mathrm{N}_{ij}\rangle\,. \tag{6.17}$$

The N-dependent part can be safely aggregated with the large smooth term $E_{\mathrm{sm}}(N)$, and it turns out that the residual-interaction term is in this case proportional to the eigenvalue $S(S+1)$ of the total spin square $\hat{\boldsymbol{S}}^2_{\mathrm{tot}}$ of the dot.

As was pointed out by Aleiner and coworkers (Kurland *et al* 2000, Aleiner *et al* 2002) this result is to be expected and is just the consequence of the general symmetries of our problem. Indeed, the description we have used for the eigenstates of the non-interacting system is, within an energy band centred at the Fermi energy and of width the Thouless energy, equivalent to a random-matrix model. This means that as long as one considers an energy scale smaller than the Thouless energy (which is assumed here), there is no preferred direction in the Hilbert space, and any physical quantity should, after averaging over the ensemble, yield a result which is invariant under rotation of the Hilbert

space. As a consequence, if fluctuations are neglected, the residual-interaction Hamiltonian

$$\hat{H}_{\rm RI} = \frac{1}{2} \sum_{\substack{i,j,k,l \\ \sigma\sigma'}} V_{ijkl} c^\dagger_{i\sigma} c^\dagger_{j\sigma'} c_{l\sigma'} c_{k\sigma} \tag{6.18}$$

with

$$V_{ijkl} \stackrel{\rm def}{=} \int {\rm d}\boldsymbol{r}\, {\rm d}\boldsymbol{r}' \varphi^*_i(\boldsymbol{r}) \varphi^*_j(\boldsymbol{r}') \varphi_l(\boldsymbol{r}') \varphi_k(\boldsymbol{r}) \tag{6.19}$$

should have a 'universal form', i.e. should be expressed only in terms of the invariants, which, without time-reversal symmetry, are the number operator $\hat{N}$ and the total spin square $\hat{\boldsymbol{S}}^2_{\rm tot}$.

Using the random-plane-wave model we can get an explicit expression of this universal-Hamiltonian form, including the values of the various parameters. Indeed, inserting (2.39) in (6.19) one has

$$\begin{aligned} V_{ijkl} = & \sum_{\mu\mu'\nu\nu'} a^*_{i\mu} a^*_{j\nu} a_{l\nu'} a_{k\mu'} \\ & \times \int {\rm d}\boldsymbol{r}\, {\rm d}\boldsymbol{r}' \exp\left(\frac{\rm i}{\hbar} [\boldsymbol{r} \cdot (\boldsymbol{p}_{\mu'} - \boldsymbol{p}_\mu) + \boldsymbol{r}' \cdot (\boldsymbol{p}_{\nu'} - \boldsymbol{p}_\nu)] \right) \\ & \times V_{\rm sc}(\boldsymbol{r} - \boldsymbol{r}'). \end{aligned} \tag{6.20}$$

With $\langle a^*_{i\mu} a^*_{j\nu} a_{l\nu'} a_{k\mu'} \rangle = \langle a^*_{i\mu} a_{k\mu'} \rangle \langle a^*_{j\nu} a_{l\nu'} \rangle + \langle a^*_{i\mu} a_{l\nu'} \rangle \langle a^*_{j\nu} a_{k\mu'} \rangle = \frac{1}{M\mathcal{A}} [\delta_{ik}\delta_{\mu\mu'} \cdot \delta_{jl}\delta_{\nu\nu'} + \delta_{il}\delta_{\mu\nu'} \cdot \delta_{jk}\delta_{\nu\mu'}]$, one gets

$$\begin{aligned} \hat{H}_{\rm RI} = & \frac{1}{2} \sum_{\substack{i,j \\ \sigma\sigma'}} \left[\frac{\hat{V}_{\rm sc}(0)}{\mathcal{A}} c^\dagger_{i\sigma} c^\dagger_{j\sigma'} c_{j\sigma'} c_{i\sigma} + \frac{\langle \hat{V}_{\rm sc} \rangle_{\rm f.s.}}{\mathcal{A}} c^\dagger_{i\sigma} c^\dagger_{j\sigma'} c_{i\sigma'} c_{j\sigma} \right] \\ & + \text{fluctuating terms}. \end{aligned} \tag{6.21}$$

We can then use the equalities

$$\begin{aligned} \sum_{\substack{i,j \\ \sigma\sigma'}} c^\dagger_{i\sigma} c^\dagger_{j\sigma'} c_{j\sigma'} c_{i\sigma} &= \hat{N}(\hat{N} - 1), \\ \sum_{\substack{i,j \\ \sigma\sigma'}} c^\dagger_{i\sigma} c^\dagger_{j\sigma'} c_{i\sigma'} c_{j\sigma} &= -\hat{N}^2/2 + 2\hat{N} - 2\hat{\boldsymbol{S}}^2_{\rm tot} \end{aligned}$$

to write the residual-interaction part of the Hamiltonian as the sum of two terms $\hat{H}_{\rm RI} = \hat{H}^{(N)}_{\rm RI} + \hat{H}^{(S)}_{\rm RI}$. The $\hat{N}$-dependent part $\hat{H}^{(N)}_{\rm RI} = (\hat{V}_{\rm sc}(0)/2\mathcal{A})\hat{N}(\hat{N}-1) - (\langle \hat{V}_{\rm sc} \rangle_{\rm f.s.}/\mathcal{A})[(\hat{N}/4)(\hat{N}-4)]$ can be aggregated with the smooth term $E_{\rm sm}(N)$ in (6.6), while the spin part can be expressed as

$$\hat{H}^{(S)}_{\rm RI} = -\frac{\langle \hat{V}_{\rm sc} \rangle_{\rm f.s.}}{\mathcal{A}} \hat{\boldsymbol{S}}^2_{\rm tot} = \Delta\, f^a_0 \hat{\boldsymbol{S}}^2_{\rm tot}. \tag{6.22}$$

We obtain in this relatively pedestrian way that, as expected, when fluctuations are neglected, from general symmetry considerations, the residual interaction is, up to a term which depends smoothly on the total number of particles, proportional to $\hat{\boldsymbol{S}}^2_{\rm tot}$. We moreover obtain that the proportionality constant is $-\langle \hat{V}_{\rm sc} \rangle_{\rm f.s.}/\mathcal{A}$ which should, as before, be interpreted as $\Delta\, f^a_0$.

We now understand that the basic ingredient missing in the constant-interaction model was the existence of the term $\hat{H}^{(S)}_{\rm RI}$. This term tends to polarize the spin of the quantum dot and is of the same order (the mean level spacing Δ) as the cost in one-particle energy associated with moving a particle in higher orbitals. Because the numerical value of $|f^0_a|$ is smaller than one-half, the one-particle energy cost is, *on average*, always numerically larger than the spin polarization term. However, the fluctuations of the one-particle energies ϵ_i taking place also on the scale Δ imply that, depending on the actual value of the ϵ_is, the ground state may actually have a non-minimal spin. This in return will modify the quantities such as peak-spacing distributions. Figure 11 shows the distributions obtained within this model for $r_s = 1$.

6.2.2. Time-reversal invariant systems. Physical effects not contained in the universal Hamiltonian are going to further modify the peak-spacing and spin distributions. Before considering them, let us return to the question of time-reversal invariance, assuming again chaotic dynamics. When this symmetry is present the random matrix is no longer invariant under all unitary transformations, but instead under the smaller group of orthogonal transformations. In addition to $\hat{N}$ and $\hat{S}$, such transformations leave $\hat{T} = \sum_i c_{i\uparrow} c_{i\downarrow}$ also invariant. Taking into account that the residual-interaction Hamiltonian should be invariant under a global phase change of the unperturbed one-particle eigenstates (and thus of the $c_{i\sigma}$, implying that only the product $\hat{T}^\dagger \hat{T}$ should be involved), and that $\hat{H}_{\rm int}$ contains only four-fermion products, we see that an extra term

$$\hat{H}^{(T)}_{\rm RI} = -J_T \hat{T}^\dagger \hat{T} \tag{6.23}$$

should be added to the general form of the universal Hamiltonian (Kurland *et al* 2000, Aleiner *et al* 2002).

Using the form of the plane-wave model valid for time-reversal invariant systems (see discussion below (2.40)), we can as before express the interaction matrix element V_{ijkl} through (6.20). Now, however, $\langle a^*_{i\mu} a^*_{j\nu} a_{l\nu'} a_{k\mu'} \rangle = (1/M\mathcal{A})[\delta_{ik}\delta_{\mu\mu'} \cdot \delta_{jl}\delta_{\nu\nu'} + \delta_{il}\delta_{\mu\nu'} \cdot \delta_{jk}\delta_{\nu\mu'} + \delta_{ij}\delta_{\mu,-\nu} \cdot \delta_{kl}\delta_{\nu',-\mu'}]$, where the last contribution is specifically due to time-reversal invariance. One obtains

$$\langle V_{iijj} \rangle_{\rm TRI} = \langle V_{iiii} \rangle_{\rm TRNI} \delta_{ii} + \frac{1}{\mathcal{A}} \langle \hat{V}_{\rm sc} \rangle_{\rm f.s.}, \tag{6.24}$$

where $\langle V_{iiii} \rangle_{\rm TRNI}$ is the mean value of the completely diagonal matrix element in the time-reversal non-invariant case.

We obtain in this way that J_T equals J_S. What makes the discussion of systems with time-reversal invariance somewhat more difficult is the need to consider higher-order perturbation terms. Indeed, while $\hat{N}$ and $\hat{S}^2$ commute with the unperturbed Hamiltonian, the product $\hat{T}^\dagger \hat{T}$ does not. In particular, the evaluation of second-order corrections in the residual interactions (see (6.27) in the next subsection) shows that the matrix elements associated with the promotion to an empty orbital of two electrons (with opposite spins) occupying the same orbital are now of the order of the mean level spacing Δ. This correction is thus by no means small.

We recognize however in $\hat{H}^{(T)}_{\rm RI}$ the usual pairing Hamiltonian used in the study of superconductivity (except that

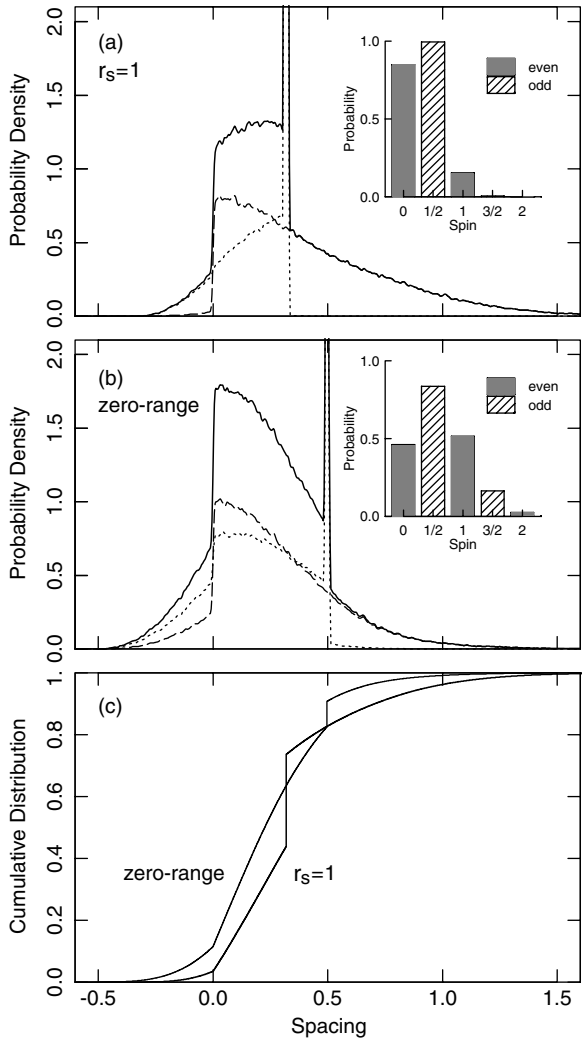

Figure 11. The probability density of Coulomb-blockade peak spacings obtained from the universal-Hamiltonian model at zero temperature. The total distribution (solid) as well as that for N even (dashed) and odd (dotted) is given for two strengths of interactions: (*a*) $r_s = 1$ and (*b*) the zero-range interaction limit $V_{sc}(\boldsymbol{r}-\boldsymbol{r}') = g_s^{-1}\nu_0\delta(\boldsymbol{r}-\boldsymbol{r}')$. The presence of a δ-function in the distribution is particularly clear in the cumulative distribution functions (the integral of the probability density) shown in (*c*). Insets show the probability of occurrence of ground-state spins in the two cases. The spacing is in units of the mean level separation Δ, and the origin corresponds to the classical spacing e^2/C. Reprinted with permission from Ullmo and Baranger (2001). Copyright 2001 by the American Physical Society.

the interaction here is repulsive). It is well known (Abrikosov *et al* 1963) that the important higher-order terms are, as in section 3.2, the Cooper series shown in figure 1. In the same way as for the magnetic response, the main role of these higher-order terms is therefore to renormalize the interaction *in the Cooper channel* according to (4.44) (for $d = 2$). This argument is often used to neglect $\hat{H}_{\rm RI}^{(T)}$ since the renormalized coupling constant goes to zero in the limit $g \to \infty$. However, for typical numbers of particles in the studied experimental dots (e.g. from 340 to 1000 for Patel *et al* (1998) or about 200 for Lüscher *et al* (2001)) the 'large' logarithm $g_s^{-1}\ln(k_F L) \simeq g_s^{-1}\ln(4\pi N/g_s)$ remains in the range [3.5, 4.4]. The higher-order terms therefore reduce the effects of the interactions in the Cooper channel (i.e. a smaller effective parameter J_T should be used) but do not eliminate them completely.

The role of the renormalization in the Cooper channel is presumably the reason why density functional calculations in the local spin density approximation, while they agree very well with the kind of Fermi-liquid description given here for time-reversal non-invariant systems (Ullmo *et al* 2005), significantly overestimate the role of residual interactions in the time-reversal invariant case. The higher-order terms do not appear to be treated correctly in this approach (Jiang *et al* 2003a, 2003b, Ullmo 2004).

6.3. Beyond the universal Hamiltonian

In figure 11 one sees that predictions derived at zero temperature from the universal Hamiltonian are noticeably different from the ones ((6.4) and (6.5)) obtained within the constant-interaction model. In particular, as shown in the inset, the exchange term (6.22) may give rise to a non-zero proportion of non-naive (i.e. different from zero or one-half) ground-state spins. However, even if one accounts for some experimental noise that would smooth some of the sharpest features, the peak-spacing distributions derived in this way do not have the uni-modal/Gaussian-like shape observed experimentally. It is clear that the universal Hamiltonian cannot be the full story. Nevertheless it seems not unreasonable to assume that it provides a decent starting point, which needs to be supplemented by a few other physical effects before a complete description is reached. Among the possible candidates, those that come naturally to the mind are (i) scrambling (Blanter *et al* 1997, Ullmo and Baranger 2001, Usaj and Baranger 2002, Jiang *et al* 2005) and gate effects (Vallejos *et al* 1998, Ullmo and Baranger 2001, Usaj and Baranger 2002, Jiang *et al* 2005), (ii) fluctuations of the residual-interaction terms (Blanter *et al* 1997, Ullmo and Baranger 2001, Usaj and Baranger 2002) and contributions beyond order one (Jacquod and Stone 2000, 2001, Usaj and Baranger 2002) and finally (iii) temperature effects (Usaj and Baranger 2001, 2002). I shall consider each of them separately and end with a discussion about the importance of the more or less chaotic character of the actual dynamics within the dots (Ullmo *et al* 2003).

6.3.1. Scrambling and gate effects. In addition to residual-interaction terms (6.7), there is one noticeable difference between the Fermi-liquid approach that we follow here and the constant-interaction model. Indeed, we have in principle a well-defined procedure to specify the self-consistent confining potential $U_{\rm mf}(\boldsymbol{r})$ seen by the electrons: for a given experimental configuration, it can be obtained by solving the Thomas–Fermi equations (2.51) and (2.52). (Note it is important not to use here for $U_{\rm mf}(\boldsymbol{r})$ the potential obtained from a self-consistent Hartree Fock, or density functional, calculation, as this would mix the scrambling and the gate effects with (some treatment of) the residual interactions.) As one extra electron is added into the quantum dot, or as the voltage of the control gate is changed (without changing the number of electrons in the dot) from $V_g^*(N-1 \to N)$ to $V_g^*(N \to N+1)$, the potential

$U_{\rm mf}(\boldsymbol{r})$ will be modified to a new value $U_{\rm mf}(\boldsymbol{r})+\delta U_{\rm mf}(\boldsymbol{r})$. As a consequence, the one-particle energies ϵ_i, and therefore the corresponding contribution to the ground-state energy, will be modified. The fluctuating part of this energy change is referred to as scrambling (for the variation of N) and gate effects (Vallejos *et al* 1998) (for the variation of $V_{\rm g}$).

An evaluation of the magnitude is analytically possible for the simple geometry of a circular billiard, with in addition (for the gate effect) the assumption that one is using a 'universal gate', i.e. one which is featureless and of the same size as (or larger than) the quantum dot. Under these assumptions, both effects appear to have a variance scaling as $1/g$, to be of the same size and to be comparable in magnitude to the fluctuations of the residual interactions that I shall discuss below (Ullmo and Baranger 2001, Aleiner *et al* 2002, Usaj and Baranger 2002).

A more careful analysis reveals that a realistic modelling of the geometry of the quantum dots, which implies the numerical solution of the Thomas–Fermi self-consistent equations, gives a drastically different picture (Jiang *et al* 2005). Indeed because in practice lateral plunger gates are used rather than the kind of 'universal' ones assumed above, the quantum dots are affected asymmetrically by the gates, and gate effects turns out to be stronger than scrambling. On the other hand, the very smooth confinement associated with a realistic potential $U_{\rm mf}(\boldsymbol{r})$ is much more easily screened than the hard-wall boundaries of a billiard. This turns out to noticeably diminish the magnitude of both scrambling and gate effects: in the configuration studied in Jiang *et al* (2005), very small fluctuations (less than a per cent of the mean-level spacing for the root mean square (rms)) is obtained for scrambling, so that it can presumably be neglected in actual experiments. Because of the use of a lateral plunger gate, gate effects are—again in the configuration studied in Jiang *et al* (2005)—not as small as scrambling, giving rise to fluctuations of the order of 7% of a mean level spacing. This figure remains however smaller than the noise level for all the dots studied in Patel *et al* (1998) (though marginally smaller for the quieter one, used for figure 7).

Since some particular care has been exercized by Lüscher *et al* to minimize gate effects (the lateral gate is not so narrow, and the higher electronic density makes screening more effective) it can be assumed that the quantum dot studied in Lüscher *et al* (2001) shows even smaller gate effects than their evaluation in Jiang *et al* (2005).

6.3.2. Fluctuations of the residual-interaction terms and higher-order correction. Screening and gate effects correspond to changes in the one-particle energies when the smooth effective confining potential is modified for one or another reason. They lead to variations of the parameters of the universal Hamiltonian, but remain in some sense contained within this description.

One may, however, consider terms, associated with the fluctuations of the residual interactions, which are corrections to the universal Hamiltonian. For instance, the off-diagonal (i.e. $(i,j)\neq(k,l)$) coefficients V_{ijkl} (6.19) are zero on average, but have a non-zero variance which can be evaluated easily within the random-plane-wave model. For instance, if $i\neq k,l$ and $j\neq k,l$, considering for simplicity the zero-range approximation $V_{\rm sc}(\boldsymbol{r}-\boldsymbol{r}')=\nu_0^{-1}\delta(\boldsymbol{r}-\boldsymbol{r}')$, and using (2.39) and (2.40) together with the Gaussian character of the $a_{i\mu}$s, one can write

$$\langle|V_{ijkl}|^2\rangle=\frac{1}{\nu_0^2}\frac{1}{(M\mathcal{A})^4}\times\sum_{\mu\nu\tau\eta}\int{\rm d}\boldsymbol{r}\,{\rm d}\boldsymbol{r}'\exp\left[\frac{\rm i}{\hbar}(\boldsymbol{p}_\mu+\boldsymbol{p}_\nu-\boldsymbol{p}_\tau-\boldsymbol{p}_\eta)(\boldsymbol{r}-\boldsymbol{r}')\right]. \tag{6.25}$$

Once the momenta are constrained to be on the Fermi circle (or sphere, this seems to be irrelevant here), the condition $\boldsymbol{p}_\mu+\boldsymbol{p}_\nu=\boldsymbol{p}_\tau+\boldsymbol{p}_\eta$ implied by the integration over space imposes $\boldsymbol{p}_\mu=\boldsymbol{p}_\tau+{\rm O}(\hbar/L)$ and $\boldsymbol{p}_\nu=\boldsymbol{p}_\eta+{\rm O}(\hbar/L)$ or the converse (the ${\rm O}(\hbar/L)$ originates from the width given to the Fermi surface in the RPW model). As a consequence, using that the number of plane waves M scales as the dimensionless conductance g, we get

$$\frac{\langle|V_{ijkl}|^2\rangle}{\Delta^2}\propto\frac{1}{g^2}. \tag{6.26}$$

We see that the smallness of the typical size of the off-diagonal elements is not so much due to the weakness of the interactions (in some sense, $\nu_0^{-1}\delta(\boldsymbol{r}-\boldsymbol{r}')$ is of order one once put in the proper units), but rather originates from the self-averaging associated with the integration over the space of fluctuating quantities.

As the matrix elements are small in the semiclassical limit $g\to\infty$, one can expect for instance that the second-order correction to the ground-state energy

$$E_0^{(2)}=\sum_{j\neq0}\frac{|\langle\Psi_j^N|H_{\rm RI}|\Psi_0^N\rangle|^2}{E_0^{(0)}-E_j^{(0)}} \tag{6.27}$$

also scales as some power of $1/g$. The analysis is made somewhat more complicated by the fact that the number of one-particle levels within the Thouless energy grows with g, and thus also the number of one-particle–one-hole and two-particle–two-hole excitations involved in the summation. A careful analysis performed by Usaj and Baranger (2002) shows nevertheless that the typical size of the second-order correction to the addition energy scales as Δ/g, is numerically already extremely small (less than 2% of Δ) for $N=500$ and can be safely neglected. This furthermore gives us extra confidence that the kind of Fermi-liquid perturbative approach that we are following is indeed valid.

The largest terms neglected by the universal-Hamiltonian description are therefore associated with the fluctuations of the diagonal residual-interaction terms $M_{ij}=V_{ijij}$ and $N_{ij}=V_{ijji}$ that we are going to evaluate more carefully now in the case of a two-dimensional quantum dot.

As before, we shall base our calculation on the random-plane-wave model. It turns out that the variances of the M_{ij}s and N_{ij}s (expressed in units of the mean level spacing Δ) have a dependence on the size of the system. To correctly reproduce this size dependence one needs the second version of the random-plane-wave model, in which condition (2.41) is

imposed on the states used in expansion (2.39), giving a width $\sim\hbar/L$ to the Fermi surface. In this way, one can write the M_{ij}s as

$$M_{ij} = \sum_{\mu_1,\mu_2,\mu_3,\mu_4} a_{i\mu_1} a^*_{i\mu_2} a_{j\mu_3} a^*_{j\mu_4} \delta_{\boldsymbol{p}_{\mu_1}-\boldsymbol{p}_{\mu_2},-\boldsymbol{p}_{\mu_3}+\boldsymbol{p}_{\mu_4}} \hat{V}_{\rm sc}(\boldsymbol{p}_{\mu_1}-\boldsymbol{p}_{\mu_2})$$
$$= \sum_{\boldsymbol{q}} \hat{V}_{\rm sc}(\boldsymbol{q}) W_{i\boldsymbol{q}} W^*_{j\boldsymbol{q}}, \tag{6.28}$$

where one introduces the definition

$$W_{i\boldsymbol{q}} \equiv \sum_{\boldsymbol{p}_{\mu_1}-\boldsymbol{p}_{\mu_2}=\boldsymbol{q}} v_{i\mu_1} v^*_{i\mu_2}. \tag{6.29}$$

The random-matrix model implies

$$\langle a_{i\boldsymbol{k}_1} a^*_{j\boldsymbol{k}_2}\rangle = (k_{\rm F}L)^{-1}\delta_{ij}\delta_{\boldsymbol{p}_1\boldsymbol{p}_2} \qquad \text{if } \delta k < \pi/L, \tag{6.30}$$
$$= 0 \qquad \text{if } \delta k > \pi/L$$

with $\delta k = ||\boldsymbol{k}_1| - k_i|$ and $k_i = \sqrt{2m\epsilon_i}/\hbar$. From this, one deduces

$$\mathrm{var}(M_{i\neq j}) \simeq \frac{1}{A^2}\sum_{\boldsymbol{q}\neq 0} \hat{V}^2_{\rm sc}(\boldsymbol{q})\langle|W_{i\boldsymbol{q}}|^2\rangle\langle|W_{j\boldsymbol{q}}|^2\rangle. \tag{6.31}$$

$|W_{j\boldsymbol{q}}|^2$ can be interpreted as $(2\pi k_i)^{-2}$ times the area of the intersection of two rings of diameter k_i and width $2\pi/L$, centred at a distance $|\boldsymbol{q}| = q$. Simple geometry gives, for $2\pi/L \leqslant |\boldsymbol{q}| \leqslant 2k_i - 2\pi/L$,

$$\langle|W_{i\boldsymbol{q}}|^2\rangle \simeq \frac{4}{(qL)\sqrt{(2k_iL)^2-(qL)^2}}. \tag{6.32}$$

One obtains for $i \simeq j$

$$\mathrm{var}(M_{i\neq j}) \simeq \frac{8}{\pi A^2}\int_{\pi/L}^{2k-\pi/L}\frac{\mathrm{d}q}{q}\frac{V_{\rm sc}(q)^2}{(2kL)^2-(qL)^2}. \tag{6.33}$$

The variance of M_{ii} and N_{ij} and the covariance between M_{ij} and N_{ij} can be computed along the same lines, and one gets

$$\mathrm{var}(N_{i\neq j}) \simeq \frac{2}{\pi A^2}\int_{\pi/L}^{2k-\pi/L}\frac{\mathrm{d}q}{q}\frac{[\hat{V}_{\rm sc}(q)+\hat{V}_{\rm sc}(2k)]^2}{(2kL)^2-(qL)^2}, \tag{6.34}$$

$$\langle M_{i\neq j}N_{i\neq j}\rangle - \langle \mathrm{M}_{i\neq j}\rangle\langle N_{i\neq j}\rangle$$
$$\simeq \frac{4}{\pi A^2}\int_{\pi/L}^{2k-\pi/L}\frac{\mathrm{d}q}{q}\frac{\hat{V}_{\rm sc}(q)[\hat{V}_{\rm sc}(q)+\hat{V}_{\rm sc}(2k)]}{(2kL)^2-(qL)^2}. \tag{6.35}$$

The diagonal part of the direct residual interaction has an extra contribution because of the additional fashion in which the wave-functions can be paired:

$$\mathrm{var}(\mathrm{M}_{ii}) \simeq 2\mathrm{var}(\mathrm{M}^2_{i\neq j})$$
$$+\frac{8}{\pi A^2}\int_{\pi}^{2k-\pi/L}\frac{dq}{q}\frac{\hat{V}_{\rm sc}(q)[\hat{V}_{\rm sc}(0)+\hat{V}_{\rm sc}(\sqrt{(2k)^2-q^2})]}{(2kL)^2-(qL)^2}. \tag{6.36}$$

In the zero-range interaction limit, the expressions for the variance of the Ms and Ns simplify considerably and one finds in this case

$$\mathrm{var}(M_{ij}) = \mathrm{var}(N_{i\neq j}) = \frac{3\Delta^2}{4\pi}\frac{\ln(kL)}{(kL)^2}(1+3\delta_{ij}). \tag{6.37}$$

Note that the decay of the wave-function correlations appearing in the variance produces a factor of $1/k_{\rm F}L$ in the root mean square compared with the mean. The $\ln(kL)$ factor is special for two dimensions; it comes from the $1/kL$ decay of the wave-function correlator in this case.

The variance of M_{ij}s and N_{ij}s scales as $1/g^2$. When adding an extra electron of spin $\tilde{\sigma}$ in the orbital $\tilde{j}$, the variation of the residual interactions (cf (6.7))

$$\delta E^{\rm RI} = \sum_{i\sigma} n_{i\sigma}\mathrm{M}_{i\tilde{j}} - \sum_{i} n_{i\tilde{\sigma}}N_{i\tilde{j}} \tag{6.38}$$

involves in principle a summation over all occupied orbitals. The energy range within which fluctuations take place is however given by the Thouless energy $E_{\rm Th}$. Thus when evaluating the fluctuations of $\delta E^{\rm RI}$, only a number scaling as $g = E_{\rm Th}/\Delta$ of $M_{i\tilde{j}}$ and $N_{i\tilde{j}}$ should be considered as independent. As a result the variance of $\delta E^{\rm RI}$ scales as $g \times 1/g^2 = 1/g$ (and the rms as $1/\sqrt{g}$).

The contributions of the residual interactions to the second difference (6.2) then depend on whether or not the Nth and $(N+1)$th particles occupy the same orbital $\tilde{j}$. In the former case (assuming for simplicity that all orbitals are either doubly occupied or empty before the Nth electron is added) only $M_{\tilde{j},\tilde{j}}$ survive the difference $\delta^2 E^{\rm RI} \equiv \delta E^{\rm RI}[N \to (N+1)] - \delta E^{\rm RI}[(N-1) \to N]$. The variance of $\delta^2 E^{\rm RI}$ then scales as $1/g^2$. This implies in particular that the Dirac delta peak visible in figure 11 is only marginally affected by the fluctuations of the residual interaction. If however the last electron is added into a different orbital, there is no cancellation between $\delta E^{\rm RI}[N \to (N+1)]$ and $\delta E^{\rm RI}[(N-1) \to N]$. Typical values of $\delta^2 E^{\rm RI}$ then scale as $\delta E^{\rm RI}$, i.e. as $1/\sqrt{g}$. For relatively small dots ($N \simeq 100$) this can lead to fluctuations of the order of 10% of a mean level spacing. The fluctuations of the residual interactions therefore give rise to a contribution to the fluctuations of the second energy difference $\delta^2 E_N$ which, for N even (and more precisely when the Nth and $(N+1)$th electrons are added to different orbitals), is parametrically larger (rms $\sim 1/\sqrt{g}$) than the fluctuations due to higher-order terms and numerically larger than the scrambling and gate effects discussed in section 6.3.1.

6.3.3. Finite temperature. Up to this point, we have considered scrambling and gate effects, which can be considered as being due to variations of the one-particle part of the universal Hamiltonian, and fluctuations of residual-interaction terms which are genuine corrections to this Hamiltonian. They give rise to fluctuations with an rms scaling[11] as $1/\sqrt{g}$ and prefactors which, for experimentally realistic parameters, are $<1\%\Delta$ for scrambling, about $7\%\Delta$ for gate effects and of the order of $10\%\Delta$ for residual-interaction fluctuations.

These figures have to be compared with the rms of the experimental noise which, for the dots studied in Patel *et al* (1998), is equal to $8\%\Delta$ for dot 1 (whose data

[11] Note that for scrambling and gate effects, this scaling has been properly derived only in the case of billiard systems, and not for the more realistic case of smooth confinement.

have been used to construct figures 7 and 8), 17%Δ for dot 5, 22%Δ for dot 4 and 40%Δ or above for the four remaining ones.

For dots with a reasonably low level of experimental noise, these extra fluctuating terms (namely, scrambling, gate effects, residual-interaction fluctuations and noise itself) can blur the sharp features of distributions such as the one depicted in figure 11. Nevertheless, they cannot prevent the distribution of the second ground-state energy difference $\delta^2 E_N$ from remaining bi-modal and therefore incompatible with the experimental peak-spacing distributions.

Usaj and Baranger pointed out that an analysis done at zero temperature, and thus concerning only ground-state properties, was however inadequate to interpret the present experiments. For instance, the dots studied in Patel *et al* (1998) were at a temperature ranging from 20% to 60% of a mean level spacing. If one had in mind that the mean level spacing gives the scale of the first many-body excitation, such a difference between T and Δ seemed enough to justify a zero temperature approach, at least for the smallest of the dots (largest Δ). This is especially true for the chaotic system, since level repulsion ensures that the proportion of small spacings is small ($\simeq 8 \times 10^{-3}$ for spacings smaller than $0.2\,\Delta$ in the Gaussian unitary ensemble). Therefore, within the constant-interaction model, the probability of an excited state being populated because of thermal fluctuations could be considered negligible for the smallest dots and reasonably small for the larger ones.

The presence of the exchange term (6.22) makes however a drastic difference in this respect. Consider for instance $\delta E_{S=1,S=0}$, the difference in energy between the $S = 1$ and the $S = 0$ lowest-energy states (assuming N even). It equals on average $\Delta - 2J_S$, that is, for $r_s = 1$ ($J_s \simeq 0.34$), about 30% of the mean level spacing. Moreover level repulsion does not help anymore since it affects only the small spacings. If one assumes GUE fluctuations for the one-particle energies, the probability that $|\delta E_{S=1,S=0}| \leqslant 0.2\Delta$ is $\simeq 0.29$. In other words, even for the smallest of the dots studied in Patel *et al* (1998), there is almost one chance out of three that both the $S = 0$ and the $S = 1$ states are both significantly occupied.

In addition, even when most of the conduction is provided by the ground state, the fact that different-spin states have different degeneracies, and thus different entropies $\mathcal{S} = \ln(2S + 1)$, will modify the conduction peak positions when $T \neq 0$.

The finite temperature linear conductance near a $N - 1 \to N$ transition can be obtained in the rate equation approximation as (Beenakker 1991, Meir and Wingreen 1992, Usaj and Baranger 2001,2002)

$$G(V_g) = \frac{e^2}{\hbar k_B T}\, P_{eq}^N \sum_\alpha \frac{\Gamma_\alpha^L \Gamma_\alpha^R}{\Gamma_\alpha^L + \Gamma_\alpha^R}\, w_\alpha, \tag{6.39}$$

where P_{eq}^N is the *equilibrium* probability that the quantum dot contains N electrons, $\Gamma_\alpha^{L(R)}$ is the partial width of the single-particle level α due to tunnelling to the left (right) lead and w_α is a weight factor given by

$$w_\alpha = \sum_{i,j,\sigma} F_{eq}(j|N) \left|\langle \Psi_j^N | c_{\alpha,\sigma}^\dagger | \Psi_i^{N-1}\rangle\right|^2 \times \frac{1}{1 + \exp[-\beta(E_j - E_i)]}. \tag{6.40}$$

In (6.40), $\mathcal{H}_{QD}|\Psi_j^N\rangle = E_j|\Psi_j^N\rangle$, so that '$j$' labels the many-body states of the quantum dot, and $F_{eq}(j|N)$ is the conditional probability that the eigenstate j is occupied given that the quantum dot contains N electrons.

From this, one can derive the temperature dependence of the peak positions (maxima of $G(V_g)$) when the sole ground states have a notable occupation probability as (Usaj and Baranger 2001, 2002)

$$\mu = E_0^N - E_0^{N-1} - k_B T \ln\left[\frac{2S_0^N + 1}{2S_0^{N-1} + 1}\right] + 2(C_g E_c/e)\delta V_g \tag{6.41}$$

which, up to a factor of $1/2$, amounts to replacing the ground-state energies E_0^N by the free energies $F^N = E_0^N + k_B T \mathcal{S}$.

The general case (conduction through more than one state) leads to more complicated expressions, but can be obtained (Usaj and Baranger 2001, 2002). Both effects—conduction through excited states and displacement of the peaks due to entropy—affect the spacing distribution: at $k_B T \simeq 0.2\Delta$ they already dominate the fluctuation of the residual interactions. This is illustrated in figure 12—taken from Usaj and Baranger (2001)—where it is seen that, once scrambling, gate effects, fluctuation of the residual interactions are already taken into account, raising the temperature from 10% to 20% of the mean level spacing suppresses the bi-modality of the peak-spacing distribution. Already at $T = 20\%\Delta$, this distribution is in reasonable agreement with the experimental result shown in figure 7. As soon as the temperature is further increased (e.g. $T = 30\%\Delta$ for the data in figure 8) or the level of experimental noise becomes significant, one should expect little (or no) even/odd effect or asymmetry in the peak-spacing distributions.

6.3.4. Non-chaotic dots. As we have just seen, starting from a universal-Hamiltonian description, the peak-spacing distributions measured by Patel *et al* can be understood within an approach where finite temperature effects and (experimental) noise—except for the quietest dot—are the most important ingredients. Conversely, the fact that noise and temperature play an important role implies that other features of the modelling are less critical and in that sense are not really probed by these experiments.

The size of the dot studied by Luscher (2001) is however significantly smaller, leading to a ratio $T/\Delta \simeq 5\%$ such that temperature cannot be responsible for the absence of bi-modality in the peak-spacing distribution. The noise level in Lüscher *et al* (2001) is not quoted, but is presumably small enough not to significantly affect the spacing distributions either (Ensslin 2007). The approach based on the universal Hamiltonian plus corrections does not therefore appear to be able to explain the distributions shown in figure 9. Other

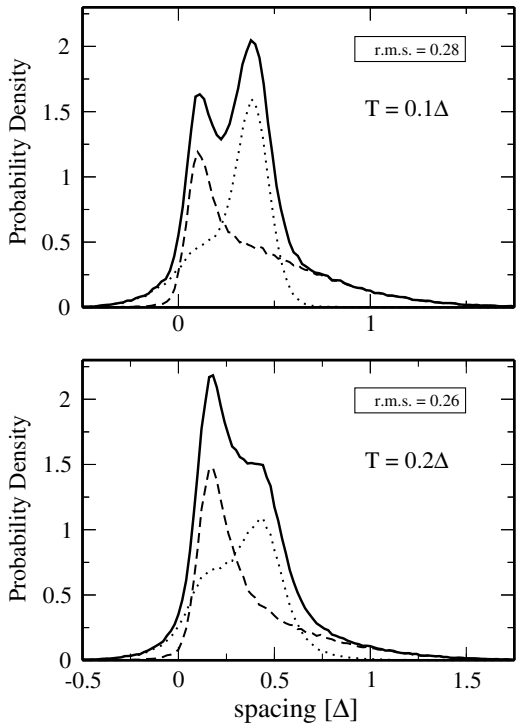

Figure 12. Finite temperature Coulomb-blockade peak-spacing distribution obtained once, in addition to the universal Hamiltonian, scrambling, gate effects, fluctuations of the residual interactions and, more importantly, finite temperature effects, is taken into account. The dotted line corresponds to N odd, the dashed line to N even and the solid one to the total (odd plus even) distribution. $N = 500$ ($g \approx 6$), $J_S = 0.32\Delta$ and $k_B T = 0.1\Delta$ (0.2Δ) in the top (bottom) plot. Reprinted with permission from Usaj and Baranger (2001). Copyright 2001 by the American Physical Society.

mechanisms have to be introduced to understand the statistical properties of peak spacings.

Interestingly, one issue, to which usually little attention is paid, is to know whether using a chaotic model for the dynamics of the electrons in the dot is adequate.

There are in fact good reasons for focusing on chaotic dynamics, the main one being that the behaviour of chaotic systems is universal (in the sense that this behaviour does not depend on the details of the system as long as the latter is in the chaotic regime). Working in the chaotic regime, both experimentally and theoretically, one (happily) avoids messy system-specific considerations.

It remains nevertheless that, even when some care has been exercized, as in Patel *et al* (1998), to bring the quantum dots in the chaotic regime, it is extremely difficult to design a system with smooth confining potential that is without question in the chaotic regime: no known smooth Hamiltonian system is mathematically proved to be in the chaotic regime; furthermore, as any numerical simulations of the classical dynamics of low-dimensional systems readily demonstrate, it is extremely difficult, especially in the presence of a magnetic field, to choose a confining potential without any obvious regions of regular motion.

Clearly the point is not to decide whether any experimental system is in the chaotic regime in the strict mathematical sense, but, for a given setup, how close the system is to fully developed chaos and, from a general perspective, how much the predictions based on the assumption that the dynamics is chaotic are robust with respect to that hypothesis. In other words, the question which has to be answered is how much chaotic dynamics are representative, for what concerns the residual interactions, of the larger class of mixed (i.e. partly chaotic, partly regular) dynamics that one is going to find in practice in experiments.

One consideration may indicate that residual interactions, and as a consequence the ground-state spin and peak-spacing distributions, are sensitive to the degree of regularity of the system under investigation. Indeed, using for simplicity the short range approximation $V_{\text{short range}}(\boldsymbol{r} - \boldsymbol{r}') = \nu_0^{-1}\delta(\boldsymbol{r} - \boldsymbol{r}')$, one can express the completely diagonal matrix element as $V_{iiii} = \mathrm{M}_{ii} = \nu_0^{-1}\int \mathrm{d}\boldsymbol{r}|\varphi_i(\boldsymbol{r})|^4$. Up to the factor ν_0^{-1}, M_{ii} is therefore the inverse participation ratio of the state φ_i, a measure of how much the latter is localized.

Of all possible dynamics, chaotic systems are however the ones showing the least localization, as their wave-functions are spread out uniformly across the whole energetically accessible domain. Integrable and mixed systems on the other hand display various forms of phase-space localization (in the sense that the Wigner or Husimi transforms of the wave-functions are concentrated in some portion of the phase space). The mechanisms underlying this kind of localization (not to be confused with Anderson localization) range from the relatively trivial quantization on invariant tori to more subtle effects of partial barriers[12], but are known in any case to be quite pervasive in mixed systems, even when the phase-space proportion of genuinely regular motion is not very large.

What these considerations imply is that although chaotic systems represent most presumably a universality class as far as residual-interaction effects are concerned, they might be the class for which *residual interactions are the least effective* when considered from the more general point of view of the range of possible dynamics. To go beyond the kind of qualitative arguments used above is complicated by the lack of simple models (such as the random-plane-wave model) for the wave-function fluctuations of mixed systems. What is possible however is to consider some specific example of smooth Hamiltonian systems showing, as a function of some external parameter, various kinds of dynamics. One then can see in these particular cases whether the actual wave-functions fluctuations used as an entry for the computation of the residual interactions induce strong modifications with respect to the chaotic predictions for the ground-state spin or addition-energy distributions.

A convenient choice, introduced by Ullmo *et al* (2003), is the coupled quartic oscillator system ($\boldsymbol{r} = (x, y)$, $r = |\boldsymbol{r}|$)):

$$\hat{H} = \frac{\left(\boldsymbol{p} - \kappa\sqrt{a(\lambda)}x^2\frac{\boldsymbol{r}}{r}\right)^2}{2} + a(\lambda)\left(\frac{x^4}{b} + by^4 + 2\lambda x^2y^2\right). \tag{6.42}$$

Here, $b = \pi/4$, $a(\lambda)$ is a convenient scaling factor chosen so that the mean number of states with energy smaller than ϵ

[12] For instance, Cantori (MacKay *et al* 1984a, 1984b,1987) or stable and unstable manifolds (Bohigas *et al* 1990,1993).

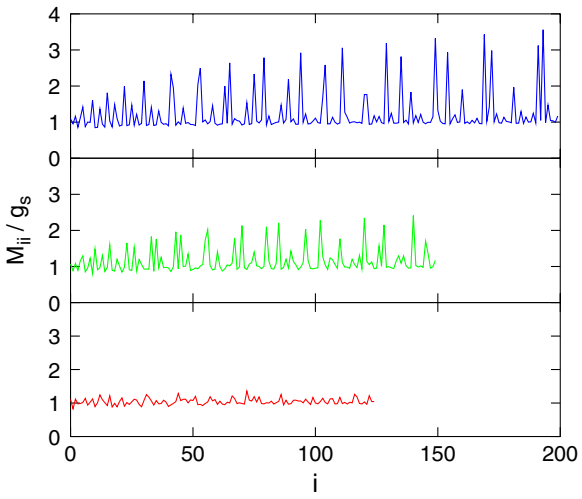

Figure 13. Inverse participation ratio as a function of the orbital index for the symmetry class (+, +). From top down: $(\lambda, \kappa) = (+0.20, 1.00)$ (nearly integrable), $(-0.20, 1.00)$ (mixed) and $(-0.80, 1.00)$ (mostly chaotic). Reprinted with permission from Ullmo *et al* (2003). Copyright 2003 by the American Physical Society.

Table 1. Probabilities $P(S = 2)$, $P(S = 5/2)$ to find a spin two (even N) or five halves (odd N) ground state and average value $\langle \delta S \rangle$ of the ground-state spin augmentation ($\delta S = S$ or $(S - 1/2)$ for even or odd number of particles, respectively), for various dynamical regimes (values of λ) with $\kappa = 1.0$ and $J_s = 0.4$. The last column is the RMT/RPW prediction (Ullmo and Baranger 2001) valid for the hard-chaos regime. Reprinted with permission from Ullmo *et al* (2003). Copyright 2003 by the American Physical Society.

λ	+0.20	−0.20	−0.80	RMT/RPW
$P(S = 2)$	0.13	0.16	0.07	0.01
$P(S = 5/2)$	0.08	0.10	0.02	0.00
$\langle \delta S \rangle$	0.51	0.54	0.38	0.23

is given by $N(\epsilon) = \epsilon^{3/2}$ and λ is the coupling between the oscillators. The parameter κ is chosen such that time-reversal invariance is completely broken.

In figure 13, values of sets of diagonal terms M_{ii} are represented for one symmetry class in various dynamical regimes, showing as expected that their behaviour is very sensitive to the nature of the classical dynamics. Table 1 further shows that this also drastically affects the spin distribution. Indeed, for model (6.42) there is, in the mixed regime, a significant proportion of ground-state spin 2 or 5/2, whereas, as predicted by the universal-Hamiltonian approach, such 'large' spins are essentially absent in the chaotic case. As discussed in Ullmo *et al* (2003), the presence of a large proportion of non-trivial spin is associated with distributions of spacings $\delta^2 E_N$ which differ significantly from the ones expected in the hard-chaos regime. This example illustrates that the question of non-chaoticity, although it has attracted less attention than other issues such as scrambling or fluctuations of residual interactions, may play a significant role in explaining the difference between universal-Hamiltonian predictions and experimental observations and may possibly be as important as the question of temperature.

7. Conclusion

In this review, I have introduced some of the tools from the field of quantum chaos which may be applied to the understanding of various many-body effects in mesoscopic physics. Among these tools, a first group is related to the semiclassical approximations of Green's function. They provide a link between the quantum properties of fully coherent systems and the classical propagation of trajectories within their classical counterparts. This link gives a very intuitive picture for many quantal properties of interest. In particular it makes it possible to introduce naturally the classical probability $P^{\epsilon}_{\rm cl}(\boldsymbol{r}, \boldsymbol{r}', t)$ (cf the M-formula (2.24)) which is central in the understanding of diffusive or chaotic quantum dots. Another set of tools is related to random-matrix theory, and the closely related random-plane-wave models, allowing for a statistical description of individual eigenstates of classically chaotic systems.

The main body of the review, however, has been devoted to the application of these tools to a selected set of examples of physical interest. In particular, I have discussed in detail how the 'semiclassical-Green's-function-based' approximations can be used to compute the interaction contribution to the orbital magnetic response of mesoscopic systems. For diffusive dynamics, I have shown that it was possible to recover in this way, in a simple and transparent manner, most of the results derived previously by diagrammatic perturbation techniques. This approach made it possible furthermore to address the ballistic regime and in particular non-chaotic geometries which are beyond the scope of applicability of the more traditional methods. Another illustration was provided by the mesoscopic fluctuations of Kondo properties for a magnetic impurity in a bounded, fully coherent electron gas, in the temperature regime such that a perturbative renormalization-group treatment can be applied. Here again, semiclassical techniques made it possible to relate some relatively non-trivial properties of the quantum system to the propagation of classical trajectories.

In the last section, turning to an energy scale $\sim\Delta$ for which the semiclassical approximations of Green's function are generally not applicable, I have discussed how the statistical properties of individual wave-functions derived from random ensembles could be applied to the study of peak spacings and ground-state-spin statistics in Coulomb-blockade experiments. In the chaotic regime, I have presented in particular the 'universal-Hamiltonian' description derived by Aleiner and coworkers, in a leading semiclassical (i.e. here $1/g$) approximation, from a generic random-matrix argument. I have furthermore shown how the parameters of this universal Hamiltonian, as well as the evaluation of the leading corrections, can be obtained from the random-plane-wave models. Finally I have discussed some important modifications expected for non-chaotic dots and their possible experimental relevance.

From these various examples emerges a general picture of what the 'quantum chaos' based approach advocated in this review brings to the understanding of the many-body physics of mesoscopic systems. I would like, for the rest

of this concluding section, to discuss it on more general grounds.

In this respect, one important class of systems is such that either the dynamics is genuinely diffusive (i.e. disordered systems) or it is assumed that there is no interesting difference between the actual dynamics and (some limit of) a diffusive one. Ballistic chaotic systems under some circumstances fall into the latter category. Furthermore, extension of the nonlinear super-symmetric σ-model to billiard systems with diffusive boundaries permits many important statistical properties of chaotic systems to be addressed (Blanter *et al* 1998, 2001b) (as long as the former represents a good model for the latter). In these cases, compared with traditional diagrammatic (Altshuler and Aronov1985, Akkermans and Montambaux 2007) or more modern (Efetov 1999, Blanter *et al* 1998, 2001b) techniques, the approach proposed in this review provides mainly an alternative route to the results. Its main advantage is then that this alternative route is closer to the actual physics considered. Indeed, most of the relevant parameters (Thouless energy, transport mean free path) and more generally the physics (in the sense of extracting scales and qualitative behaviours) of these systems are usually discussed in terms of classical quantities (classical probability of return, time to diffuse to the boundary, etc). The semiclassical approach developed here makes it therefore possible to perform the calculations with the same 'language' as the physical discussion and is therefore usually more transparent and intuitive.

For disordered systems this advantage has however to be balanced with the respective strengths of the other approaches. The super-symmetric nonlinear σ-model techniques (Efetov 1999) for instance can address stronger disorders, for which Anderson localization begins to develop, whereas semiclassical methods, as well as diagrammatic perturbations, are limited to the 'good conductor,' i.e. diffusive, regime. In the same way, when the properties of individual wave-functions are considered, and more generally when the physics of interest takes place on the scale of the mean level spacing Δ, super-symmetric nonlinear σ-models provide more systematic (and controlled) ways of performing calculations in the diffusive regime. The manipulation of the random-plane-wave models may on the other hand sometimes involve a little bit of artwork, but it is more flexible in nature and can be adapted to other dynamical regimes (Bäker and Schubert 2002a, 2002b).

Another issue which has to be kept in mind when addressing disordered systems is the one of Hikami boxes (Hikami 1981). In a semiclassical language (see section C3.1 of Akkermans and Montambaux (2007) for a more detailed discussion), a Hikami box can be described as a restricted region of space where two pairs of trajectories closely following each other change partners. An illustration is given in figure 14.

Because the length scale associated with Hikami boxes (namely the mean free path) is well separated from the classical scales associated with diffusion, their computation is not particularly difficult in the diagrammatic approach. Hikami boxes turn out to be more delicate to handle in a purely

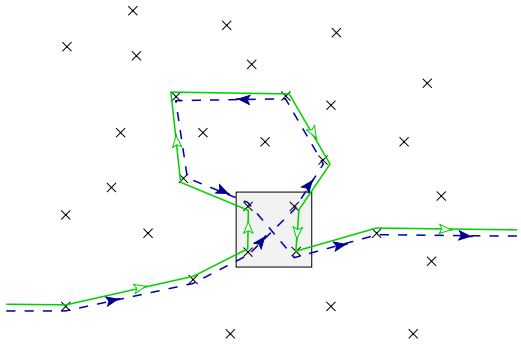

Figure 14. Illustration of an 'Hikami box' (shaded region in this figure). In this particular example the two trajectories switch from following the same path to following the time-reversal path. Such a configuration would typically be found in the calculation of weak localization.

semiclassical description, in particular because questions of current conservation have to be treated with care. Recent works[13] show that these difficulties can actually be overcome, but the level of technicality involved becomes then at least as high as with the diagrammatic approach. The usefulness of the semiclassical approaches when processes related to Hikami boxes are involved is then not anymore their simplicity but the mere fact that they can be applied to a wider class of problems, being not by construction limited to disordered problems.

For questions related to many-body effects in mesoscopic systems, the quantum chaos based approach described in this review therefore serves two purposes. One is to provide a way to perform needed calculations which remains very closely related to the qualitative physics discussed and is therefore very transparent. In this respect it is presumably the best first step into this field for either theoreticians or experimentalists.

It is, furthermore, the only way to address any experimental system which cannot be properly described by diffusive or fully chaotic dynamics. From this perspective, it is interesting to come back to the interpretation of the experimental results of Patel *et al* (1998) and of Lüscher *et al* (2001). In the first case (Patel *et al* 1998), some care has been exercized to bring the dots under study into the chaotic regime (although they are presumably not genuinely there). Furthermore, the value of r_s (i.e. the strength of the interactions) and the relatively high ($\geqslant 20\%\Delta$) temperature make it such that experimental data are compatible with the chaotic modelling of the dynamics (Usaj and Baranger 2001, 2002). On the other hand, the dots studied by Lüscher *et al* have an essentially square shape, and it is much less likely that the associated dynamics are in the fully chaotic regime. Furthermore a smaller value of r_s, and more importantly of the temperature ($\sim 0.05\Delta$), makes their data incompatible with chaotic modelling even if one includes the effects of the gate, scrambling, residual-interaction fluctuations and temperature.

As seen in the last subsection of section 6, the qualitative behaviour of non-chaotic systems can, in some

[13] See for instance Aleiner and Larkin (1996), Richter and Sieber (2002), Adagideli (2003), Muller *et al* (2004, 2005, 2007), Heusler and Haake (2004, 2006), Whitney and Jacquod (2005, 2006), Rahav and Brouwer (2005), Brouwer and Rahav (2006), Jacquod and Whitney (2006).

circumstances, be drastically different. The experimental results of Lüscher *et al* (2001) provide at least one unambiguous example where assuming diffusive or chaotic behaviour is not a reasonable starting point. It therefore demonstrates the interest of having an approach not making too much of an assumption concerning the nature of the classical dynamics within the system, so that at least the question of whether anything new, or interesting, could happen in other dynamical regimes could, at least, be asked. My hope is that this review provides a step in this direction.

Acknowledgments

This review has benefited from many discussions on the various aspects it covers, and in particular with Harold Baranger, Oriol Bohigas, Rodolfo Jalabert, Patricio Leboeuf, Gilles Montambaux, Christophe Texier and Gonzalo Usaj, who has furthermore provided some of the figures included in the Coulomb-blockade section. Harold Baranger, Rodolfo Jalabert, Gilles Montambaux, Christophe Texier, Steve Tomsovic and Marcel Veneroni have in addition read preliminary versions of the paper. Their comments and suggestions have greatly improved the readability of its content.

Appendix A. Screening of the coulomb interaction in a generic quantum dot

The purpose of this appendix is to address the question of screening of the Coulomb interaction in a generic quantum dot. This issue has been studied in the case of diffusive systems (Blanter *et al* 1997, Aleiner *et al* 2002), and I will essentially follow here the approach proposed in section 2.3.2 of Aleiner *et al* (2002). The main motivation will be to illustrate how the semiclassical approach presented in section 2 can be used to generalize some results derived in the more traditional framework of diffusive systems. Here however the exercise will turn out to be somewhat academic since I will need to perform at one point an 'uncontrolled' (read incorrect here) approximation, leading in the end to an unphysical result (equations (A.31) and (A.32) in place of the expected ones (2.51) and (2.52)). Nevertheless, the calculation is in itself instructive enough to be detailed. Identifying clearly the uncontrolled step of the derivation may furthermore help in clarifying the condition of applicability of the original result derived for the diffusive regime, which might turn out to be useful.

In the bulk, the RPA-screened interaction is obtained by considering the Dyson equation for the dressed interaction (see the discussion in section 9 of Fetter and Walecka (1971)):

$$V_{\rm dressed}(\boldsymbol{r}_1,\boldsymbol{r}_2,\omega) = V_{\rm coul}(\boldsymbol{r}_1-\boldsymbol{r}_2) + \int {\rm d}\boldsymbol{r}\int {\rm d}\boldsymbol{r}' V_{\rm coul}(\boldsymbol{r}_1-\boldsymbol{r})\Pi(\boldsymbol{r},\boldsymbol{r}',\omega)V_{\rm dressed}(\boldsymbol{r}',\boldsymbol{r}_2,\omega), \tag{A.1}$$

which is exact if all the one-particle irreducible diagrams are included for the polarization operator Π but gives the RPA approximation if only the (lowest order) bubble diagram

$$\Pi^0(\boldsymbol{r},\boldsymbol{r}',\omega) = g_{\rm s}\int_{-\infty}^{+\infty}\frac{{\rm d}\omega'}{2i\pi}G(\boldsymbol{r},\boldsymbol{r}',\omega+\omega')G(\boldsymbol{r}',\boldsymbol{r},\omega') \tag{A.2}$$

is kept. $G(\boldsymbol{r},\boldsymbol{r}',\omega) = \Theta(\omega)G^R(\boldsymbol{r},\boldsymbol{r}',\omega)+\Theta(-\omega)G^A(\boldsymbol{r},\boldsymbol{r}',\omega)$ is the unperturbed time ordered Green's function, with $\Theta(x)$ the Heaviside function and $g_{\rm s}=2$ is the spin degeneracy factor. In the zero-frequency low-momentum limit one gets (in the bulk) $\Pi^0(\boldsymbol{r},\boldsymbol{r}',\omega=0)\simeq -g_{\rm s}\nu_0\delta(\boldsymbol{r}-\boldsymbol{r}')$, with ν_0 the local density of states per spin (2.13). Inserting this expression for Π^0 in (A.1) gives (2.46) and (2.47).

Let us now consider a mesoscopic system and assume that its typical dimensions are much larger than the screening length. One then expects that the residual screened Coulomb interaction should be very similar to the one in the bulk, and it is therefore natural to approach the question from the same viewpoint. In this case however Green's function is not known exactly, so one needs to resort to semiclassical approximations of $G^{R,A}$ in the expression of Π^0. The difficulty encountered then is that semiclassical approximations are valid for high energies (high ω), and in particular one cannot expect the semiclassical expressions for $G(\boldsymbol{r},\boldsymbol{r}',\omega)$ to be accurate if ω is not much larger than the mean level spacing Δ of the system.

Following Aleiner *et al* (2002), the idea is then, in the spirit of the renormalization-group approach, to integrate out only the 'fast variable' (high-energy part) for which a semiclassical approximation can be used and to deal with the low energy physics by some other methods (based for instance on a random-matrix description (Murthy and Mathur 2002, Murthy and Shankar 2003)). Using the exact expression for the polarization bubble

$$\Pi^0(\boldsymbol{r},\boldsymbol{r}',\omega) = g_{\rm s}\sum_{nn'}\Theta(-\epsilon_n\epsilon_{n'})\frac{\varphi_n^*(\boldsymbol{r}')\varphi_n(\boldsymbol{r})\varphi_{n'}^*(\boldsymbol{r})\varphi_{n'}(\boldsymbol{r}')}{\omega+\epsilon_{n'}-\epsilon_n}(-{\rm sgn}(\epsilon_n)) \tag{A.3}$$

with $(\epsilon_n,\varphi_n(\boldsymbol{r}))$ the one-particle energies and eigenstates, we see that this can be achieved by restricting the sum in the above expression to the pair (n,n') such that at least one energy is outside a band centred at the Fermi energy $\epsilon_{\rm F}$ (taken as the origin of energies) and of width ϵ^* chosen such that $\Delta \ll \epsilon^* \ll E_{\rm Th}$, and whose precise value (once in this range) is expected to be irrelevant. Up to an unimportant boundary term, this is equivalent to restricting the sum to particle–hole energies $\epsilon_{n'}-\epsilon_n$ larger (in absolute value) than ϵ^*. Introducing $\Pi^{R,A}(\boldsymbol{r},\boldsymbol{r}',\omega)\stackrel{\rm def}{=}\lim_{\eta\to 0+}\Pi^0(\boldsymbol{r},\boldsymbol{r}',\omega\pm i\eta)$, the retarded and advanced polarization bubbles, one can therefore write the polarization operator in which only the fast modes are integrated out as

$$\hat{\Pi}_{\epsilon^*}(\boldsymbol{r}',\boldsymbol{r},\tilde{\omega}=0) = \frac{1}{2i\pi}\int\frac{{\rm d}\omega}{\omega}\left[\Pi^R(\boldsymbol{r},\boldsymbol{r}',\omega)-\Pi^A(\boldsymbol{r},\boldsymbol{r}',\omega)\right]\Theta(|\omega|-\epsilon^*). \tag{A.4}$$

The insertion of $\hat{\Pi}_{\epsilon^*}$ in (A.1) will then give the effective interaction describing the low energy ($\leqslant\epsilon^*$) physics of the quantum dot.

Appendix A.1. Calculation of the polarization loop

Let us first consider positive energies $\omega > 0$. Noting that phase cancellation is possible only for the product $G^A G^R$, but not for $G^R G^R$ or $G^A G^A$, one has

$$\Pi^R(\boldsymbol{r},\boldsymbol{r}',\omega) = g_s \int_{-\omega}^{0} \frac{\mathrm{d}\omega'}{2i\pi} G^R(\boldsymbol{r},\boldsymbol{r}',\omega'+\omega+i\eta) G^A(\boldsymbol{r}',\boldsymbol{r},\omega') \tag{A.5}$$

and

$$\Pi^A(\boldsymbol{r},\boldsymbol{r}',\omega) = \Pi^R(\boldsymbol{r}',\boldsymbol{r},\omega)^*. \tag{A.6}$$

Using the semiclassical expressions (2.3) and keeping only the diagonal approximation in which a trajectory j is paired with itself to cancel the oscillating phases, one gets

$$[G^R(\boldsymbol{r},\boldsymbol{r}',\omega+\omega')G^A(\boldsymbol{r}',\boldsymbol{r},\omega')]_{\mathrm{diag}} = \sum_{j:\boldsymbol{r}\to\boldsymbol{r}'} \frac{4\pi^2}{(2\pi\hbar)^{d+1}} |D_j|^2 \exp[\mathrm{i}(S_j(\omega+\omega') - S_j(\omega'))/\hbar]. \tag{A.7}$$

In this equation, one would then like to perform a Taylor expansion of the action

$$(S_j(\omega+\omega') - S_j(\omega')) = (\partial S_j/\partial\epsilon)\omega = t_j\omega, \tag{A.8}$$

where the last equality comes from (2.7). Inserting the unity $\int_0^\infty \delta(t-t_j)$ we obtain

$$[G^R(\boldsymbol{r},\boldsymbol{r}',\omega+\omega')G^A(\boldsymbol{r}',\boldsymbol{r},\omega')]_{\mathrm{diag}} = \frac{4\pi^2}{(2\pi\hbar)^{d+1}} \int_0^\infty \mathrm{d}t \sum_{j:\boldsymbol{r}\to\boldsymbol{r}'} |D_j|^2 \delta(t-t_j) \exp[\mathrm{i}t\omega/\hbar] \tag{A.9}$$

$$= \frac{2\pi\nu_0(\boldsymbol{r}')}{\hbar} \int_0^\infty \mathrm{d}t\, P^\epsilon_{\mathrm{cl}}(\boldsymbol{r},\boldsymbol{r}',t) \exp[\mathrm{i}t\omega/\hbar] \tag{A.10}$$

$$= 2\pi\nu_0(\boldsymbol{r})\hat{P}^\epsilon_{\mathrm{cl}}(\boldsymbol{r},\boldsymbol{r}',\omega), \tag{A.11}$$

where we have used the M-formula (2.24) and $\hat{P}^\epsilon_{\mathrm{cl}}$ is the Fourier transform of the classical probability P^ϵ_{cl}. Interestingly enough $[G^R(\omega+\omega')G^A(\omega')]_{\mathrm{diag}}$ is independent of ω', so that finally

$$\Pi^R(\boldsymbol{r},\boldsymbol{r}',\omega) = -\mathrm{i}\omega g_s \nu_0(\boldsymbol{r}')\hat{P}^\epsilon_{\mathrm{cl}}(\boldsymbol{r},\boldsymbol{r}',\omega). \tag{A.12}$$

Note that the fact that we have computed Π^R, i.e. that $\omega \equiv \omega + \mathrm{i}\eta$, is what is making the Fourier transform in (A.10) convergent. If we had computed Π^A the above approach would have lead to divergences. Π^A should therefore be derived from Π^R using (A.6), giving

$$\Pi^A(\boldsymbol{r},\boldsymbol{r}',\omega) = \mathrm{i}\omega g_s \nu_0(\boldsymbol{r})\hat{P}^\epsilon_{\mathrm{cl}}(\boldsymbol{r}',\boldsymbol{r},\omega). \tag{A.13}$$

For negative ω, Π^A should be calculated first and Π^R derived from it with (A.6), leading to the same result.

Here, one rather important remark is in order. Expression (A.8) assumes obviously that ω is small. This is usually not a significant constraint since the actions S_i are classical quantities, so that the relevant scale is the Fermi energy (or bandwidth) ϵ_{F}. It is therefore enough that $\omega \ll \epsilon_{\mathrm{F}}$ to apply (A.8). However the integral on the left-hand side of (A.4) is not limited to the neighbourhood of the Fermi surface. Replacing $\Pi^{R,A}$ by approximations (A.12) and (A.13) will be incorrect on the edge of the energy band, which will be associated with short distances $|\boldsymbol{r}-\boldsymbol{r}'| < \lambda_{\mathrm{F}}$. This will be the cause of the problems that we shall encounter later on. Let us ignore this issue for the time being and come back to this discussion when it will become obvious that the results obtained in this way are unphysical.

Then, inserting (A.12) and (A.13) into (A.4) and writing $\Theta(x) = 1 - \Theta(-x)$ we get

$$\hat{\Pi}_{\epsilon^*}(\boldsymbol{r}',\boldsymbol{r},\tilde{\omega}=0) = -g_s \int_{-\infty}^{+\infty} \frac{\mathrm{d}\omega}{2\pi} [\nu_0(\boldsymbol{r}')\tilde{P}^\epsilon_{\mathrm{cl}}(\boldsymbol{r},\boldsymbol{r}',\omega) + \nu_0(\boldsymbol{r})\tilde{P}^\epsilon_{\mathrm{cl}}(\boldsymbol{r},\boldsymbol{r}',\omega)](1-\Theta(\epsilon^*-|\omega|)). \tag{A.14}$$

The term proportional to one in the integrand of (A.14) gives rise to $\int(\mathrm{d}\omega/2\pi)\tilde{P}^\epsilon_{\mathrm{cl}}(\boldsymbol{r},\boldsymbol{r}',\omega) = P^\epsilon_{\mathrm{cl}}(\boldsymbol{r},\boldsymbol{r}',t=0)$. To evaluate the remaining term, it is useful to discuss the weight function $\Theta(\epsilon^*-|\omega|)$. Its precise form is irrelevant here, and, rather than the actual Heaviside step function, I shall assume that $\Theta(\epsilon^*-|\omega|)$ is actually a smooth function $\Theta_{\epsilon^*}(\omega)$ which is zero for $|\omega| \gg \epsilon^*$ and one for $|\omega| \ll \epsilon^*$. To fix the idea one can think for instance of $\Theta_{\epsilon^*}(\omega) = \exp(-(1/2)(\omega/\epsilon^*)^2)$, but this precise form will not play any particular role. If one introduces $\tilde{\Theta}_{\epsilon^*}(t)$, the Fourier transform of $\Theta_{\epsilon^*}(\omega)$, one has, with $t^* = \hbar/\epsilon^*$,

$$\tilde{\Theta}_{\epsilon^*}(t) \simeq 1/t^* \qquad \text{for t} \ll \text{t}^*, \tag{A.15}$$

$$= 0 \qquad \text{for t} \gg \text{t}^*, \tag{A.16}$$

$$\int_0^\infty \mathrm{d}t\, \tilde{\Theta}_{\epsilon^*}(t) = \Theta_{\epsilon^*}(\omega=0) = 1. \tag{A.17}$$

Assuming furthermore that $\tilde{\Theta}_{\epsilon^*}(t)$ is a positive function (this hypothesis can be easily relaxed), we see that $\tilde{\Theta}_{\epsilon^*}(t)$ is a density probability (since it is positive and normalized to one) which selects trajectories shorter than t^*. We can thus write

$$\hat{\Pi}_{\epsilon^*}(\boldsymbol{r}',\boldsymbol{r},\tilde{\omega}=0) = -g_s[\nu_0(\boldsymbol{r}')P^\epsilon_{\mathrm{cl}}(\boldsymbol{r},\boldsymbol{r}',t=0) - \tfrac{1}{2}(\nu_0(\boldsymbol{r}')\langle P^\epsilon_{\mathrm{cl}}(\boldsymbol{r},\boldsymbol{r}',t)\rangle_{t\leqslant t^*} + \nu_0(\boldsymbol{r})\langle P^\epsilon_{\mathrm{cl}}(\boldsymbol{r}',\boldsymbol{r},t)\rangle_{t\leqslant t^*})], \tag{A.18}$$

where $\langle f(t)\rangle_{t\leqslant t^*} \stackrel{\mathrm{def}}{=} \int_0^\infty \mathrm{d}t\, f(t)\tilde{\Theta}_{\epsilon^*}(t)$ is the average over time t lesser than t^* of the function $f(t)$.

Now $P^\epsilon_{\mathrm{cl}}(\boldsymbol{r},\boldsymbol{r}',t=0) = \delta(\boldsymbol{r}-\boldsymbol{r}')$. Furthermore, the condition $\Delta \ll \epsilon^* \ll E_{\mathrm{Th}}$ is equivalent to $t_f \ll t^* \ll t_H$, with $t_H = \hbar/\Delta$ the Heisenberg time and t_{f} the time of flight across the system (for ballistic systems) or time needed to diffuse to the boundary (for diffusive systems). We see that the choice of ϵ^* is made precisely so that (i) semiclassical approximations are valid, but also (ii) that most of the range $[0,t^*]$ is such that *for diffusive or chaotic systems* (the case of an integrable or a mixed system should be investigated in this respect), the motion can be assumed to be randomized. Assuming ergodicity we can therefore write

$$\langle P^\epsilon_{\mathrm{cl}}(\boldsymbol{r},\boldsymbol{r}',t)\rangle_{t\leqslant t^*} \simeq \frac{\int \mathrm{d}\boldsymbol{p}\delta(\epsilon_{\mathrm{F}} - H(\boldsymbol{r},\boldsymbol{p}))}{\int \mathrm{d}\boldsymbol{r}''\mathrm{d}\boldsymbol{p}''\delta(\epsilon_{\mathrm{F}} - H(\boldsymbol{r}'',\boldsymbol{p}''))} = \Delta\nu_0(\boldsymbol{r}). \tag{A.19}$$

This eventually leads to

$$\hat{\Pi}_{\epsilon^*}(\boldsymbol{r}', \boldsymbol{r}, \tilde{\omega} = 0) = -g_s[\nu_0(\boldsymbol{r})\delta(\boldsymbol{r} - \boldsymbol{r}') - \nu_0(\boldsymbol{r})\nu_0(\boldsymbol{r}')\Delta], \tag{A.20}$$

where one recognizes the first term as the zero-frequency low-momentum bulk polarization $\Pi^0_{\text{bulk}}(\boldsymbol{r}', \boldsymbol{r}, \tilde{\omega} = 0) = -g_s\nu_0(\boldsymbol{r})\delta(\boldsymbol{r} - \boldsymbol{r}')$, and I will denote by

$$\Pi_{\text{l.r.}} \stackrel{\text{def}}{=} g_s\nu_0(\boldsymbol{r})\nu_0(\boldsymbol{r}')\Delta \tag{A.21}$$

the remaining long range part. For billiard systems for which $\nu_0(\boldsymbol{r}) = (\mathcal{A}\Delta)^{-1} = \text{const.}$, with $\mathcal{A}$ the volume of the system, (A.20) is for instance exactly equation (60) of Aleiner *et al* (2002).

Appendix A.2. Self-consistent equation

In the bulk, both the Coulomb interaction (2.42) and the polarization operator Π^0_{bulk} are translation invariant and the Dyson equation (A.1) can be solved in the momentum representation as

$$\hat{V}_{\text{dressed}}(\boldsymbol{q}) = \frac{\hat{V}_{\text{coul}}(\boldsymbol{q})}{1 - \hat{V}_{\text{coul}}(\boldsymbol{q})\hat{\Pi}^0_{\text{bulk}}(\boldsymbol{q})}. \tag{A.22}$$

The resulting interaction is then short ranged, effectively much weaker than the original Coulomb interaction, and is therefore well adapted for a perturbative treatment.

The difficulty that one encounters in the mesoscopic case is twofold. First, the lack of translational invariance for Π_{ϵ^*} makes, in principle, (A.1) impossible to solve in closed form for a generic spatial variations of $\nu_0(\boldsymbol{r})$. Second, we know that even at the level of electrostatics, the effects of the interactions cannot be small since they will at minima considerably rearrange the static charges within the system. Therefore, even if (A.1) could be solved, there is little chance that the resulting dressed interaction could be effectively used in a perturbative approach starting from the non-interacting electrons' Hamiltonian.

For a quantum dot with a fixed number $(N+1)$ of electrons, one way to solve both these difficulties is to derive a self-consistent equation following one of the standard derivations of the Hartree Fock approximation (Thouless 1961). For this purpose, let us note that any one-body potential $\tilde{U}(\boldsymbol{r})$ can be written formally as the two-body interaction

$$\tilde{V}(\boldsymbol{r}, \boldsymbol{r}') = \frac{1}{N}(\tilde{U}(\boldsymbol{r}) + \tilde{U}(\boldsymbol{r}')) \tag{A.23}$$

since, using for instance a second quantization formalism,

$$\frac{1}{2}\int \mathrm{d}\boldsymbol{r}\,\mathrm{d}\boldsymbol{r}'\hat{\Psi}^\dagger(\boldsymbol{r})\hat{\Psi}^\dagger(\boldsymbol{r}')\tilde{V}(\boldsymbol{r}, \boldsymbol{r}')\hat{\Psi}(\boldsymbol{r}')\hat{\Psi}(\boldsymbol{r}) = \int \mathrm{d}\boldsymbol{r}\hat{\Psi}^\dagger(\boldsymbol{r})\tilde{U}(\boldsymbol{r})\hat{\Psi}(\boldsymbol{r}). \tag{A.24}$$

As a consequence, the total Hamiltonian, as well as the formalism presented in the first part of this appendix, is unmodified if the confining potential $U_{\text{ext}}(\boldsymbol{r})$ and the Coulomb potential $V_{\text{coul}}(\boldsymbol{r}, \boldsymbol{r}')$ are, respectively, replaced by

$$U(\boldsymbol{r}) = U_{\text{ext}}(\boldsymbol{r}) + \tilde{U}(\boldsymbol{r}), \tag{A.25}$$

$$V(\boldsymbol{r}, \boldsymbol{r}') = V_{\text{coul}}(\boldsymbol{r}, \boldsymbol{r}') - \tilde{V}(\boldsymbol{r}, \boldsymbol{r}'). \tag{A.26}$$

One then has freedom in the choice of the function $\tilde{U}(\boldsymbol{r})$ to simplify the Dyson equation. In particular, if we can impose that

$$\int \mathrm{d}\boldsymbol{r}\int \mathrm{d}\boldsymbol{r}' V(\boldsymbol{r}_1, \boldsymbol{r})\Pi_{\text{l.r.}}(\boldsymbol{r}, \boldsymbol{r}')V_{\text{dressed}}(\boldsymbol{r}', \boldsymbol{r}_2) \equiv 0, \tag{A.27}$$

the Dyson equation (A.1) would then have the usual 'bulk-like' form

$$V_{\text{dressed}}(\boldsymbol{r}_1, \boldsymbol{r}_2) = V(\boldsymbol{r}_1, \boldsymbol{r}_2) - \int \mathrm{d}\boldsymbol{r}\int \mathrm{d}\boldsymbol{r}' V(\boldsymbol{r}_1, \boldsymbol{r})\Pi^0_{\text{bulk}}(\boldsymbol{r} - \boldsymbol{r}')V_{\text{dressed}}(\boldsymbol{r}', \boldsymbol{r}_2), \tag{A.28}$$

which, if $\nu_0(\boldsymbol{r})$ and $\tilde{U}(\boldsymbol{r})$ vary slowly on the scale of the bulk screening length κ^{-1}, has the same solution (2.46) and (2.47) as in the bulk.

Now, equation (A.27) might seem at first sight difficult to solve since it involves the unknown function $V_{\text{dressed}}(\boldsymbol{r}', \boldsymbol{r}_2)$. However, since $\Pi_{\text{l.r.}}(\boldsymbol{r}, \boldsymbol{r}')$ does not actually correlate $\boldsymbol{r}$ and $\boldsymbol{r}'$, the two integrals in (A.27) actually decouple, and a sufficient condition to solve this equation is that $\int \mathrm{d}\boldsymbol{r}V(\boldsymbol{r}_1 - \boldsymbol{r})\nu_0(\boldsymbol{r}) \equiv 0$, i.e.

$$\int \mathrm{d}\boldsymbol{r}V_{\text{coul}}(\boldsymbol{r}_1 - \boldsymbol{r})\nu_0(\boldsymbol{r}) = \frac{1}{N}\int \mathrm{d}\boldsymbol{r}\nu_0(\boldsymbol{r})(\tilde{U}(\boldsymbol{r}) + \tilde{U}(\boldsymbol{r}_1)). \tag{A.29}$$

The constant term $\int \mathrm{d}\boldsymbol{r}\nu_0(\boldsymbol{r})\tilde{U}(\boldsymbol{r})/N$ is irrelevant here as it can be eliminated by a constant shift of $\tilde{U}$. One therefore obtains in this way the self-consistent equation

$$\tilde{U}(\boldsymbol{r}_1) = N\Delta\int \mathrm{d}\boldsymbol{r}V_{\text{coul}}(\boldsymbol{r}_1 - \boldsymbol{r})\nu_0(\boldsymbol{r}). \tag{A.30}$$

In other words what we have obtained for the self-consistent potential are the equations

$$U_{\text{mf}}(\boldsymbol{r}) = U_{\text{ext}}(\boldsymbol{r}) + \tilde{N}\Delta\int \mathrm{d}\boldsymbol{r}'\nu_0(\boldsymbol{r}')V_{\text{coul}}(\boldsymbol{r}, \boldsymbol{r}'), \tag{A.31}$$

$$\nu_0(\boldsymbol{r}) = \int \frac{\mathrm{d}\boldsymbol{p}}{(2\pi\hbar)^d}\delta(\mu - U_{\text{mf}}(\boldsymbol{r}) - \boldsymbol{p}^2/2m). \tag{A.32}$$

Appendix A.3. Discussion (C&P)

The above result has a few nice characteristics and one, rather unpleasant, feature. On the bright side, we see that it allows us to clearly separate the two consequences of the long range Coulomb interaction: on the one hand, the appearance of a self-consistent potential (obtained from equation (A.30)) and, on the other hand, the screening process leading to the usual 'bulk' form ((2.46) and (2.47)) of the screened interaction (provided that $\tilde{U}(\boldsymbol{r})$ (and thus $\tilde{V}(\boldsymbol{r}, \boldsymbol{r}')$) varies slowly on the scale of the screening length).

What makes (A.30) less useful however is that it is obviously incorrect. Indeed we know that whatever self-consistent equation we end up writing, it should contain in some approximation the electrostatic equilibrium of the problem. This is not the case here. If the self-consistent potential $U_{\text{mf}}(\boldsymbol{r}) \stackrel{\text{def}}{=} U_{\text{ext}}(\boldsymbol{r}) + \tilde{U}(\boldsymbol{r})$ obtained from (A.30) is well approximated by a constant (giving for instance a

billiard system with weak disorder as was considered in Blanter *et al* (1997) and Aleiner *et al* (2002)), and assuming $(N+1) \gg 1$, one can do the replacement $N\Delta\nu(\boldsymbol{r}) \to n(\boldsymbol{r})$ in (A.30) and write instead

$$\tilde{U}(\boldsymbol{r}_1) = \int \mathrm{d}\boldsymbol{r} V_{\mathrm{coul}}(\boldsymbol{r}_1 - \boldsymbol{r}) n(\boldsymbol{r}), \tag{A.33}$$

i.e. (2.51) and (2.52), which is just the Thomas Fermi equation, from which a plain electrostatic is obtained by neglecting the kinetic energy term $\mathcal{T}_{\mathrm{TF}}[n]$ in (2.48). However for a generic confining potential $U_{\mathrm{ext}}(\boldsymbol{r})$, solutions of (A.30) will not in general be an approximation of the solution of (A.33).

What we see is that, in some sense, equation (A.30) is 'aware' of the properties of the system near the Fermi energy (the density of states $\nu_0(\boldsymbol{r})$), but misses the relevant information at large energies, of the order of the bandwidth. This is to be expected since the polarization operator Π^*_ϵ (A.20) involves only the local density of states at the Fermi energy $\nu_0(\boldsymbol{r})$. This can be tracked back to approximation (A.8) where the action $S(\omega)$ has been linearized near the Fermi energy, eliminating in this way any information relevant to the large (i.e. $\sim \epsilon_{\mathrm{F}}$) energies.

Appendix B. Magnetization and persistent current

In this appendix, I re-derive briefly (for sake of completeness) the basic expressions (3.2) and (4.26) of magnetization and persistent current which are the starting points of the discussion in sections 3 and 4. I follow here the presentation given in Desbois *et al* (1998).

Let us therefore consider a two-dimensional gas ($d = 2$) of electrons confined by a potential $U(\boldsymbol{r})$ ($\boldsymbol{r} = (x, y)$ are the coordinates inside the plane and $\hat{\boldsymbol{z}}$ the unit vector in the perpendicular direction) and interacting through $V(\boldsymbol{r} - \boldsymbol{r}')$. The total Hamiltonian of the system is therefore expressed as $\hat{H} = \hat{H}_0 + \hat{H}_{\mathrm{int}}$ with

$$\hat{H}_0 \stackrel{\mathrm{def}}{=} \int \mathrm{d}\boldsymbol{r} \hat{\Psi}^\dagger(\boldsymbol{r}) \left[\frac{1}{2m} (-\mathrm{i}\hbar\boldsymbol{\nabla} - e\boldsymbol{A}(\boldsymbol{r}))^2 + U(\boldsymbol{r}) \right] \hat{\Psi}(\boldsymbol{r})$$

the non-interacting part ($\boldsymbol{A}(\boldsymbol{r})$ is the vector potential) and

$$\hat{H}_{\mathrm{int}} \stackrel{\mathrm{def}}{=} \frac{1}{2} \int \mathrm{d}\boldsymbol{r}\, \mathrm{d}\boldsymbol{r}' \hat{\Psi}^\dagger(\boldsymbol{r}) \hat{\Psi}^\dagger(\boldsymbol{r}') V(\boldsymbol{r} - \boldsymbol{r}') \hat{\Psi}(\boldsymbol{r}') \hat{\Psi}(\boldsymbol{r}),$$

the interacting part (which is however not going to play any role here). One may furthermore introduce the current density operator

$$\hat{\jmath}(\boldsymbol{r}) = e\hat{\Psi}^\dagger(\boldsymbol{r}) \boldsymbol{v} \hat{\Psi}(\boldsymbol{r})$$

with

$$\boldsymbol{v} \stackrel{\mathrm{def}}{=} \frac{1}{m}(-\mathrm{i}\hbar\boldsymbol{\nabla} - e\boldsymbol{A}(\boldsymbol{r}))$$

the velocity. The variation of the Hamiltonian corresponding to a variation $\delta\boldsymbol{A}$ of the vector potential is then expressed as

$$\delta\hat{H} = -\frac{1}{2} \int \mathrm{d}\boldsymbol{r} \, [\hat{\jmath}(\boldsymbol{r}) \delta\boldsymbol{A}(\boldsymbol{r}) + \delta\boldsymbol{A}(\boldsymbol{r}) \hat{\jmath}(\boldsymbol{r})].$$

Appendix B.1. Uniform perpendicular magnetic field

Let us first consider the case where the variation $\delta\mathbf{A}$ corresponds to a uniform magnetic field $\boldsymbol{B} = \delta B_z \hat{\boldsymbol{z}}$. Equation (3.2) basically states that the magnetization $M_z \stackrel{\mathrm{def}}{=} \langle \hat{M}_z \rangle$, with

$$\hat{M}_z \stackrel{\mathrm{def}}{=} \frac{1}{2} \int \mathrm{d}\boldsymbol{r} (\boldsymbol{r} \times \hat{\jmath}) \cdot \hat{\boldsymbol{z}},$$

is the variable conjugated to δB_z. Indeed, choosing for convenience the symmetric gauge

$$\delta\boldsymbol{A} = \frac{\delta B_z}{2} (\hat{\boldsymbol{z}} \times \boldsymbol{r})$$

and, noting that $(\hat{\boldsymbol{z}} \times \boldsymbol{r})$ and $\boldsymbol{v}$ commute, we have

$$\delta\hat{H} = -\frac{\delta B_z}{2} \int \mathrm{d}\boldsymbol{r} [\hat{\jmath}(\boldsymbol{r}) \cdot (\hat{\boldsymbol{z}} \times \boldsymbol{r}) + (\hat{\boldsymbol{z}} \times \boldsymbol{r}) \cdot \hat{\jmath}(\boldsymbol{r})] = -\delta B_z \hat{M}_z.$$

We see that $\hat{M}_z$ is indeed conjugated to δB_z, and the variation of the grand potential (3.1) gives (3.2).

Appendix B.2. Flux line

Let us now consider a half-infinite line $\mathcal{D} = \{\boldsymbol{r}_0 + \alpha\hat{\boldsymbol{u}};\ (\alpha > 0)\}$ originating from $\boldsymbol{r}_0$ and directed along the unit vector $\hat{\boldsymbol{u}} = (\cos\theta_0, \sin\theta_0)$. One can define the current operator across $\mathcal{D}$

$$\hat{I}^{\mathrm{orb}}(\boldsymbol{r}_0, \theta_0) \stackrel{\mathrm{def}}{=} \int_{\mathcal{D}} \mathrm{d}|\boldsymbol{r} - \boldsymbol{r}_0| \frac{(\boldsymbol{r} - \boldsymbol{r}_0) \times \hat{\jmath}(\boldsymbol{r})}{|\boldsymbol{r} - \boldsymbol{r}_0|} \cdot \hat{\boldsymbol{z}},$$

or if no current escapes to infinity then $\langle I^{\mathrm{orb}} \rangle$ has no θ_0 dependence

$$\hat{I}^{\mathrm{orb}}(\boldsymbol{r}_0) \stackrel{\mathrm{def}}{=} \frac{1}{2\pi} \int \mathrm{d}\boldsymbol{r} \frac{(\boldsymbol{r} - \boldsymbol{r}_0) \times \hat{\jmath}(\boldsymbol{r})}{|\boldsymbol{r} - \boldsymbol{r}_0|^2} \cdot \hat{\boldsymbol{z}}\,.$$

Introducing the vector potential

$$\boldsymbol{A}_{\boldsymbol{r}_0}(\boldsymbol{r}) \stackrel{\mathrm{def}}{=} \frac{1}{2\pi} \Phi \frac{\hat{\boldsymbol{z}} \times (\boldsymbol{r} - \boldsymbol{r}_0)}{|\boldsymbol{r} - \boldsymbol{r}_0|^2}$$

we see that the corresponding magnetic field is $\boldsymbol{B} = \boldsymbol{\nabla} \times \boldsymbol{A}_{\boldsymbol{r}_0} = \Phi\delta(\boldsymbol{r} - \boldsymbol{r}_0)\hat{\boldsymbol{z}}$ and therefore describes a flux line Φ at $\boldsymbol{r}_0$. Following the same steps as above, we find the variation of the Hamiltonian associated with a variation $\delta\Phi$ of the flux to be

$$\begin{aligned} \delta\hat{H} &= -\delta\Phi \int \mathrm{d}\boldsymbol{r}\ \hat{\Psi}^\dagger(\boldsymbol{r}) \frac{1}{2\pi} \frac{\hat{\boldsymbol{z}} \times (\boldsymbol{r} - \boldsymbol{r}_0)}{|\boldsymbol{r} - \boldsymbol{r}_0|^2} \cdot \boldsymbol{v} \hat{\Psi}(\boldsymbol{r}) \\ &= -\delta\Phi \hat{I}^{\mathrm{orb}}(\boldsymbol{r}_0). \end{aligned} \tag{B.1}$$

The orbital current $\hat{I}^{\mathrm{orb}}(\boldsymbol{r}_0)$ is thus conjugated to the flux Φ, which, noting $I \stackrel{\mathrm{def}}{=} \langle I^{\mathrm{orb}} \rangle$, as before directly implies (4.26).

Appendix C. List of symbols

- $a_{i\mu}$: random-plane-wave coefficient (see (2.39))
- a_j: area enclosed by the trajectory j
- $\boldsymbol{A}(\boldsymbol{r})$: vector potential
- $\boldsymbol{B}$: magnetic field
- β: $1/k_{\mathrm{B}}T$
- β_{RMT}: random-matrix ensemble parameter
- C: quantum dot total capacitance

- $C_{\rm g}$: gate dot capacitance
- $\hat{c}^{\dagger}_{\alpha\sigma}$, $\hat{c}_{\alpha\sigma}$: creation and destruction operators
- χ: magnetic susceptibility
- $\chi_{\rm L}$: Landau susceptibility
- $\chi_{\rm loc}$: local susceptibility
- D: diffusion coefficient
- D_j: determinant describing the stability of the trajectory j (cf (2.5))
- D_0: original bandwidth of the Kondo problem
- $D_{\rm eff}$: running bandwidth of the Kondo problem
- Δ: one-particle mean level spacing
- e (<0): particle (electron) charge
- ϵ_κ: one-body energy
- E_N: many-body ground-state energy of a N-particle quantum dot
- $E\{n_{i\sigma}\}$: energy of the many-body state corresponding to the occupation numbers $\{n_{i\sigma}\}$
- $E_{\rm sm}(N)$: smooth part of $E\{n_{i\sigma}\}$
- $E^{\rm RI}\{n_{i\sigma}\}$: contribution of the residual interactions to $E\{n_{i\sigma}\}$
- $E_{\rm c}$: charging energy
- $E_{\rm Th}$: Thouless energy
- $\mathcal{E}_{\rm ext}$: confinement part of the Thomas Fermi functional
- $\mathcal{E}_{\rm coul}$: Coulomb part of the Thomas Fermi functional
- f_0^a: Fermi-liquid parameter
- $f(\epsilon-\mu)$: Fermi function
- $f_\chi(T/T_{\rm K})$: universal function describing the susceptibility for the (bulk) Kondo problem
- $\mathcal{F}_{\rm TF}$: Thomas Fermi functional
- g: dimensionless conductance $E_{\rm Th}/\Delta$
- $g_{\rm s}$: (=2) spin degeneracy
- $G(\boldsymbol{r},\boldsymbol{r}';\epsilon)$: (unperturbed) Green's function
- $G^A(\boldsymbol{r},\boldsymbol{r}';\epsilon)$: (unperturbed) advanced Green's function
- $G^R(\boldsymbol{r},\boldsymbol{r}';\epsilon)$: (unperturbed) retarded Green's function
- $G^R_j(\boldsymbol{r},\boldsymbol{r}';\epsilon)$: semiclassical contribution of the orbit j to the retarded Green's function (see (2.3))
- $\mathcal{G}(\boldsymbol{r},\boldsymbol{r}';\omega)$: (unperturbed) Matsubara Green's function
- $\Gamma^{\rm L(R)}_\alpha$: partial width of the single-particle level α
- $\hbar$: Planck constant
- J_0: bare coupling constant of the Kondo Hamiltonian
- $J_{\rm eff}$: renormalized coupling constant of the Kondo Hamiltonian
- J_S: universal-Hamiltonian coupling constant ($\hat{\boldsymbol{S}}^2_{\rm tot}$ term)
- J_T: universal-Hamiltonian coupling constant ($\hat{T}^\dagger\hat{T}$ term)
- $J_{\rm RPA}$: RPA approximation of J_S
- $k_{\rm F}$: Fermi wave-vector
- $k(\boldsymbol{r})$: $\hbar^{-1}\sqrt{2m(E-U(\boldsymbol{r}))}$
- κ: screening wave-vector
- ℓ: mean free path
- L: characteristic size of the system
- $L_{\rm T}$: thermal length
- L_ϕ: coherence length
- $\lambda_{\rm F}$: Fermi wavelength
- λ_0: electron–electron bare coupling constant
- $\lambda(\Lambda)$: electron–electron running coupling constant
- Λ_0: bare cutoff
- Λ: running cutoff
- $m_{\rm e}$: particle (electron) mass
- M_{ij}: screened interaction matrix element (see (6.8*a*))
- $\langle\hat{M}_z\rangle$: magnetization
- μ: chemical potential
- $\mu_{\rm mc}$: micro-canonical distribution (2.36)
- $\hat{N}$: number operator
- N_{ij}: screened interaction matrix element (see (6.8*b*))
- $\nu_{\rm loc}(\boldsymbol{r},\epsilon)$: local density of states (see (2.11))
- $\nu_0(\boldsymbol{r},\epsilon)$: Weyl (smooth) part of the local density of states (see (2.12))
- $\nu_{\rm osc}(\boldsymbol{r},\epsilon)$: oscillating part of the local density of states (see (2.15))
- $\nu_j(\boldsymbol{r},\epsilon)$: contribution of the orbit j to the oscillating part of the local density of states
- $\nu_\beta(\boldsymbol{r},T)$: thermally averaged local density of states (see (5.10))
- $n(\boldsymbol{r})$: density of particles
- $n(\boldsymbol{r},\boldsymbol{r}')$: non-diagonal element of the particle density matrix (see (3.5))
- Ω: grand potential
- $\Omega^{\rm C}$: Cooper series contribution to the grand potential
- $P^\epsilon_{\rm cl}(\boldsymbol{r},\boldsymbol{r}',t)$: classical probability to go from $\boldsymbol{r}'$ to $\boldsymbol{r}$ in a time t at energy ϵ
- $\tilde{P}^\epsilon_{\rm cl}(\boldsymbol{r},\boldsymbol{r}',\omega)$: Fourier transform of $P^\epsilon_{\rm cl}(\boldsymbol{r},\boldsymbol{r}',t)$
- $\varphi_\kappa(\boldsymbol{r})$: one-body eigenstate
- $[\varphi]_{\rm W}(\boldsymbol{r},\boldsymbol{p})$: Wigner transform of the state φ
- $p_{\rm F}$: Fermi momentum
- $P_{\rm nns}$: nearest neighbour distribution
- ϕ_0: quantum of flux
- ϕ_j: magnetic flux enclosed by the trajectory j
- Ψ^N_j: many-body eigenstate of a quantum dot with N-particles
- $\hat{\Psi}^\dagger_\sigma(\boldsymbol{r})$, $\hat{\Psi}_\sigma(\boldsymbol{r})$: creation and destruction operators
- r_s: electron gas parameter
- $R(x)$: $x/\sinh(x)$
- $\rho(\epsilon)$: total density of states
- $\rho_0(\epsilon)$: Weyl (smooth) part of the total density of states
- $\boldsymbol{S}=(S_x,S_y,S_z)$: spin operator ($=\frac{1}{2}\hbar\boldsymbol{\sigma}$)
- $\hat{\boldsymbol{S}}_{\rm tot}$: quantum dot total spin
- $\boldsymbol{\sigma}=(\sigma_x,\sigma_y,\sigma_z)$: Pauli matrices
- $\Sigma(\boldsymbol{r},\boldsymbol{r}';\omega)$: (free) particle–particle propagator (see (3.16))
- $\Sigma^{(D)}(\boldsymbol{r},\boldsymbol{r}';\omega)$: diagonal part of the particle–particle propagator
- $\Sigma_j(\boldsymbol{r},\boldsymbol{r}';\omega)$: contribution of the orbit j to the diagonal part of the particle–particle propagator
- t_j: time of travel of the orbit j
- $t_{\rm fl}$: time of flight across a ballistic structure
- $t_{\rm T}$: thermal time (see (3.8))
- $\hat{T}^\dagger$: $\sum_i \hat{c}^\dagger_{i\uparrow}\hat{c}_{i\downarrow}$
- $T_{\rm K}$: Kondo temperature (bulk case)
- $T^0_{\rm K}$: average Kondo temperature (mesoscopic case)
- $T^*_{\rm K}[\nu_\beta]$: realization dependent Kondo temperature (mesoscopic case)
- $T_{\rm K}[\nu_\beta](T)$: realization and temperature dependent Kondo temperature (mesoscopic case)
- $\mathcal{T}_{\rm TF}$: kinetic energy part of the Thomas Fermi functional
- $\Theta(u)$: Heaviside function

- $U(\boldsymbol{r})$: one-body potential
- $U_{\rm ext}(\boldsymbol{r})$: one-body external potential
- $U_{\rm mf}(\boldsymbol{r})$: one-body mean-field potential
- $V_{\rm g}$: gate voltage
- $V_{\rm g}^*$: gate voltage corresponding to a conductance peak
- $V(\boldsymbol{r}-\boldsymbol{r}')$: two-body interaction
- $V_{\rm coul}(\boldsymbol{r}-\boldsymbol{r}')$: bare Coulomb interaction
- $V_{\rm sc}(\boldsymbol{r}-\boldsymbol{r}')$: screened Coulomb interaction
- $V_{\text{short range}}(\boldsymbol{r}-\boldsymbol{r}')$: short range approximation $(=\nu_0^{-1}\delta(\boldsymbol{r}-\boldsymbol{r}'))$ of the screened interaction
- V_{ijkl}: screened interaction matrix element (see (6.19))
- $\hat{V}_{\rm sc}(\boldsymbol{q})$: Fourier transform of the screened Coulomb interaction
- $\langle\hat{V}_{\rm sc}\rangle_{\rm f.s.}$: Fermi surface average of $\hat{V}_{\rm sc}(\boldsymbol{q})$
- ζ_j: Maslov index of orbit j

References

Abrikosov A A 1965 *Physics* **2** 5–20
Abrikosov A, Gorkov L and Dzyaloshinski I 1963 *Methods of Quantum Field Theory in Statistical Physics* (Englewood Cliffs, NJ: Prentice-Hall)
Adagideli I 2003 *Phys. Rev.* B **68** 233308
Affleck I and Simon P 2001 *Phys. Rev. Lett.* **86** 2854–7
Agam O, Andreev A V, Simons B D and Altshuler B L 1997 *Phys. Rev. Lett.* **79** 1779
Ahn K H, Richter K and Lee I H 1999 *Phys. Rev. Lett.* **83** 4144–7
Akkermans E and Montambaux G 2007 *Mesoscopic Physics of Electrons and Photons* (Cambdrige: Cambdrige University Press)
Aleiner I L, Brouwer P W and Glazman L I 2002 *Phys. Rep.* **358** 309–440
Aleiner I L and Larkin A I 1996 *Phys. Rev.* B **54** 14423–44
Alhassid Y 2000 *Rev. Mod. Phys.* **72** 895–968
Altshuler B, Aronov A and Zyuzin A 1983 *Sov. Phys.—JETP* **57** 889
Altshuler B L and Aronov A G 1985 *Electron–Electron Interactions in Disordered Systems* ed A L Efros and M Pollak (Amsterdam: North-Holland) pp 1–153
Alt H, Graf H D, Harney H L, Hofferbert R, Lengeler H, Richter A, Schardt P and Weidenmüller H A 1995 *Phys. Rev. Lett.* **74** 62–5
Ambegaokar V and Eckern U 1990*a* *Europhys. Lett.* **13** 733
Ambegaokar V and Eckern U 1990*b* *Phys. Rev. Lett.* **65** 381–4
Anderson P W 1970 *J. Phys. C: Solid State Phys.* **3** 2436–41
Andreev A V, Agam O, Simons B D and Altshuler B L 1996 *Phys. Rev. Lett.* **76** 3947–50
Andrei N 1980 *Phys. Rev. Lett.* **45** 379–82
Argaman N, Imry Y and Smilansky U 1993 *Phys. Rev.* B **47** 4440–57
Argaman N 1996 *Phys. Rev.* B **53** 7035–54
Arnold V 1989 *Mathematical Methods of Classical Mechanics* (New York: Springer)
Aslamazov L G and Larkin A I 1975 *Sov. Phys.—JETP* **40** 321–7
Bäcker A and Schubert R 2002*a* *J. Phys. A: Math. Gen.* **35** 527–38
Bäcker A and Schubert R 2002*b* *J. Phys. A: Math. Gen.* **35** 539–64
Balian R and Bloch C 1972 *Ann. Phys. (N.Y.)* **69** 76–160
Baranger H U, Ullmo D and Galzman L I 2000 *Phys. Rev.* B **61** R2425
Beenakker C W J 1991 *Phys. Rev.* B **44** 1646–56
Berkovits R 1998 *Phys. Rev. Lett.* **81** 2128–31
Berry M V and Tabor M 1977 *J. Phys. A: Math. Gen.* **10** 371–9
Berry M V 1977 *J. Phys. A: Math. Gen.* **10** 2083–91
Berry M V 1985 *Proc. R. Soc. Lond.* A **400** 229–51
Blanter Y M, Mirlin A D and Muzykantskii B A 1997 *Phys. Rev. Lett.* **78** 2449–52
Blanter Y M, Mirlin A D and Muzykantskii B A 1998 *Phys. Rev. Lett.* **80** 4161–4
Blanter Y M, Mirlin A D and Muzykantskii B A 2001a *Phys. Rev.* B **63** 235315
Blanter Y M, Mirlin A D and Muzykantskii B A 2001b *Phys. Rev.* B **63** 235315
Bogomolny E 1988 *Physica* D **31** 169–89
Bohigas O, Giannoni M J and Schmit C 1984a *Phys. Rev. Lett.* **52** 1–4
Bohigas O, Giannoni M J and Schmit C 1984b *J. Physique Lett.* **45** 1015–22
Bohigas O and Leboeuf P 2002 *Phys. Rev. Lett.* **88** 092502
Bohigas O, Tomsovic S and Ullmo D 1990 *Phys. Rev. Lett.* **65** 5–8
Bohigas O, Tomsovic S and Ullmo D 1993 *Phys. Rep.* **223** 43–133
Bohigas O 1991 *Chaos and Quantum Physics* ed M J Giannoni *et al* (Amsterdam: North-Holland) pp 87–199
Borda L, Zaránd G, Hofstetter W, Halperin B I and von Delft J 2003 *Phys. Rev. Lett.* **90** 026602
Bouchiat H and Montambaux G 1989 *J. Physique* **50** 2695–707
Brody T A, Flores J, French J B, Mello P A, Pandey A and Wong S S M 1981 *Rev. Mod. Phys.* **53** 385–479
Brouwer P W, Oreg Y and Halperin B I 1999 *Phys. Rev.* B **60** R13977–80
Brouwer P W and Rahav S 2006 *Phys. Rev.* B **74** 075322
Burdin S 2007 private communication
Cerruti N R and Tomsovic S 2002 *Phys. Rev. Lett.* **88** 054103
Chandrasekhar V, Webb R A, Brady M J, Ketchen M B, Gallagher W J and Kleinsasser A 1991 *Phys. Rev. Lett.* **67** 3578–81
Chang A M, Baranger H U, Pfeiffer L N, West K W and Chang T Y 1996 *Phys. Rev. Lett.* **76** 1695–8
Choi M S, Lopez R and Aguado R 2005 *Phys. Rev. Lett.* **95** 067204
Cohen A, Richter K and Berkovits R 1999 *Phys. Rev.* B **60** 2536–40
Cornaglia P S and Balseiro C A 2002*a* *Phys. Rev.* B **66** 115303
Cornaglia P S and Balseiro C A 2002*b* *Phys. Rev.* B **66** 174404
Cornaglia P S and Balseiro C A 2003 *Phys. Rev. Lett.* **90** 216801
Craig N J, Taylor J M, Lester E A, Marcus C M, Hanson M P and Gossard A C 2004 *Science* **304** 565–7
Creagh S C, Robbins J M and Littlejohn R G 1990 *Phys. Rev.* A **42** 1907–22
Crépieux A and Lacroix C 2000 *Phys. Rev.* B **61** 6785–9
Deblock R, Bel R, Reulet B, Bouchiat H and Mailly D 2002 *Phys. Rev. Lett.* **89** 206803
Delande D, Bommier A and Gay J C 1991 *Phys. Rev. Lett.* **66** 141–4
Delande D and Gay J C 1986 *Phys. Rev. Lett.* **57** 2006–9
Derode A, Roux P and Fink M 1995 *Phys. Rev. Lett.* **75** 4206–9
Desbois J, Ouvry S and Texier C 1998 *Nucl. Phys.* B **528** 727–45
Dobrosavljević V, Kirkpatrick T R and Kotliar B G 1992 *Phys. Rev. Lett.* **69** 1113–6
Eckern U, Schwab P and Ambegaokar V 2004 *Phys. Rev. Lett.* **93** 209701
Eckern U 1991 *Z. Phys.* B **42** 389
Efetov K 1999 *Supersymmetry in Disorder and Chaos* (Cambdrige: Cambdrige University Press)
Ensslin K 2007 private communication
Entin-Wohlman O, Imry Y and Aharony A 2003 *Phys. Rev. Lett.* **91** 046802
Fetter A and Walecka J 1971 *Quantum Theory of Many-Particle Systems* (New York: McGraw-Hill)
Fiete G A, Hersch J S, Heller E J, Manoharan H C, Lutz C P and Eigler D M 2001 *Phys. Rev. Lett.* **86** 2392–5
Fink M, Cassereau D, Derode A, Prada C, Roux P, Tanter M, Thomas J L and Wu F 2000 *Rep. Prog. Phys.* **63** 1933–95
Fink M 1997 *Phys. Today* **50** 34–40
Folk J A, Marcus C M, Berkovits R, Kurland I L, Aleiner I L and Altshuler B L 2001 *Phys. Scr.* T **90** 26
Folk J A, Patel S R, Godijn S F, Huibers A G, Cronenwett S M, Marcus C M, Campman K and Gossard A C 1996 *Phys. Rev. Lett.* **76** 1699–702
Fowler M and Zawadowzki A 1971 *Solid State Commun.* **9** 471–6

Franzese G, Raimondi R and Fazio R 2003 *Europhys. Lett.* **62** 264–70
Galpin M R, Logan D E and Krishnamurthy H R 2005 *Phy. Rev. Lett.* **94** 186406
Gefen Y, Braun D and Montambaux G 1994 *Phys. Rev. Lett.* **73** 154
Glazman L and Pustilnik M 2005 *Nanophysics: Coherence and Transport* ed H Bouchiat *et al* (Amsterdam: Elsevier) pp 427–78
Glazman L and Raikh M 1988 *Pis'ma Zh. Eksp. Teor. Fiz.* **47** 378
Glazman L and Raikh M 1988 *JETP Lett.* **47** 452
Gmachl C, Capasso F, Narimanov E E, Nöckel J U, Stone A D, Faist J, Sivco D L and Cho A Y 1998 *Science* **280** 1556–64
Goldhaber-Gordon D, Shtrikman H, Mahalu D, Abusch-Magder D, Meirav U and Kastner M 1998 *Nature* **391** 156
Goldstein H 1964 *Mécanique Classique* (Paris: Presses Universitaire de France)
Grabert H and Devoret M H (ed) 1992 *Single Charge Tunneling* (London: Plenum)
Gutzwiller M C 1970 *J. Math. Phys.* **11** 1791–806
Gutzwiller M C 1971 *J. Math. Phys.* **12** 343–58
Gutzwiller M C 1990 *Chaos in Classical and Quantum Mechanics* (New York: Springer)
Gutzwiller M 1991 *Chaos and Quantum Physics* ed M J Giannoni *et al* (Amsterdam: North-Holland) p 201
Hannay J H and Ozorio de Almeida A M 1984 *J. Phys. A: Math. Gen.* **17** 3429
Held K, Eisenberg E and Altshuler B L 2003 *Phys. Rev. Lett.* **90** 106802
Hensinger W K *et al* 2001 *Nature* **412** 52–5
Heusler S, Muller S, Braun P and Haake F 2006 *Phys. Rev. Lett.* **96** 066804
Hewson A 1993 *The Kondo Problem to Heavy Fermions* (Cambridge: Cambridge University Press)
Hikami S 1981 *Phys. Rev.* B **24** 2671–9
Hirose K and Wingreen N S 1999 *Phys. Rev.* B **59** 4604–7
Hirose K and Wingreen N S 2002 *Phys. Rev.* B **65** 193305-1–4
Hortikar S and Srednicki M 1998 *Phys. Rev. Lett.* **80** 1646–9
Hur K L, Simon P and Loss D 2007 *Phys. Rev.* B **75** 035332
Jacquod P and Stone D A 2000 *Phys. Rev. Lett.* **84** 3938–41
Jacquod P and Stone A D 2001 *Phys. Rev.* B **64** 214416
Jacquod P and Whitney R S 2006 *Phys. Rev.* B **73** 195115
Jalabert R A, Stone A D and Alhassid Y 1992 *Phys. Rev. Lett.* **68** 3468–71
Jariwala E M Q, Mohanty P, Ketchen M B and Webb R A 2001 *Phys. Rev. Lett.* **86** 1594–7
Jiang H, Baranger H U and Yang W 2003a *Phys. Rev.* B **68** 165337
Jiang H, Baranger H U and Yang W 2003b *Phys. Rev. Lett.* **90** 026806
Jiang H, Ullmo D, Yang W and Baranger H U 2005 *Phys. Rev.* B **71** 085313
Kaplan L 2000 *Phys. Rev.* E **62** 3476–88
Kaul R K, Ullmo D, Chandrasekharan S and Baranger H U 2005 *Europhys. Lett.* **71** 973–9
Kaul R, Zaránd G, Chandrasekharan S, Ullmo D and Baranger H 2006 *Phys. Rev. Lett.* **96** 176802
Kaul R, Zaránd G, Chandrasekharan S, Ullmo D and Baranger H 2008 in preparation
Kettemann S and Mucciolo E R 2006 *Pis'ma Zh. Eksp. Teor. Fiz.* **83** 284
Kettemann S and Mucciolo E R 2006 *JETP Lett.* **83** 240
Kettemann S and Mucciolo E R 2007 *Phys. Rev.* B **75** 184407
Kettemann S 2004 *Quantum Information and Decoherence in Nanosystems* ed D C Glattli *et al* (Vietnam: Gioi Publishers) p 259 (*Preprint* cond-mat/0409317)
Kogan A, Granger G, Kastner M A, Goldhaber-Gordon D and Shtrikman H 2003 *Phys. Rev.* B **67** 113309
Kondo J 1964 *Prog. Theor. Phys.* **32** 37
Koskinen M, Manninen M and Reimann S M 1997 *Phys. Rev. Lett.* **79** 1389–92
Kouwenhoven L P, Marcus C M, McEuen P L, Tarucha S, Wetervelt R M and Wingreen N S 1997 *Mesoscopic Electron Transport* ed L L Sohn *et al* (Dordrecht: Kluwer) pp 105–214
Kravtsov V E and Altshuler B L 2000 *Phys. Rev. Lett.* **84** 3394–7
Kubo R 1964 *J. Phys. Soc. Japan* **19** 2127
Kudrolli A, Kidambi V and Sridhar S 1995 *Phys. Rev. Lett.* **75** 822–5
Kurland I L, Aleiner I L and Altshuler B L 2000 *Phys. Rev.* B **62** 14886–97
Leeuwen J 1921 *J. Physique* **2** 361
Lee I H, Rao V, Martin R M and Leburton J P 1998 *Phys. Rev.* B **57** 9035–42
Lévy L P, Dolan G, Dunsmuir J and Bouchiat H 1990 *Phys. Rev. Lett.* **64** 2074–7
Lévy L, Reich D, Pfeiffer L and West K 1993 *Physica* B **189** 204
Lewenkopf C H and Weidenmuller H A 2005 *Phys. Rev.* B **71** 121309
Leyvraz F and Seligman T H 1997 *Phys. Rev. Lett.* **79** 1778
Le Hur K, Simon P and Borda L 2004 *Phys. Rev.* B **69** 045326
Le Hur K and Simon P 2003 *Phys. Rev.* B **67** 201308
Lindemann S, Ihn T, Heinzel T, Zwerger W, Ensslin K, Maranowski K and Gossard A 2002 *Phys. Rev.* B **66** 195314
Lüscher S, Heinzel T, Ensslin K, Wegscheider W and Bichler M 2001 *Phys. Rev. Lett.* **86** 2118–21
MacKay R S, Meiss J D and Percival I C 1984a *Physica* D **13** 55
MacKay R S, Meiss J D and Percival I C 1984b *Phys. Rev. Lett.* **52** 697–700
MacKay R S, Meiss J D and Percival I C 1987 *Physica* D **27** 1
Mailly D, Chapelier C and Benoit A 1993 *Phys. Rev. Lett.* **70** 2020–3
Makarovski A, Liu J and Finkelstein G 2007a *Phys. Rev. Lett.* **99** 066801
Makarovski A, Zhukov A, Liu J and Finkelstein G 2007b *Phys. Rev.* B **75** 241407
Martins G B, Busser C A, Al-Hassanieh K A, Anda E V, Moreo A and Dagotto E 2006 *Phys. Rev. Lett.* **96** 066802
McDonald S W and Kaufman A N 1988 *Phys. Rev.* A **37** 3067–86
Mehta M L 1991 *Random Matrices* 2nd edn (London: Academic)
Meir Y and Wingreen N S 1992 *Phys. Rev. Lett.* **68** 2512–15
Miller M, Ullmo D and Baranger H U 2005 *Phys. Rev.* B **72** 045305
Mirlin A D 2000 *Phys. Rep.* **326** 259–382
Mohanty P, Jariwala E, Ketchen M and Webb R 1996 *Quantum Coherence and Decoherence* ed K Fujikawa and Y Ono (Amsterdam: Elsevier)
Mohanty P 1999 *Ann. Phys., Lpz.* **8** 549–58
Montambaux G 1996 *J. Physique* **6** 1
Mouchet A, Miniatura C, Kaiser R, Grémaud B and Delande D 2001 *Phys. Rev.* E **64** 016221
Muller S, Heusler S, Braun P, Haake F and Altland A 2004 *Phys. Rev. Lett.* **93** 014103
Muller S, Heusler S, Braun P, Haake F and Altland A 2005 *Phys. Rev.* E **72** 046207
Müller S, Heusler S, Braun P and Haake F 2007 *New J. Phys.* **9** 12
Murthy G and Mathur H 2002 *Phys. Rev. Lett.* **89** 126804
Murthy G and Shankar R 2003 *Phys. Rev. Lett.* **90** 066801
Narimanov E E, Baranger H U, Cerruti N R and Tomsovic S 2001 *Phys. Rev.* B **64** 235329
Narimanov E E, Cerruti N R, Baranger H U and Tomsovic S 1999 *Phys. Rev. Lett.* **83** 2640–3
Ng T K and Lee P A 1988 *Phys. Rev. Lett.* **61** 1768–71
Nöckel J U and Stone A D 1997 *Nature* **385** 45
Nozières P 1974 *J. Low Temp. Phys.* **17** 31
Oh S, Zyuzin A Y and Serota R A 1991 *Phys. Rev.* B **44** 8858–68
Olofsson H, Aberg S, Bohigas O and Leboeuf P 2006 *Phys. Rev. Lett.* **96** 042502
Ong T T, Baranger H U, Higdon D M, Patel S R and Marcus C M 2001 Parity effect in the coulomb blockade peak spacing distribution of quantum dots, unpublished
Oreg Y and Goldhaber-Gordon D 2003 *Phys. Rev. Lett.* **90** 136602

Ozorio de Almeida A M 1988 *Hamiltonian systems: Chaos and Quantization* (Cambridge: Cambridge University Press)

Patel S R, Cronenwett S M, Stewart D R, Huibers A G, Marcus C M, Duruöz C I, Harris J S, Campman K and Gossard A C 1998 *Phys. Rev. Lett.* **80** 4522–5

Patel S R, Stewart D R, Marcus C M, Gökçedağ M, Alhassid Y, Stone A D, Duruöz C I and Harris J S 1998 *Phys. Rev. Lett.* **81** 5900–3

Peres A 1984 *Phys. Rev.* A **30** 504–8

Pines D and Nozières P 1966 *Theory of Quantum Liquids* vol I (New York: Benjamin)

Porter C E 1965 *Statistical Theories of Spectra: Fluctuations* (New York: Academic)

Potok R M, Rau I G, Shtrikman H, Oreg Y and Goldhaber-Gordon D 2007 *Nature* **446** 167–71

Pradhan P and Sridhar S 2000 *Phys. Rev. Lett.* **85** 2360–3

Pradhan P and Sridhar S 2002 *Pramana-J. Phys.* **58** 333–41

Prado S D, de Aguiar M A M, Keating J P and de Carvalho R E 1994 *J. Phys. A: Math. Gen.* **27** 6091–106

Rahav S and Brouwer P W 2005 *Phys. Rev. Lett.* **95** 056806

Reulet B, Ramin M, Bouchiat H and Mailly D 1995 *Phys. Rev. Lett.* **75** 124–7

Richter K and Sieber M 2002 *Phys. Rev. Lett.* **89** 206801

Richter K, Ullmo D and Jalabert R A 1996*a* *J. Math. Phys.* **37** 5087

Richter K, Ullmo D and Jalabert R A 1996*b* *Phys. Rep.* **276** 1

Richter K, Ullmo D and Jalabert R A 1996*c* *Phys. Rev.* B **54** R5219–22

Richter K 2000 *Semiclassical Theory of Mesoscopic Quantum Systems* (New York: Springer)

Rokhinson L P, Guo L J, Chou S Y and Tsui D C 2001 *Phys. Rev.* B **63** 035321

Rupp T, Alhassid Y and Malhotra S 2002 *Phys. Rev.* B **65** 193304

Schechter M, Oreg Y, Imry Y and Levinson Y 2003 *Phys. Rev. Lett.* **90** 026805

Schechter M, Oreg Y, Imry Y and Levinson Y 2004 *Phys. Rev. Lett.* **93** 209702

Schmid A 1991 *Phys. Rev. Lett.* **66** 80–3

Shankar R 1994 *Rev. Mod. Phys.* **66** 129

Simmel F, Abusch-Magder D, Wharam D A, Kastner M A and Kotthaus J P 1999 *Phys. Rev.* B **59** R10441–44

Simmel F, Heinzel T and Wharam D A 1997 *Europhys. Lett.* **38** 123–8

Simon P and Affleck I 2002 *Phys. Rev. Lett.* **89** 206602

Simon P, Lopez R and Oreg Y 2005 *Phys. Rev. Lett.* **94** 086602

Simon P, Salomez J and Feinberg D 2006 *Phys. Rev.* B **73** 205325

Sivan U, Berkovits R, Aloni Y, Prus O, Auerbach A and Ben-Yoseph G 1996 *Phys. Rev. Lett.* **77** 1123–6

Sohn L L, Schön G and Kouwenhoven L P (ed) 1997 *Mesoscopic Electron Transport* (Dordrecht: Kluwer)

Srednicki M 1996 *Phys. Rev.* E **54** 954–5

Sridhar S 1991 *Phys. Rev. Lett.* **67** 785–8

Steck D A, Oskay W H and Raizen M G 2001 *Science* **293** 274–8

Steck D A, Oskay W H and Raizen M G 2002 *Phys. Rev. Lett.* **88** 120406

Heusler S, Sebastian Müller P B and Haake F 2004 *J. Phys. A: Math. Gen.* **37** L31–7

Stöckmann H J and Stein J 1990 *Phys. Rev. Lett.* **64** 2215–18

Stopa M 1993 *Phys. Rev.* B **48** 18340–3

Stopa M 1996 *Phys. Rev.* B **54** 13767–83

Tanatar B and Ceperley D M 1989 *Phys. Rev.* B **39** 5005

Thimm W B, Kroha J and von Delft J 1999 *Phys. Rev. Lett.* **82** 2143–6

Thouless D J 1961 *The Quantum Mechanics of Many-Body Systems* (New York: Academic)

Tomsovic S, Ullmo D and Bäcker A 2007 Residual coulomb interaction fluctuations in chaotic systems: the boundary, random plane waves, and semiclassical theory *Preprint* 0712.0225

Újsághy O, Zaránd G and Zawadowski A 2001 *Solid State Commun.* **117** 167–77

Ullmo D, Baranger H U, Richter K, von Oppen F and Jalabert R A 1998 *Phys. Rev. Lett.* **80** 895–9

Ullmo D and Baranger H U 2001 *Phys. Rev.* B **64** 245324

Ullmo D, Jiang H, Yang W and Baranger H U 2004 *Phys. Rev.* B **70** 205309

Ullmo D, Jiang H, Yang W and Baranger H U 2005 *Phys. Rev.* B **71** 201310

Ullmo D, Nagano T, Tomsovic S and Baranger H U 2001 *Phys. Rev.* B **63** 125339

Ullmo D, Nagano T and Tomsovic S 2003 *Phys. Rev. Lett.* **90** 176801

Ullmo D, Richter K, Baranger H, von Oppen F and Jalabert R 1997 *Physica* E **1** 268

Ullmo D, Richter K and Jalabert R A 1995 *Phys. Rev. Lett.* **74** 383–6

Urbina J D and Richter K 2003 *J. Phys. A: Math. Gen.* **36** L495–L502

Urbina J D and Richter K 2004 *Phys. Rev.* E **70** 015201

Urbina J D and Richter K 2007 *Eur. Phys. J. Special Topics* **145** 255–69

Usaj G and Baranger H U 2001 *Phys. Rev.* B **64** 201319

Usaj G and Baranger H U 2002 *Phys. Rev.* B **66** 155333

Usaj G and Baranger H U 2003 *Phys. Rev.* B **67** 121308

Vallejos R O, Lewenkopf C H and Mucciolo E R 1998 *Phys. Rev. Lett.* **81** 677–80

van der Wiel W G, Franceschi S D, Fujisawa T, Elzerman J M, Tarucha S and Kouwenhoven L P 2000 *Science* **289** 2105–08

Vavilov M G and Glazman L I 2005 *Phys. Rev. Lett.* **94** 086805

von Oppen F and Riedel E K 1991 *Phys. Rev. Lett.* **66** 84–7

von Oppen F and Riedel E K 1993 *Phys. Rev.* B **48** 9170–3

von Oppen F, Ullmo D and Baranger H 2000 *Phys. Rev.* B **62** 1935–42

von Oppen F 1994 *Phys. Rev.* B **50** 17151–61

Voros A 1979 *Stochastic Behaviour in Classical and Quantum Hamiltonian Systems* ed G Casati and G Ford (Berlin: Springer) p 334

Walker P N, Gefen Y and Montambaux G 1999a *Phys. Rev. Lett.* **82** 5329–32

Walker P N, Montambaux G and Gefen Y 1999b *Phys. Rev.* B **60** 2541–53

Weinmann D, Häusler W and Kramer B 1996 *Ann. Phys., Lpz.* **5** 652–95

Whitney R S and Jacquod P 2005 *Phys. Rev. Lett.* **94** 116801

Whitney R S and Jacquod P 2006 *Phys. Rev. Lett.* **96** 206804

Wiegmann P B 1980 *Sov. Phys.—JETP Lett.* **31** 392

Wilson K G 1975 *Rev. Mod. Phys.* **47** 773–840

Wintgen D and Friedrich H 1986 *Phys. Rev. Lett.* **57** 571–4

Wintgen D 1987 *Phys. Rev. Lett.* **58** 1589–92

Yoo J, Chandrasekharan S, Kaul R K, Ullmo D and Baranger H U 2005 *Phys. Rev.* B **71** 201309

Zaránd G and Udvardi L 1996 *Phys. Rev.* B **54** 7606–9

Zhuravlev A, Zharekeshev I, Gorelov E, Lichtenstein A I, Mucciolo E R and Kettemann S 2007 *Phys. Rev. Lett.* **99** 247202